Doctoral Thesis

Seismic Performance of Composite Walls with

Encased Steel Braces (ESB walls)

submitted in satisfaction of the requirements for the degree of Doctor
of Technical Science at the Vienna University of Technology (TU Wien), Faculty of Civil
Engineering

Dissertation

Seismische Leistung von Verbundstoffwänden mit ummantelten Stahlstützen (ESB-Wände)

ausgeführt zum Zwecke der Erlangung des akademischen Grades eines Doktors der
technischen Wissenschaft eingereicht an der Technischen Universität Wien Fakultät für
Bauingenieurwesen von

Dipl.-Ing. Ali Khazei
Matrikelnummer 0125279
Leopold - Steiner - Gasse 51/2/1
1190 - Wien

Betreuer: Univ. Prof. Dipl.-Ing. Dr.techn. Kolbitsch
TU Wien, Institut für Hochbau, Baudynamik und Gebäudetechnik
Karlsplatz 13/208-02, A-1040 Wien

Gutachter: Univ. Prof. Dipl.-Ing. Dr.techn. Rudolf Heuer
TU Wien, Institut für Hochbau, Baudynamik und Gebäudetechnik
Karlsplatz 13/208-01, A-1040 Wien

Gutachter: Univ. Prof. Dipl.-Ing. Dr.techn. Rainer Flesch
TU Graz, Institut für Betonbau, im Fach Baudynamik
8010 Graz, Lessingstraße 25

WIEN Februar 2020

Danksagung

An dieser Stelle möchte ich all jenen danken, die durch ihre fachliche und Persönliche Unterstützung zum Gelingen dieser Doktorarbeit beitragen haben.

Besonderer Dank gebührt Herrn Univ. Prof. Dipl.-Ing. Dr. techn. Kolbitsch, Univ. Prof. Dipl.-Ing. Dr. techn. Rudolf Heuer und Univ. Prof. Dipl.-Ing. Dr. techn. Rainer Flesch für die Betreuung meiner Dissertation und den Zahlreichen wissenschaftlichen Ratschlägen, welche stets zur Verbesserung der Arbeit beitragen haben.

Ebenfalls bedanke mich bei meiner Frau und meinen Eltern für ihre persönliche Unterstützung

Acknowledgement

At this point I would like to thank all those who have contributed to the success of this doctoral thesis by their professional and personal support.

Special thanks are due to Univ. Prof. Dipl.-Ing. Dr. techn. Kolbitsch, Univ. Prof. Dipl.-Ing. Dr. techn. Rudolf Heuer and Univ. Prof. Dipl.-Ing. Dr. techn. Rainer Flesch for supervising my doctoral thesis and for the numerous scientific advices which have always contributed to the improvement of the work.

I would also like to thank my wife and my parents for their personal support.

Abstract

The composite wall with encased steel braces (ESB wall) is a novel type of steel–concrete composite wall that consists of a steel braced frame embedded in reinforced concrete. This arrangement is supposed to enhance the seismic performance of the wall, as the steel columns encased in the boundary elements can increase the flexural strength of the wall and the steel braces encased in the web can increase the shear strength. ESB walls have seen use in super tall building structures constructed in regions of high seismicity. The ESB walls are commonly used on stories where the shear force demand is very high. Currently, no design guidelines exist for the design of ESB Walls in the Eurocode. More research is required before a distinct set of guidelines can be prescribed for the design of ESB Walls. The present research will investigate behavior of composite walls with encased steel braces (ESB walls). Time history analysis will be performed to examine the shear strength and stiffness of the ESB walls. In this study, two frames with three floors and five floors will be modeled in ABAQUS software. Then the X- shaped braces and inverted V brace is added to frames. Later, reinforced concrete shear wall will be added to braced frames, so the steel braces encased in the reinforced concrete shear wall. Time history analysis, on the braced frames will be done Compare and note with each other.

The results of the study are in good agreement with those of previous studies. However, none of these studies examined the effect of using V- and X-shaped struts and shear walls simultaneously, nor did they examine which struts reinforce the structures more strongly against earthquake vibrations. This has led the study to examine the effect of these reinforcements under various earthquakes. In future studies, reinforced concrete structures can also be used in addition to steel structures, and the results can be compared. In addition, these braces can also be used in other parts of the building. To meet this objective, one can use the very important data provided in this thesis, and ultimately better and more accurate results can be extracted using this approach.

The main aim of this thesis is to study the effect of increasing the number of floors on how to extend the stress on the building structure. To this end, the number of floors increased from three to five. Therefore, it can be concluded that an increase in the number of floors also more than 5 storey causes stress values, but these modes are quite consistent with the three- and five-storey buildings.

Kurzfassung

Die Verbundwand mit ummantelten Stahlstreben (ESB-Wand) ist eine neuartige Stahl-Beton-Verbundwand, die aus einem in Stahlbeton eingebetteten Stahlstützrahmen besteht. Diese Anordnung soll die seismische Leistung der Wand verbessern, da die in den Begrenzungselementen eingeschlossenen Stahlstützen die Biegefestigkeit der Wand und die im Steg eingeschlossenen Stahlstreben die Scherfestigkeit erhöhen können. ESB-Wände wurden in sehr hohen Gebäudestrukturen verwendet, die in Regionen mit hoher Seismizität errichtet wurden. Die ESB-Wände werden häufig in Stockwerken verwendet, in denen die Anforderungen an die Scherkraft sehr hoch sind. Es sind weitere Forschungsarbeiten erforderlich, bevor eine bestimmte Reihe von Richtlinien für den Entwurf von ESB-Wänden vorgeschrieben werden kann. Die vorliegende Forschung wird das Verhalten von Verbundwänden mit ummantelten Stahlstreben (ESB-Wände) untersuchen. Es wird eine Analyse der Zeitgeschichte durchgeführt, um die Scherfestigkeit und Steifigkeit der ESB-Wände zu untersuchen. In dieser Studie werden zwei Rahmen mit drei und fünf Stockwerken in der Software ABAQUS modelliert. Dann werden die X- und V-und förmigen die Strebe zu den Rahmen hinzugefügt. Später wird eine Stahlbeton-Scherwand zu den ausgesteiften Rahmen hinzugefügt, so dass die Stahlstreben in die Stahlbeton-Scherwand eingeschlossen werden. Eine zeitliche Analyse der Rahmen mit den Verstrebungen wird durchgeführt. wird miteinander verglichen und notiert.Die Ergebnisse der Studie stimmen gut mit denen früherer Studien überein. Keine dieser Studien hat jedoch die Wirkung der gleichzeitigen Verwendung von V- und X-förmigen Streben und Scherwänden untersucht und auch die Frage, welche Streben die Strukturen gegen die Erdbebenschwingungen stärker verstärken.In zukünftigen Studien können neben Stahlkonstruktionen auch Stahlbetonstrukturen verwendet werden, und die Ergebnisse können verglichen werden. Zusätzlich können diese Streben auch in anderen Gebäudeteilen eingesetzt werden. Um dieses Ziel zu erreichen, kann man die sehr wichtigen Daten, die in dieser Arbeit zur Verfügung gestellt werden, verwenden, und letztlich können mit diesem Ansatz bessere und genauere Ergebnisse gewonnen werden. Der Hauptzweck dieser Arbeit ist die Untersuchung der Auswirkungen einer Erhöhung der Anzahl der Stockwerke auf die Ausdehnung der Belastung der Gebäude- struktur. Zu diesem Zweck wurde die Anzahl der Stockwerke von drei auf fünf erhöht. Daraus lässt sich schließen, dass eine Erhöhung der Geschosszahl auch über 5 GeschosseSpannungswerte verursacht, aber diese Modi sind mit den drei- und fünfstöckigen Gebäuden durchaus vereinbar.

CONTENTS

1. INTRODUCTION

1.1 GENERAL

Shear walls have long been used as lateral resistance systems. Some of the most commonly used shear walls in multi-storey buildings are reinforced concrete shear walls (RC walls) and steel plate shear walls (SPSWs). The composite plate shear walls (C-PSW) integrate the components of a steel plate shear wall as well as a reinforced concrete shear wall. Composite Steel concrete elements manufactured by steel and concrete are used worldwide almost as soon as both materials have become available for structural engineers, taking into account the two main advantages of these materials, good compressive strength of the concrete and a higher tensile strength of the steel. A composite element that can be used in conjunction with perimeter frames to obtain dual systems is the composite wall obtained from the interlocking of steel shapes in the reinforced concrete wall. Walls with additional shapes called composite steel-concrete shear walls contain one or more embedded forms of steel, usually located at the ends of the wall. Because reinforced concrete (RC) walls can provide high lateral stiffness and strength, they are widely used as the main component-resistant lateral forces in high-rise buildings. Reinforced concrete walls have been developed to increase the flexural strength and lateral deformation of the RC walls, where structural steel is embedded in the edge elements of the wall.

Some advantages of composite shear walls:

- Compared to a reinforced concrete shear wall, the composite shear walls have the equal shear strength and has more shear stiffness. The composite shear wall occupies less space, which is very useful in architecture and space utilization.

- The weight of the of composite shear wall is less than the reinforced concrete shear wall, which reduces the size of the foundation and saves costs.

- Composite shear walls can be cast in situ or prefabricated.

- The earthquake damage can cause cracking and crushing in concrete shear walls and in steel shear walls, it causes steel rupture, but in the composite shear walls, can cause yielding the steel plates and even the concrete does not crack.

- Reinforced concrete in a composite shear wall can be used as a thermal and acoustic insulation and also protects the steel sheet against fire.

The design principles for composite shear walls are included in the design of specific codes for composite steel and concrete structures (EN 1992-1-1) and in the provisions relating to the design of buildings in case of resistance to earthquakes [10]. In addition, the design principles for reinforced concrete and steel structures can be used in some cases. In Eurocode 8, part 7.10, three types of composite structural systems are defined, as shown in Figure. 1

- Type 1 – Steel or composite frame with concrete infill,
- Type 2–Concrete walls reinforced by vertical steel sections,
- Type 3 – Concrete shear wall coupled by steel or composite beams.

Type 1 – Steel or composite frame with concrete infill

Type 2 – Concrete walls reinforced by vertical steel sections

Type 3 – Concrete shear wall coupled by steel or composite beams
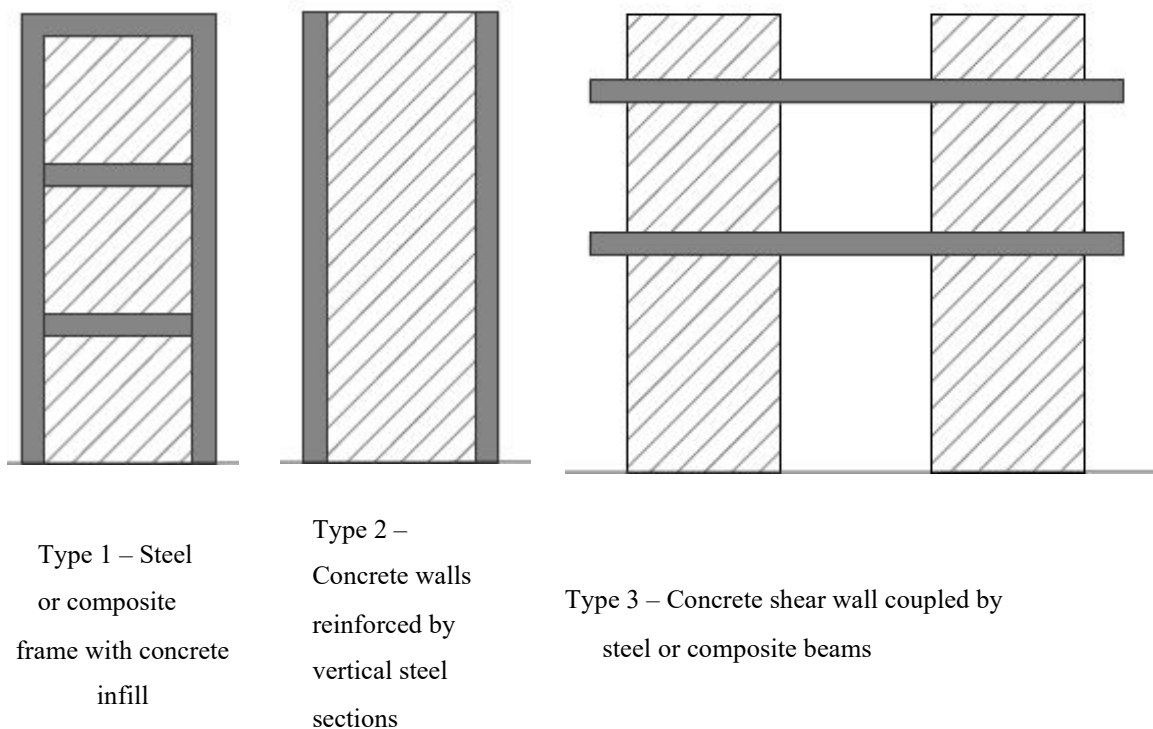
Figure 1: Composite structural systems with shear walls [8]

Although valuable research data is available from this type of system, while many of the major buildings are based on these systems, information on the seismic design of this seismic system is very limited.

Recently, a new type of composite shear wall that includes encased steel braces (ESB) has been proposed for better seismic performance of structures. This kind of Technic is supposed to enhance the seismic performance of the wall because the steel columns enclosed in the boundary elements can increase flexural strength of the wall structure and the steel braces encased in the boundary elements can heightened shear strength. The use of diagonal reinforcement elements is adopted to increase the shear strength of the walls. ESB walls have been used in super-high constructions constructed in regions of high seismicity. The ESB walls are commonly used on stories where the demand for shear force is very high (for example, the walls of the core on the lower floors or on the outrigger storey).

(a) With an encased single diagonal brace   (b) With encased X- shaped brace
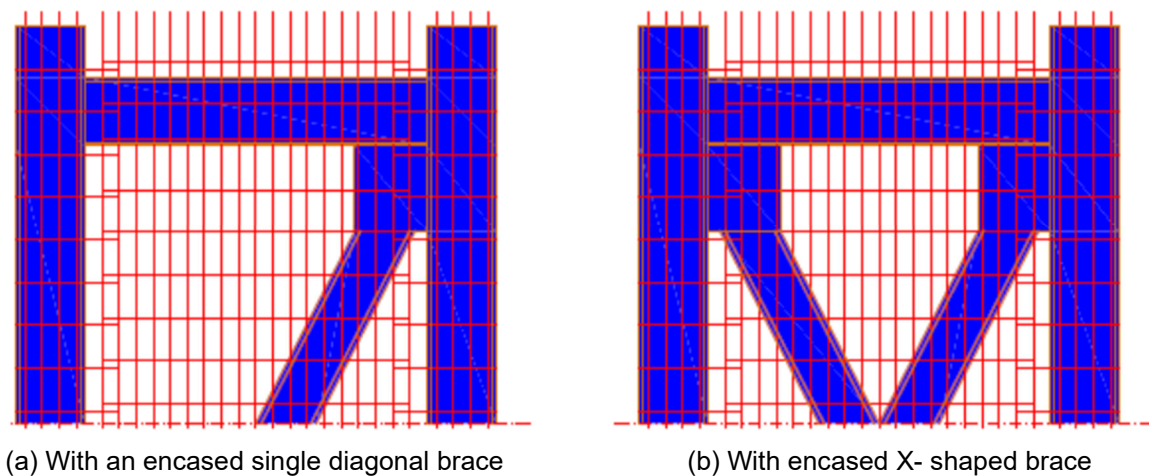
Figure 2: Composite walls with encased steel braces (ESB walls)

1.2   OBJECTIVES AND SCOPE OF THE RESEARCH

Currently there are no design guidelines for the design of ESB walls in the Eurocode. More research is needed before a separate set of guidelines can be prescribed for the design of ESB walls. As mentioned earlier, some experimental and analytical studies have been carried out in different countries on different forms of composite shear walls; different dimensions and designed to study the cyclic behavior of these structures as well as the effect of parameters such as aspect ratio, brace types, etc. Experimental and analytical studies on composite shear walls have been limited to static and quasi-static cyclic loads. ESB walls have not been studied under real seismic loads. So far, no comprehensive research has been conducted on ESB walls seismic loading. One of the objectives of this research is to evaluate the seismic performance of ESB walls. A nonlinear finite element model is developed to study the behavior of ESB walls.

1.3   OUTLINE OF THESIS

Chapter 1 presents brief introduction about the novel form of the composite wall, research significance and objective of the study.

Chapter 2 presents a comprehensive literature review on different types of shear wall namely, steel plate shear wall, profiled steel sheet shear wall, composite shear wall.

Chapter 3 describes in detail the finite element model developed to predict the behavior of the composite shear wall under earthquake loading. Some strategies in nonlinear dynamic explicit Finite Element Method (FEM) for simulating a time-history response are discussed in detail.

Chapter 4 outlines the detail of the finite element model developed to predict the behavior of the composite shear wall under impact loading.

Chapter 5 presents the main conclusions of the study along with some suitable recommendations for future work on the composite shear wall system.

2. LITERATURE REVIEW

2.1 INTRODUCTION

Shear walls are lateral load-resisting systems capable of effectively bracing a building against both wind and earthquake forces. Traditionally reinforced concrete shear walls were used in reinforced concrete building structures for many years to brace the building from lateral loads.

The system for this new type of shear wall consists of vertical infill panel one storey high and one bay wide connected to the surrounding beam-column frame. This type of shear walls is well-suited for new construction and it also offers relatively simple mean for the seismic upgrading of existing steel or concrete structures. In this chapter, the development and recent investigations on different types of this innovative shear walls are presented and some current researches on the effect of impact loading on structural elements are reviewed.

2.2 COMPOSITE SHEAR WALL

The term "composite shear wall" can be referred to shear wall which consists of reinforced concrete panel cast between steel [31] or composite shear panel attached between steel columns. Recently many researchers from all over the world mostly from United States, China, South Korea, Britain and Canada pay attention to composite shear wall.

In this study, the focus is on composite shear wall made of steel and concrete as a shear panel attached to steel columns. The composite shear panel consist of one or two steel plate with reinforced concrete which can be precast or cast in place as shown in Figure. 3. The steel plate can be connected to a precast reinforced concrete panel by using mechanical connectors like bolts and also can be attached to cast in place reinforced concrete by using shear studs or bonding a Fiber Reinforced Polymer sheet [34].
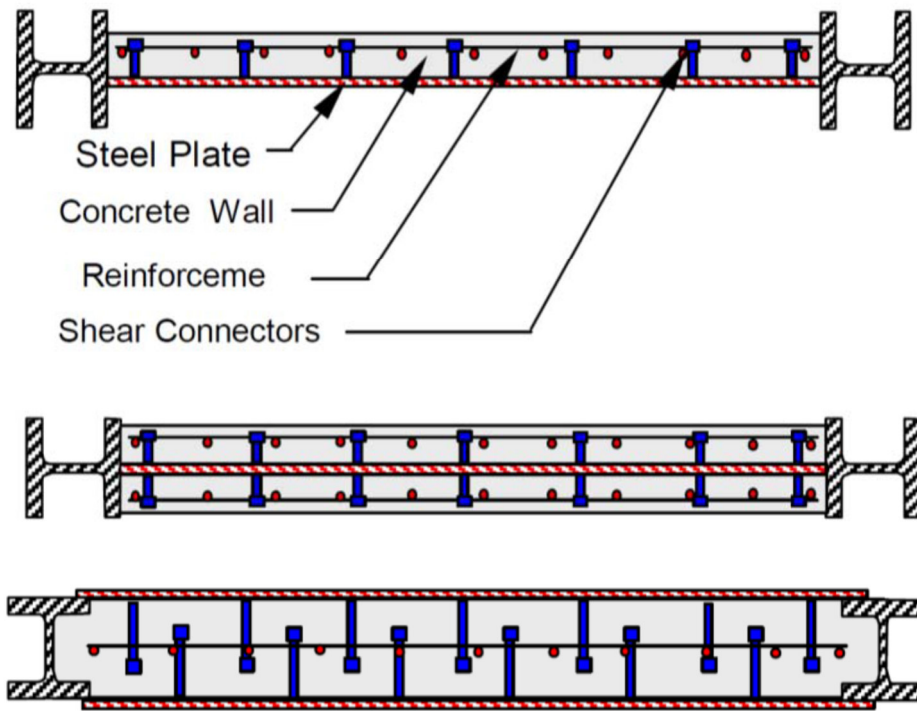
Figure 3: Types of studied composite shear wall [7]

In a composite shear wall, the concrete part restrains the steel plate and prevents the steel plate from buckling before yielding of steel. Therefore, the steel plate shear wall can resist the storey shear by yielding in shear. It should be noted that the shear yield capacity of the steel plate is significantly greater than its capacity to resist shear in yielding of diagonal tension field [7]. The main disadvantage of an unstiffened steel plate shear wall is the buckling of the compression zone of the shear wall, which results in reduction of stiffness, strength and energy dissipation capacity [35]. In a composite shear wall, concrete panel also can resist shear by developing compression diagonal field. Thus, the composite shear wall can have the most benefits of both concrete panel and steel plate shear wall.

Various types of steel and concrete composite walls have been developed and used in seismic zones. Zhao and Abolhassan [36] attached RC panels to the steel plate walls using bolts, resulting in highly ductile behavior and stable cyclic post-yielding performance. Dan et al. [2] encased vertical steel profiles into RC walls and demonstrated the effectiveness of the steel profiles in improving the seismic performance of RC shear walls.

Qian et al. [3] embedded steel tubes at the wall boundaries and fully anchored into the foundation of RC walls and proved such composite details can ensure good seismic performance under high axial load and cyclic lateral loading.

Nie et al. [37] investigated the seismic behavior of high-strength composite walls composed of concrete filled steel tubular (CFT) columns at the two boundaries and high strength concrete filled double-steel-plate wall body. Rafiei et al. [38] and Hossain et al. [39] investigated the behavior of composite shear walls consisting of two skins of profiled steel sheeting and an infill of concrete under in-plane monotonic and cyclic loading respectively, demonstrating more ductile behavior and higher energy absorbing capacity. Chen et al. [40] studied the double steel plate-high strength concrete composite walls with concrete filled steel tube boundary elements, showing high strength and excellent deformation capacity.

Zhao and Astaneh-Asl (2004) carried out experimental studies on two half-scale, one bay, three storey composite shear wall specimens [41]. The composite shear wall consisted of a reinforced concrete shear panel bolted to one side of a steel plate shear wall. The bay span and storey height of the specimens were 2.1m (7 ft). The thickness of the reinforced concrete shear panel and the flat steel plate were 76 mm (3 inch) and 4.8 mm (3/16 inch), respectively.

The properties of the specimens were identical except that in the first specimen there was a 32 mm gap between the reinforced concrete panel and the surrounding steel frame and in the second specimen there was not any gap. The authors considered the first specimen as "innovative" composite shear wall while the second specimen represents "Traditional" composite shear wall. The components of the test setup as shown in Figure. 4 are actuator, loading beam at top, reaction beam at bottom, R/C reaction blocks, and the specimen [36].
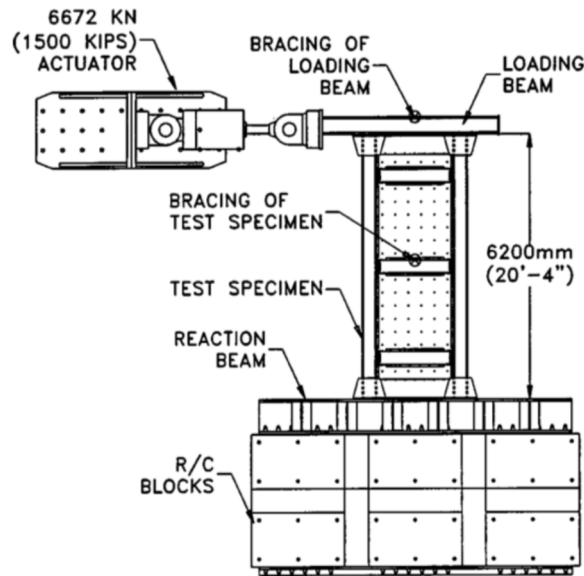
Figure 4: Experimental test setup and detail of the test specimen [36]

Cyclic displacements were applied at the top of the specimen according to the specifications for qualifying cyclic tests of beam to column connections in seismic provisions for structural steel buildings (AISC 1997). The loading sequence and failure points for both specimens are shown in Figure 5.
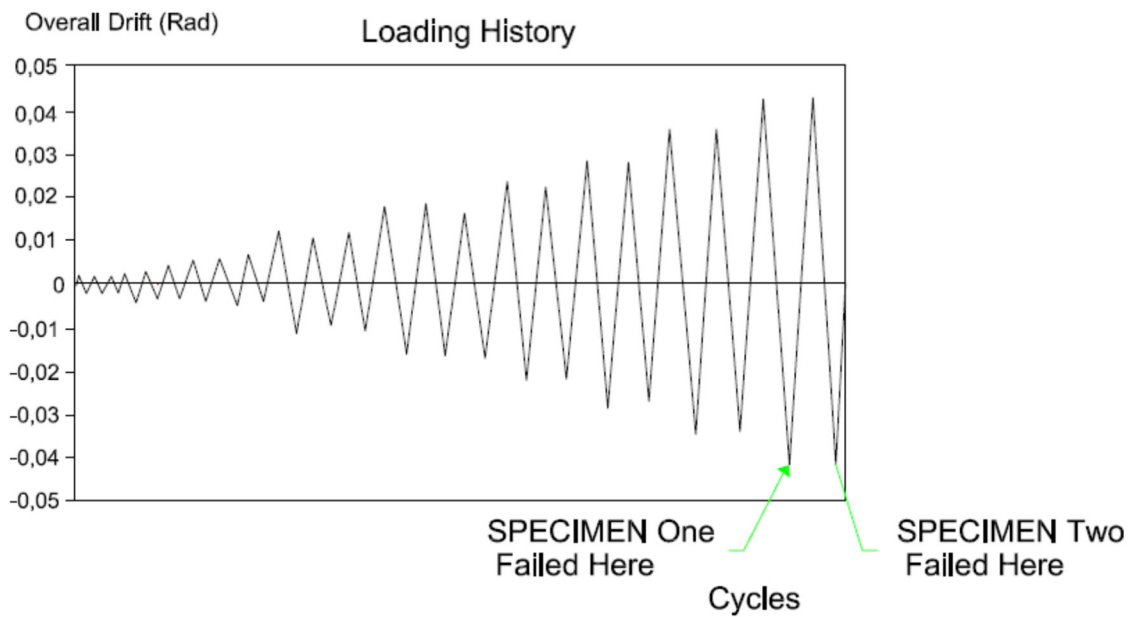
Figure 5: Time history of drift applied to two specimens [36]

It was observed that both innovative and traditional composite shear walls had high ductility and good lateral-load resisting properties. The maximum inter-storey drift was more than 5% for both specimens and they can withstand up to 4% inter-storey drift without and reduction in the shear strength.

The reinforced concrete panel by itself in both specimens did not contribute much (less than 20%) in increasing the shear strength, but it was crucial to prevent the steel plate panel from buckling. The reinforced concrete panel had less damage in first specimen (innovative) than second specimen (traditional) and also the first specimen behaved in a more ductile manner compare to the second specimen.

Rahai and Hatami (2009) investigated experimental tests on the effects of changes in shear joint spacing on the behavior of the composite shear wall [34]. The experimental tests were performed on three small scale, single bay, and one storey composite shear wall specimens consisting of 3.3 mm thick steel plate and 50 mm thick reinforced concrete panel attached to one side of the steel plate by bolts. The steel plate was connected to reinforced concrete panel by 9, 12, 24 bolts which the vertical bolts spacing varied from 222 mm to 777 mm and the horizontal bolts spacing was 222 mm for all three specimens. Cyclic loadings were applied at top of the specimens.

Cyclic loadings were applied at top of the specimens. It has been found that the decreasing distance between the bolts increases the absorbed energy in the shear wall and reduces the amount of out-of-plane displacement of steel.

The authors also performed numerical modelling of the composite shear wall using the ANSYS finite element software. The model was calibrated and verified based on the two laboratory models at Berkeley and Alberta Universities. The shear connectors were modelled using a three-dimensional beam element with 6 degrees of freedom. The steel plates, beams and columns were modelled by shell element with four nodes and six degrees of freedom per node. A solid element with eight nodes, three degrees of freedom per node for translation was used for the reinforced concrete.

The following assumptions were made to investigate the effect of the shear connector spacing on the shear wall behaviour:

- The friction between steel and concrete was neglected, and
- The steel was considered to have a bilinear behaviour.

A good agreement was observed in the hysteresis curves between numerical model and experimental results.

an experimental study on seismic behavior of mid-rise RC shear wall with concealed truss conducted Cao et all. (2009). Six specimens of mid-rise I-section shear wall with frame with the shear span ratio of 1.85 were designed. The serial numbers of them were SW1.85-1, SW1.85-2, SW1.85-3, SW1.85-4, SW1.85-5, and SW1.85-6, in which the number of 1.85 denotes the shear span ratio. Three types of the shear wall are shown in Figure 6.
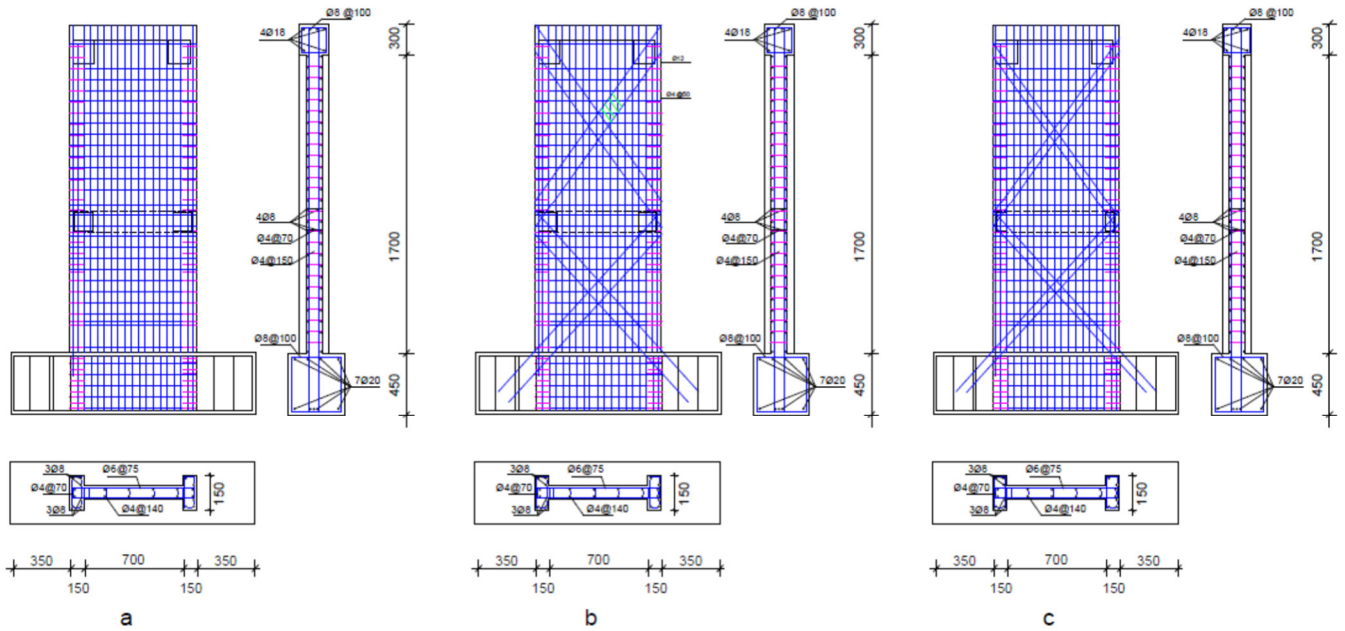
Figure 6: Reinforcement detail. (a) SW1.85-2; (b) SW1.85-3; (c) SW1.85-5 [9]

With the low-circled loading on the specimen at the height of 1.85 m to the top surface of the base on the horizontal direction, a vertical loading with a constant value P = 650 kN was applied for maintaining the axial compression ratio to 0.20 (as the designed concrete strength level) before the loading at the horizontal direction. The test setup is shown in Figure 7.
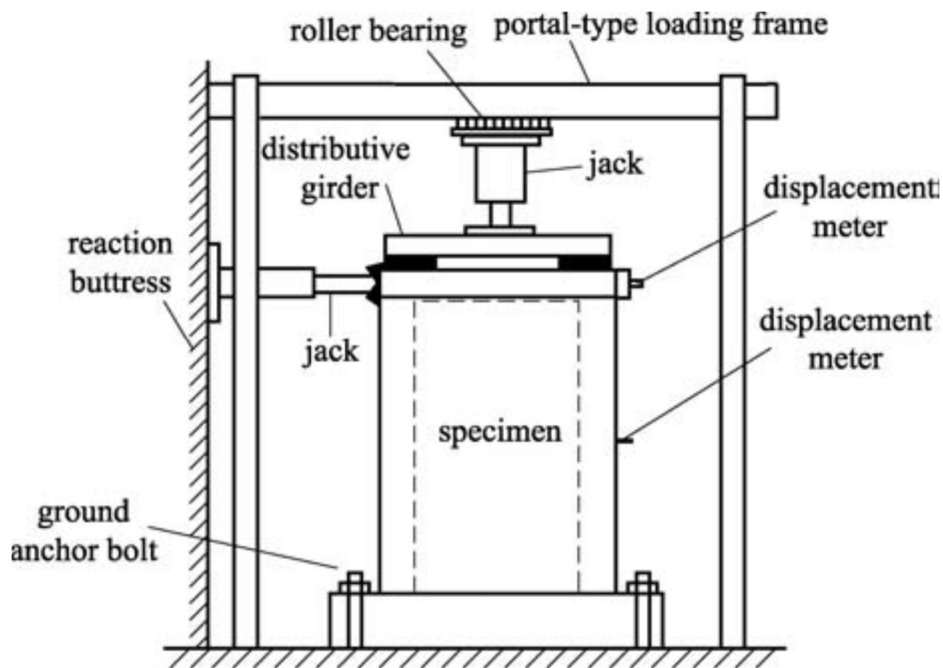
Figure 7: Test set-up [9]

This new composite shear wall includes two kinds of composition: one is the composition of two bearing systems, truss and shear wall; the other is the composition of two materials, steel and concrete, which forms a double composite shear wall. The failure mode of the mid-rise shear wall with concealed truss is quite different with that of the ordinary mid-rise shear wall. The effect of the concealed truss lies in that it slows the development of the cracking, expands the distribution area of the cracking, extends the dissipation area of the bottom plastic hinge, and improves the post stiffness and integrated seismic capacity of the shear wall [9].

Dan et al. (2011) hat examined in his work theoretically and experimentally nonlinear behavior of composite shear walls with vertical steel concealed profiles. To study the behavior of the concrete walls reinforced by vertical steel sections, a theoretical and experimental program was developed in the Civil Engineering Department at the Politehnica University of Timisoara, Romania. In Eurocode 8 part 7.10 [11] three types of composite structural systems are defined. The studied walls belong to Type 2. For this type of structural walls, the Composite Steel Reinforced Concrete Wall (CSRCW) notation will be used in the followings.

The experimental program consists of six 1:3 scale elements (CSRCW1 to 6), designed using the principles from the existing codes (Eurocode 2, Eurocode 4 and Eurocode 8) applied to composite steel–concrete elements [8,12]. The design details of all the six types of composite steel–concrete shear walls are shown in Figure 8.

(a) Horizontal sections.　　　　(b) Vertical section.
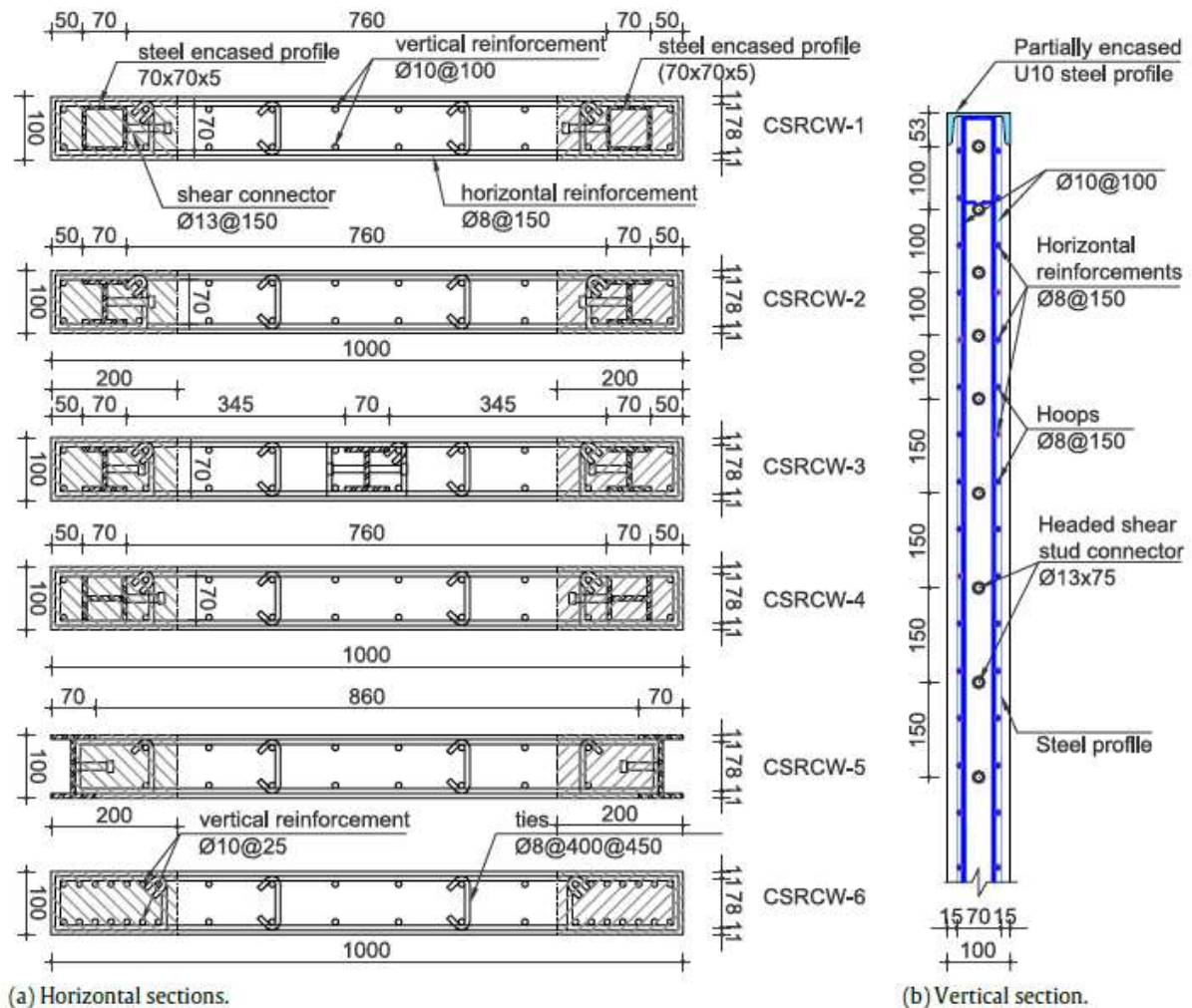
Figure 8: Details of the composite steel–concrete walls. [10]

The experimental elements differ on the arrangement of the steel shapes embedded in the cross section of the wall and on the cross-section type of the steel encased profiles. All specimens were tested based on constant vertical load and cyclically increasing horizontal (lateral) loads. The tests were performed until failure.

Using the recorded data during the tests, the following parameters are presented and discussed: maximum load capacity, stress and strain distribution in structural components (reinforcements, structural steel on concrete surface), inter- storey drifts, cracking patterns, deformation and degradation capacity. [10]

The relationship between the performance of reinforced concrete shear walls and reinforced concrete boundary columns has occupied Liao in his work.

A one-bay, one storey SRC–RC wall is selected as the analytical and testing model, as shown in Figure 9.

(a) SRC-frame and SRC-RC wall mixed structure   (b) SRC-RC wall
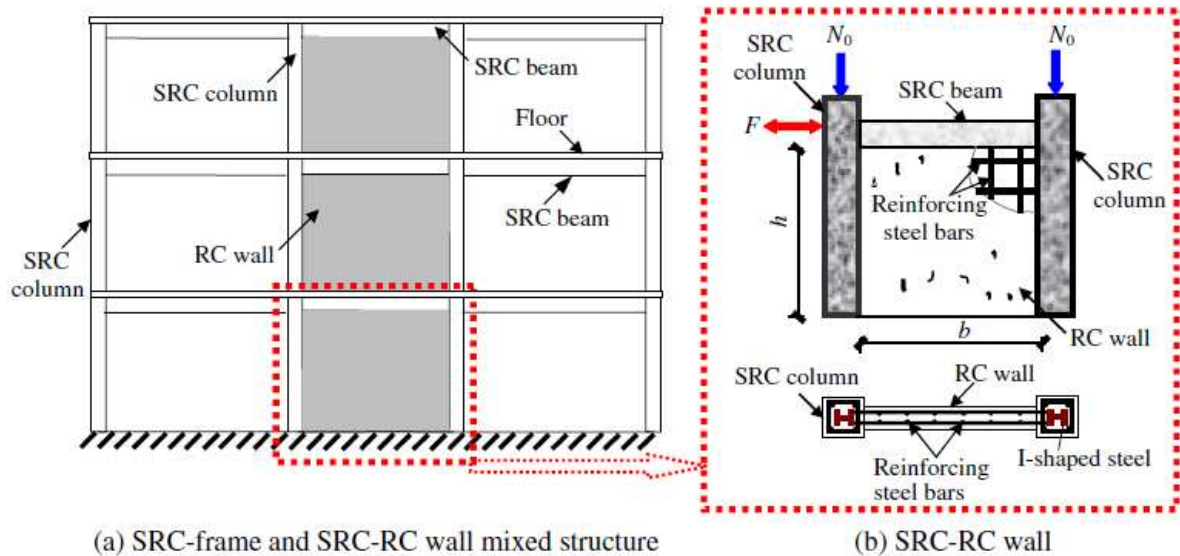
Figure 9: A schematic view of SRC–RC wall model in a real mixed structure. [13]

According to Tomii [14] and Gao [15], as a part of the overall frame system, the framed shear wall is expected to carry a larger portion of the horizontal load due to its high stiffness. A finite element (FE) model is developed to simulate the behaviour of SRC–RC walls under constant axial load and lateral loading. A series of tests, including six shear wall specimens, were conducted under cyclic loading condition to investigate the strength, ductility and energy dissipation of them, as well as to verify the FE model. This FE model is then used to examine the load transfer mechanism and to carry out a parametric analysis for SRC–RC walls. the FE model can predict the behavior of the composite shear walls with enough accuracy.

The specimens were designed and conceived to investigate the effects of the following parameters on the behavior of the composite walls: the type of vertical- side reinforcement, for example, reinforcement bars or structural steel, the position of structural steel in the cross section, the structural steel shape. All the specimens had the similar vertical reinforcement. Figure. 10. shows composite steel–concrete experimental elements.
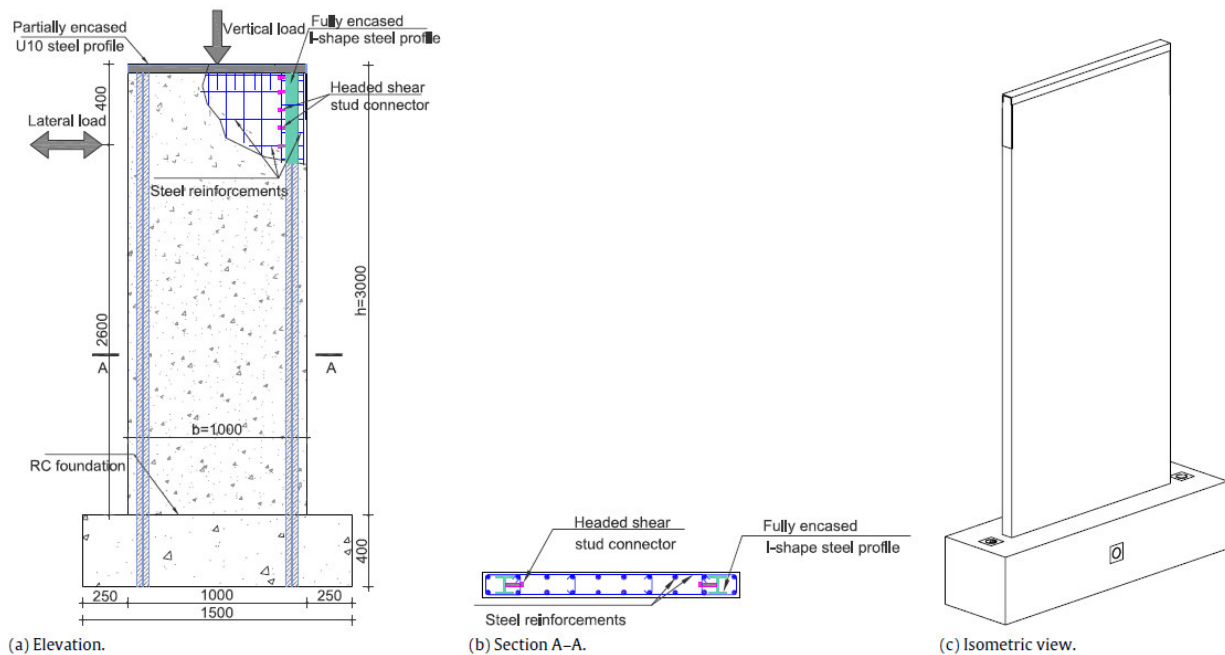
Figure 10: Composite steel–concrete experimental element [2]

it is to be considered that when bending the behavior of RC is nonlinear The non-linearity is due to the non-linear behavior of concrete and steel, the shear bolt behavior as well as the connection between steel and concrete is attributable to steel-concrete composite shear walls Therefore, the software ATENA 2D was used to analyse the proposed experimental elements in order to have a general overview related to the expected behavior during the experimental tests. The software is capable to analyze the reinforced concrete and also the composite steel–concrete elements in a plane stress state. The two-dimensional nonlinear analysis is performed using the incremental–iterative procedure [2].

Ji et al. (2016) investigated on cyclic shear behavior of composite walls with encased steel braces [16]. The prototype wall was selected from the Z15 Tower, a super-tall building of 528 m height, located in the central business district of Beijing. The wall specimens were scaled down by 0.35 in dimension and by 0.12 in shear strength capacity relative to the prototype walls, to accommodate the capacity of the loading facility. Two wall specimens (labeled SW1 and SW2) were designed, SW1 having an encased steel plate brace and SW2 having an encased I-shaped brace. The two specimens had identical geometry, as shown in Figure 11.
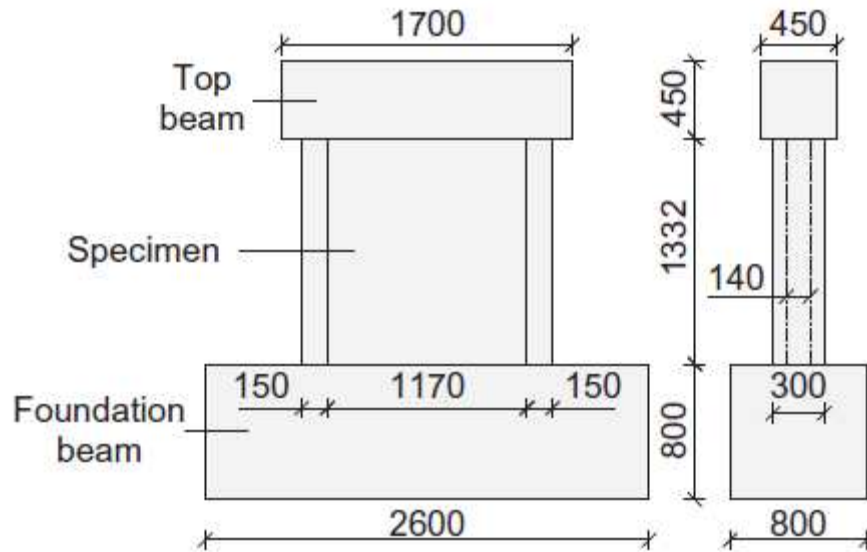
Figure 11: Overall dimensions of test specimens (mm). [16]

The test specimen was loaded using the multi-functional largescale testing facility at Tsinghua University. Figure 12. shows the test setup [17].
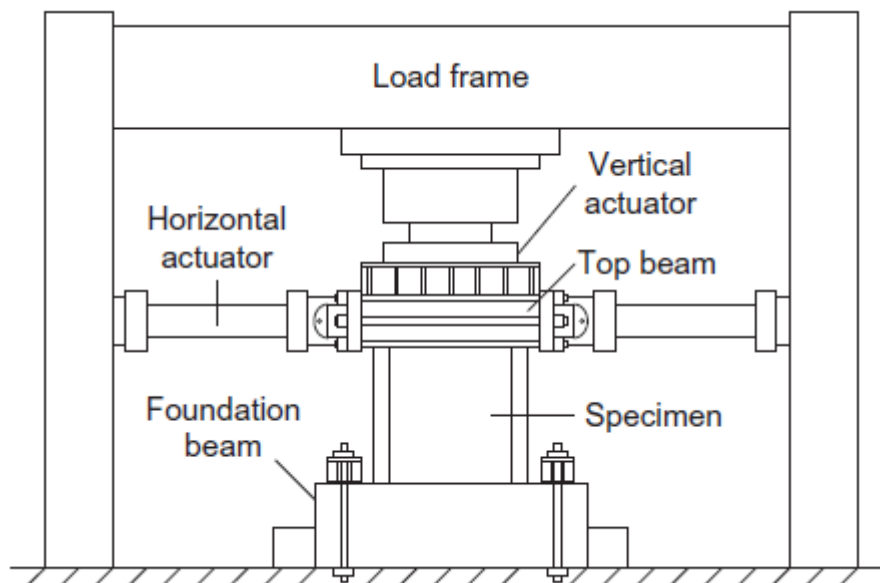
Figure 12: Test setup. [16]

The foundation beam was securely clamped to the reaction floor. The top beam was clamped to three hydraulic actuators, one in the vertical direction and the other two in the horizontal direction. A rigid steel beam was placed between the top beam and vertical actuator to distribute the vertical force uniformly on the specimen.

The vertical actuator could move horizontally to accommodate the lateral displacement of the specimen. At first, a vertical load was applied to the specimen and then it was constantly maintained during testing.

Afterwards, cyclic shear loads were applied by the two horizontal actuators. Both horizontal actuators operated simultaneously, one in pull and another in push. The horizontal loading point (i.e., the centroid of the top beam) was 1557 mm above the wall base. The shear-to-span ratio of the wall specimen was 1.06 [16].

Zhao et al. (2016) studied on hysteretic model for steel–concrete composite shear walls subjected to in-plane cyclic loading. Experimental investigations on more than one hundred SC wall specimens subjected to cyclic in-plane loading have been conducted. Of these tests, the detailed results of load and displacement of 32 specimens were presented [17], which provides a basic database for the derivations and calibrations Tabell 2.1 shows the experimental results including the axial load (N), the lateral load (Q), and the stiffness (K).

Speicmen	N(Mpa)	Cracking point				Yield point				Peak point			
		Q1(kN)	K1V(kN/mm)	K1M(kN/mm)	K1(kN/mm)	Q2(kN)	K2V(kN/mm)	K2M(kN/mm)	K2(kN/mm)	Q3(kN)	K3V(kN/mm)	K23M(kN/mm)	K3(kN/mm)
SS050	0.00	474	2380	-	-	2250	1461	-	-	3250	1001	-	-
SS100	0.00	488	2020	-	-	-	-	-	-	3224	921	-	-
SS150	0.00	420	1710	-	-	-	-	-	-	3245	773	-	-
H10T05	0.00	400	-	-	850	1310	-	-	492	2630	-	-	277
HT10T10	0.00	510	-	-	2210	2700	-	-	701	4130	-	-	298
H10T10V	3.00	1130	-	-	1890	3190	-	-	679	4980	-	-	320
H10T15	0.00	660	-	-	3090	3750	-	-	872	6700	-	-	286
H07T10	0.00	600	-	-	2570	2888	-	-	963	4710	-	-	428
H15T10	0.00	420	-	-	730	2348	-	-	398	4000	-	-	184
BS70T05	0.00	700	4290	27,21	3710	6210	1686	15,291	1519	7370	976	11,572	900
BS70T10	0.00	900	6110	26,19	5050	4280	1583	15,457	1436	5730	822	11,713	768
BS70T14	0.00	875	3880	29,15	3430	4340	1267	14,649	1167	5410	840	11,723	784
BS50T10	0.00	775	6690	80,66	6230	4590	2726	46,789	2576	6570	1593	37,672	1528
BS85T10	0.00	895	3950	13,43	3070	4150	12113	76,44	1046	5450	722	6411	649
S2-00NN	0.00	299	2167	-	2167	2338	779		779	3024	385	-	385
S2-15NN	1,47	442	2769	-	2769	2379	731		731	3166	553	-	553
S2-30NN	2,94	553	2743	-	2743	2542	704		704	3166	450	-	450
S3-00N	0.00	317	1971	-	1971	3132	867		867	3675	482	-	482
S3-15N	1,47	392	2317	-	2317	3187	880		880	3832	472	-	472
S3-30NN	2,94	393	1617	-	1617	3233	885		885	3796	535	-	535
S3-00PS	0.00	357	2110	-	2110	2726	1136		1136	3653	457	-	457
S3-00PN	0.00	276	2035	-	2035	2399	995		995	3583	431	-	431
S4-00NN	0.00	356	2880	-	2880	3580	1484		1484	4175	805	-	805
SCW1-1a	9,74	-	-	-	-	1098	-	-	471	1782	-	-	223
SCW1-1b	9,74	-	-	-	-	1072	-	-	393	1612	-	-	202
SCW1-2a	9,74	-	-	-	-	652	-	-	163	1035	-	-	77
SCW1-2b	9,74	-	-	-	-	684	-	-	187	954	-	-	83
SCW1-3	9,74	-	-	-	-	500	-	-	99	604	-	-	76
SCW1-4	8,15	-	-	-	-	700	-	-	343	962	-	-	160
SCW1-5	11,33	-	-	-	-	12,64	-	-	556	1972	-	-	248
SCW1-6	9,74	-	-	-	-	1200	-	-	417	1568	-	-	157
SCW1-7	9,74	-	-	-	-	900	-	-	440	1659	-	-	193

Table 2.1: Experimental data sets of SC walls specimens [17]

To establish a hysteretic model for SC walls subjected to cyclic in-plane load, the load–displacement relationship is simplified into a quadri-linear backbone curve, as shown in Figure 13.
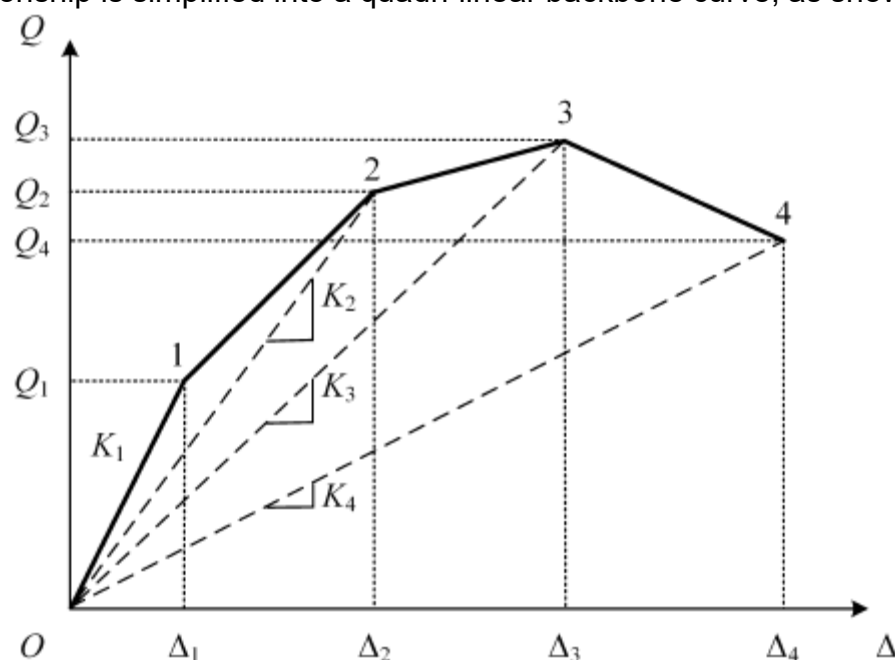
Figure 13: Quadri - linear backbone curve and turning points [17]

Conclusions shows the hysteretic response of an SC wall under cyclic in-plane load can be described by a quadri-linear model. The four turning points are cracking point, steel faceplate yield point, peak point and ultimate point, respectively [17].

Rassouli et al. (2016) conducted an experimental and numerical study on steel-concrete composite shear wall using light-weight concrete [23]. In experimental investigations, three one-storey and one-bay CSPSWs with the scale of 1:4 are designed and fabricated. The steel parts of all the specimens were fabricated and welded at a factory and then the precast reinforced concrete panels were attached to the infill steel plates of specimens by high strength bolts at the laboratory.

an experimental and numerical study on steel-concrete composite shear wall using light-weight concrete investigated Rassouli et al. (2016). In experimental examination, three one-storey one-bay CSPSWs with the scale of 1:4 are designed and fabricated. The steel parts of all the specimens were produced and welded at a factory and then at the laboratory the precast reinforced concrete panels were fixed to the infill steel plates of specimens by high strength bolts. The specimens were design in accordance with AISC341 [24]. It is adopted that the infill composite wall resists complete lateral load up to entire yield of the infill steel plate; therefore, beams and columns were plan according to capacity design method. Figure 14 shows a typical CSPSW specimen and an experimental model shows in Figure 15. [23]
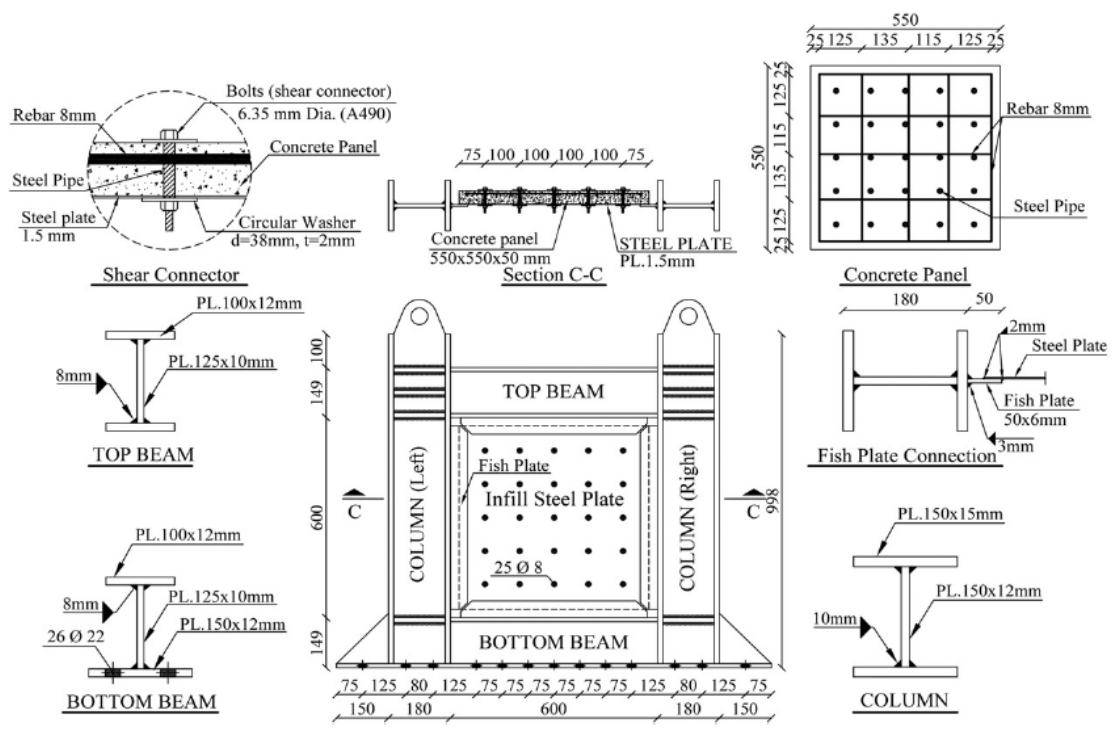
Figure 14: Details of specimen CSPSW-L [23]
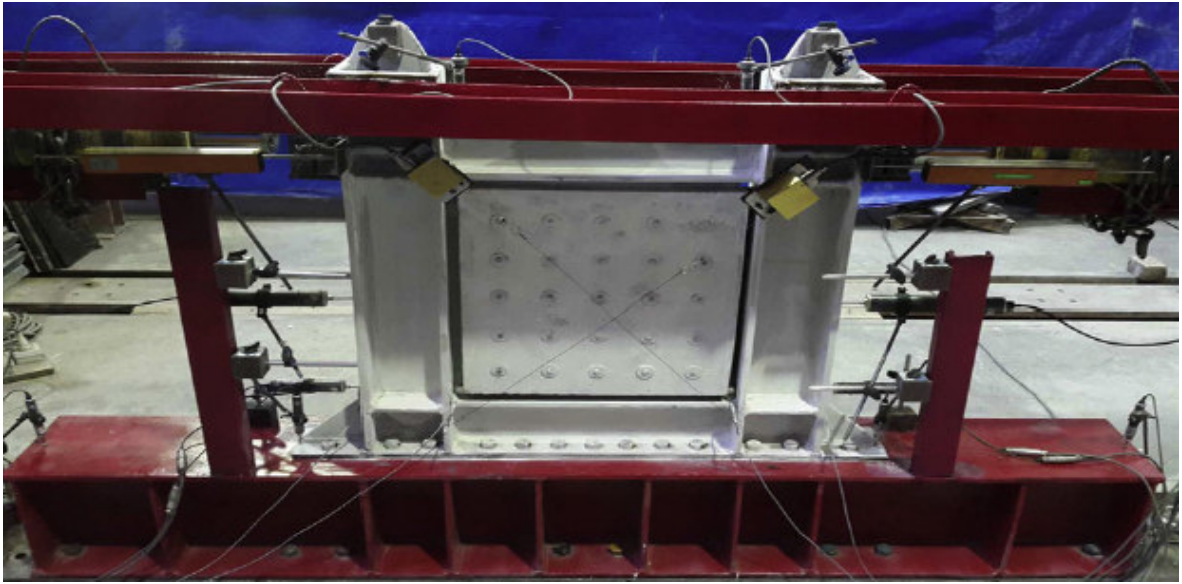
Figure 15: Specimen CSPSW-N [23]

Loading history was applied by two hydraulic jacks in accordance with ATC-24 [25]. Before the experiments, finite element models of specimens with the attained material properties were developed to predict the yield points of specimens which were approximately the same value observed during the tests. The cyclic displacement loading history of CSPSW-L is illustrated in Figure 16. [23]
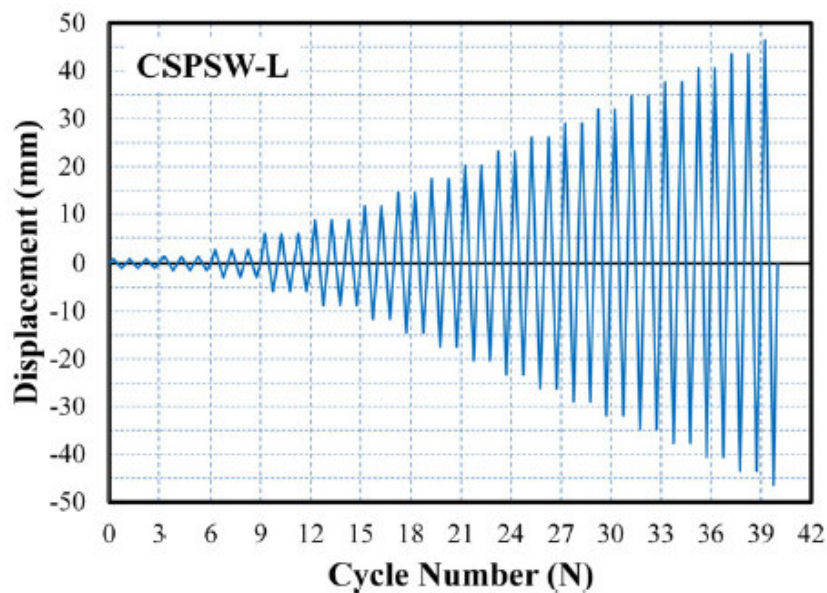
Figure 16: Cyclic displacement loading history of CSPSW-L in accordance with ATC-24. [23]

24

The quasi-static cyclic test results indicate that CSPSW with a light-weight concrete panel is a responsible lateral load-resisting system for steel structures. also, the shear capacity of the lightweight concrete specimen was approximately identical to that of the standard weight specimen. for that, it can be concluded that the new system can reduce the seismic mass and improving the behavior of steel structures

Seo et al. (2016) investigated on Steel-plate composite (SC) walls: In-plane shear behavior, database, and design [26]. The in-plane shear strength of steel-plate composite (SC)walls is governed by the onset of Von Mises yielding in the steel faceplates. The fundamental in-plane shear behavior of SC walls was reviewed using the mechanics based behavior model (MBM) that uses composite (cracked orthotropic) plate theory. The MBM idealized the in-plane shear force–shear strain behavior into three portions: (i) before concrete cracking, (ii) after concrete cracking but before steel plate yielding, and (iii) steel plate yielding. The model was verified using the experimental results of a large scale in-plane shear test of the experimental database. The experimental database of in-plane shear tests conducted on SC wall specimens in Japan, S. Korea, and the US was also compiled and described in this paper. The database included a total of 26 tests that were conducted to investigate the in-plane shear behavior of SC walls. These tests were categorized based on the specimen configuration as: (i) SC wall specimens with flange walls, and (ii) SC wall panel specimens. SC wall specimens with penetrations, specimens with ribs, and wall pier specimens without adequate boundary elements were not included in the database [26].

the seismic behavior of steel and concrete composite walls with embedded steel framework investigated Wu et al. (2016) for use in high-rise buildings. In their investigation, an alternative type of steel and concrete composite shear wall has been developed as shown in Figure 17. The steel truss embedded in the concrete wall is composed of channel steel chords at boundary elements and equal-leg double angle web braces at the wall web. By embedding a steel truss instead of steel plate in the RC wall, considerable saving in steel material and improvement in constructability can be achieved [27].
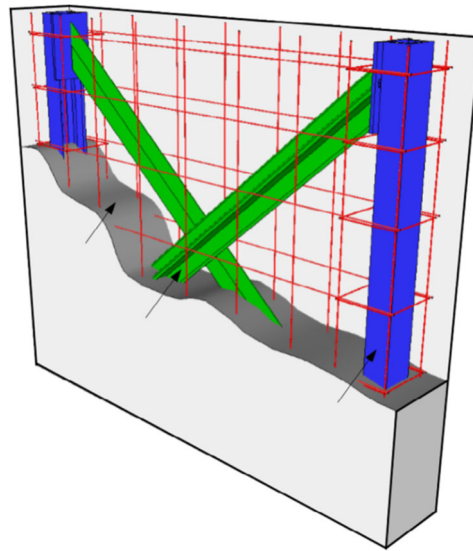
Figure 17: Proposed type of composite wall [27]

Three one-fourth scaled specimens embedded with steel truss identified by S-1, S-2 and S-3 were constructed and tested under constant axial load and reversed cyclic lateral load. All the specimens were designed according to the Chinese Code for Seismic Design of Buildings (GB50011-2010) [28], having identical overall geometric dimensions, as shown in Figure 18 [27].
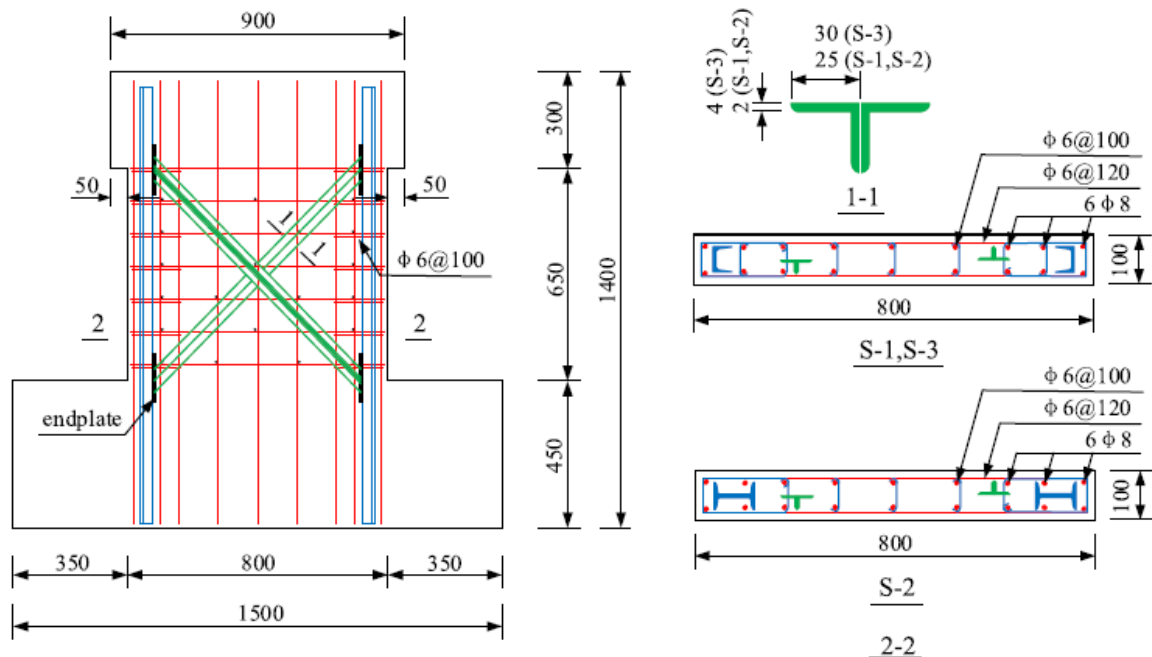
Figure 18: Detailed dimensions of the specimens [27]

The axial load and lateral cyclic load were applied to the specimens using the test setup shown in Figure 19. [27].
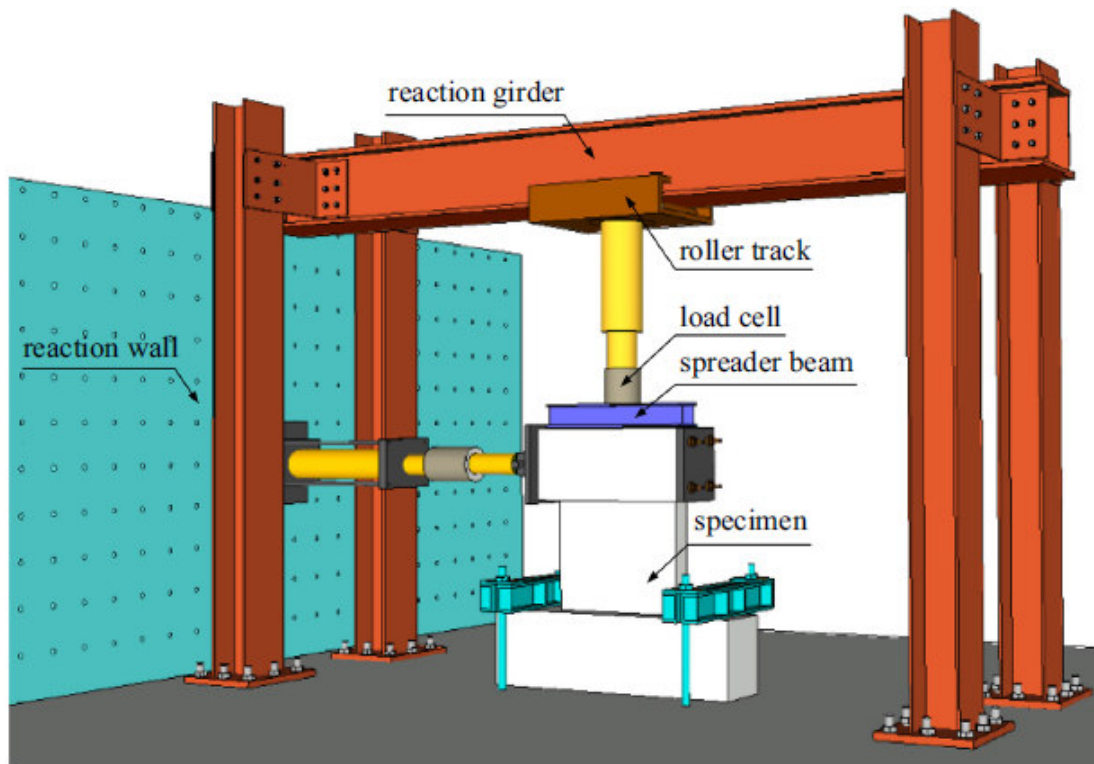
Figure 19: Test setup [27]

the amounts of embedded truss chord and web brace were the test parameters the behavior of the test specimens, including the damage formation, failure mode, hysteretic curve, stiffness and strength degradation, energy dissipation and ductility, were tested.

Test results showed that the embedded truss web braces affect significantly the hysteretic behavior of the composite walls in terms of lateral load capacity, energy dissipation and ductility, while the embedded truss chords can enhance the lateral load capacity. With a finite element model (FE models), all test results in the search for the optimal design were broadened and confirmed. Then 27 FE models that cover the practical ranges of axial load ratio, amount of embedded steel truss chord and web braces were adopted in a parametric analysis to investigate their effects on the wall performance. The results confirm that a high axial load ratio is beneficial for initial stiffness and lateral load capacity while affecting energy dissipation capacity [27].

on effective stiffness of composite shear wall with double plates and filled concrete investigated Nie et al. (2014). The composite shear walls with double steel plates and filled concrete are composed of two steel plates with studs inside, side columns made of steel tubing, and an infill of concrete. They were expanded to enlarge the building space and delay the appearance of cracks by using the steel plates as formwork. the formula for calculating the effective shear stiffness of the composite shear wall is derived from this model. The total effective stiffness is obtained by combining the effective shear stiffness and the effective flexural stiffness, in which the flexural stiffness can be obtained by the fibre model. The predictions for the effective stiffness correlate well with the results of a series of tests on composite shear walls [29].

The numerical modeling of sheet steel reinforced concrete shear walls was studied by Nguyen and Whittaker (2017 The tests were taken in the NEES laboratory at the University in Buffalo supported from the Bowen Laboratory at Purdue University. All four walls had an aspect ratio (height-to-length, H=L) of 1.0. The design variables considered in the experiments involve reinforcement ratio, tie rod and stud spacing, and connector types. Each SC wall was installed on the top of a re-usable foundation block Figure 20. Presents views of SC1 on the Foundation Block [30].
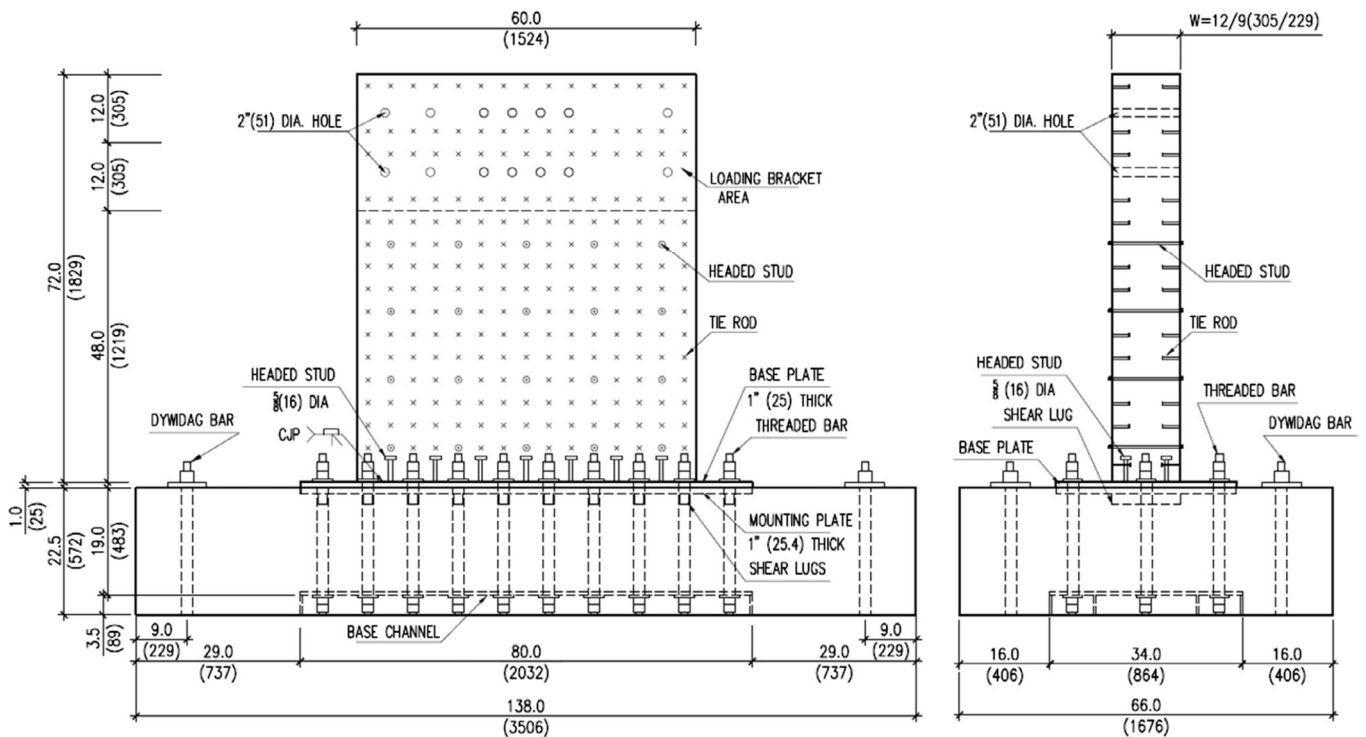
Figure 20: Elevation views of SC specimens [30]

3. FINITE ELEMENT MODELING

3.1 Introduction

Modelling of Finite Element (FE) composite wall for the development of numerical models based on experimental program was carried out. One goal of this study is to develop reliable finite element model that can simulate the behavior of composite shear wall. Based on the finite element model, a parametric study was performed to investigate the behaviour of the wall with variable steel strength, concrete strength and location/orientation of intermediate steel-concrete connectors. Further information can be found in Capital 10 (attachment).

In this study, two frames with three floors and five floors will be modeled in ABAQUS software. Then the X- shaped braces and inverted V brace is added to frames. Time history analysis, on the braced frames will be done. Later, reinforced concrete shear wall will be added to braced frames, so the steel braces encased in the reinforced concrete shear wall. This is supposed to enhance the seismic performance materials, as steel columns encased in flexural strength of the boundary walls and laminated steel braces on the web can increase shear strength. Frames behavior, before and after the addition of concrete shear wall, will be evaluated.

3.2 Material properties

3.2.1 CONCRETE MODEL

The simulations the concrete behavior in ABAQUS/CAE consists of three disparate models: the smeared cracking model, brittle cracking model and the concrete damaged plasticity model. Each model has its limitations and is useful for certain types of structures and loading conditions.

The Concrete Damage Plasticity (CDP) model [43-44] is the roughly comprehensive model and was used in the composite wall simulation of the current study. The concrete behaviour in tension, compression and cyclic loading was generally excerpted from the ABAQUS documentations [42] and presented in the following sections.

3.2.2 Behaviour of Concrete in Tension

Figure 21 shows the concrete behaviour in uniaxial loading in tension. The stress-strain response follows a linear elastic relationship until the failure stress (σ_{t0}). Beyond the failure stress, there will be a softening stress-strain response. When the concrete specimen is unloaded from any connect on the strain intenerating divide of the stress-strain curve, the unloading deal is reduced, and the elastic stiffness of the material is degraded or damaged. The degradation of the elastic stiffness is characterized by damage variable in tension (d_t), which can take value from zero, representing the undamaged material, to one, representing the total loss of strength. σ_t and σ_c are the tension and compression stresses and E_0 is the initial undamaged elastic stiffness of the material.
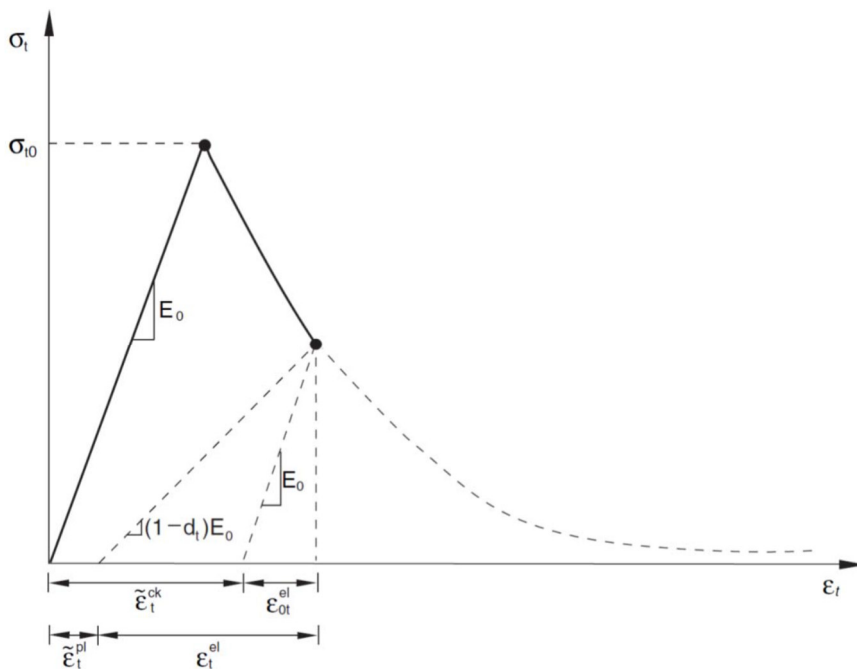
Figure 21: Response of concrete to uniaxial loading in tension [42]

The cracking strain ($\acute{\varepsilon}_t^{ck}$) is defined as the total strain (ε_t) minus the elastic strain corresponding to the undamaged material, which is:

(3.1)
$$\acute{\varepsilon}_t^{ck} = \varepsilon_t - \frac{\sigma_t}{E_0}$$

Where σ_t is tensile stress and E_0 is the initial elastic stiffness of concrete. Tension stiffening data are given in terms of the cracking strain, $\acute{\varepsilon}_t^{ck}$. The unloading data are provided to ABAQUS in terms of tensile damage curves (d_t versus $\acute{\varepsilon}_t^{ck}$) ABAQUS automatically converts the cracking strain values to plastic strain values ($\acute{\varepsilon}_t^{pl}$) using the following relationship [42]:

(3.2)
$$\acute{\varepsilon}_t^{pl} = \acute{\varepsilon}_t^{ck} - \frac{d_t}{(1 - d_t)} \frac{\sigma_t}{E_0}$$

3.2.2.1 Behaviour of Concrete in Compression

Figure 22 shows the concrete behaviour in uniaxial loading in compression. Under uniaxial compression the response is linear until the value of initial yield, σ_{c0} is reached. In the plastic regime the response is typically characterized by stress hardening followed by strain softening beyond the ultimate stress, σ_{cu}. ε_t
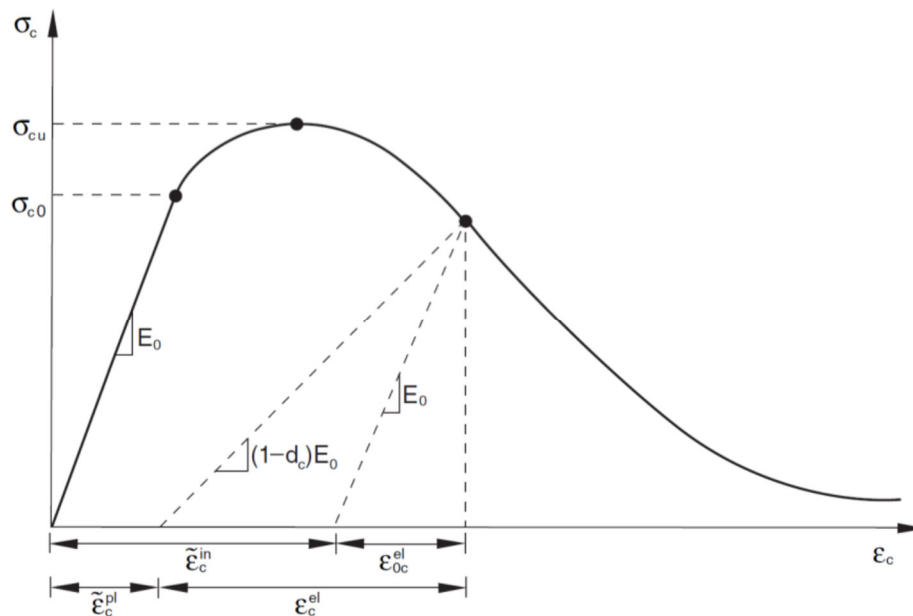
Figure 22: Response of concrete to uniaxial loading in compression [42]

The cracking strain ($\acute{\varepsilon}_t^{ck}$) is defined as the total strain (ε_t) minus the elastic strain corresponding to the undamaged material, which is:

$$(3.3) \qquad \acute{\varepsilon}_t^{ck} = \varepsilon_t - \frac{\sigma_t}{E_0}$$

Where σ_t is tensile stress and E_0 is the initial elastic stiffness of concrete. Tension stiffening data are given in terms of the cracking strain, $\acute{\varepsilon}_t^{ck}$. The unloading data are provided to ABAQUS in terms of tensile damage curves (d_t versus $\acute{\varepsilon}_t^{ck}$) ABAQUS automatically converts the cracking strain values to plastic strain values ($\acute{\varepsilon}_t^{pl}$) using the following relationship [42]:

$$(3.4) \qquad \acute{\varepsilon}_t^{pl} = \acute{\varepsilon}_t^{ck} - \frac{d_t}{(1-d_t)}\frac{\sigma_t}{E_0}$$

3.2.2.2   <u>Stress–strain Relationship in Concrete</u>

For compressive stress-strain relationship in concrete, the model proposed by Popovics was incorporated [45] to simulate the concrete behaviour in compression. In this model, the value of compressive concrete stress (f_c) is a function of concrete strain (ε_c) which can be derived from the following equation:

$$(3.5) \qquad \frac{f_c}{\hat{f}_c} = \frac{n(\varepsilon_c/\varepsilon_0)}{n - 1 + (\varepsilon_c/\varepsilon_0)^{nk}}$$

where,

f'_c = ultimate compressive strength of concrete

n = a curve-fitting factor (can be taken as $n = 0.8 + \frac{f'_c}{17}$ or $n = \frac{E_c}{E_c - E'_c}$)

E_c = initial tangent modulus (can be taken as $E_c = 6900 + 3300\sqrt{f'_c}$)

ε_0 = strain when f_c reaches f'_c , $\varepsilon_0 = \frac{f'_c}{E_c}\left(\frac{n}{n-1}\right)$

E'_c = tangent modulus of concrete at f'_c , $E'_c = f'_c/\varepsilon_0$

K a factor to control the slope of the stress-strain curve:

$if \; (\varepsilon_c/\varepsilon_0) \leq 1 \Rightarrow k = 1.0$

$if \; (\varepsilon_c/\varepsilon_0) > 1 \Rightarrow k = 0.67 + \frac{f'_c}{62} \geq 1.0$

Many researchers proposed a stress-strain relationship for concrete in tension. The strain softening part (after cracking) of the model can be linear, bi-linear or reciprocal function [46-47].

Table 3.1 shows the summary of the required parameters for calculating concrete properties where ultimate concrete compressive and tensile strengths were derived from experimental testing.

f'_c MPa	n	E_c MPa	ε_0	E'_c MPa	k : if $(\varepsilon_c/\varepsilon_0)$ > 1	f'_t MPa
51.9	3.85	30,670	0.002286	22,700	1.51	4.92
48.1	3.63	29,790	0.002229	21,580	1.45	4.68
40.2	3.16	24,500	0.002401	16,740	1.32	4.75
35.7	2.90	26,620	0.002047	17,440	1.25	3.28

Table 3.1: The summary of the concrete parameters

3.2.3   Steel Model

The steel properties that were obtained from the tensile coupon tests are nominal (engineering) stress and strain values. These nominal values were defined in terms of the initial sectional area and gauge length of the coupon. The ABAQUS software for finite element analysis uses true (Cauchy) stress and logarithmic strain. The true stress (σ_{true}) and logarithmic plastic strain (ε_{ln}^{pl}) can be derived from the tensile coupon data using the following equations [43]:

$$\sigma_{true} = \sigma_{nom}(1 + \varepsilon_{nom}) \qquad \textbf{(3.6)}$$

and

$$\varepsilon_{ln}^{pl} = ln(1 + \varepsilon_{nom}) + \frac{\sigma_{true}}{E} \qquad \textbf{(3.7)}$$

where, σ_{nom} is the nominal stress, ε_{nom} is the nominal strain and the E is the modulus of elasticity obtained from tensile coupon tests. A comparison between true and engineering stress-strain for high strength and mild strength steel are presented in Figures 23 and 24, respectively.
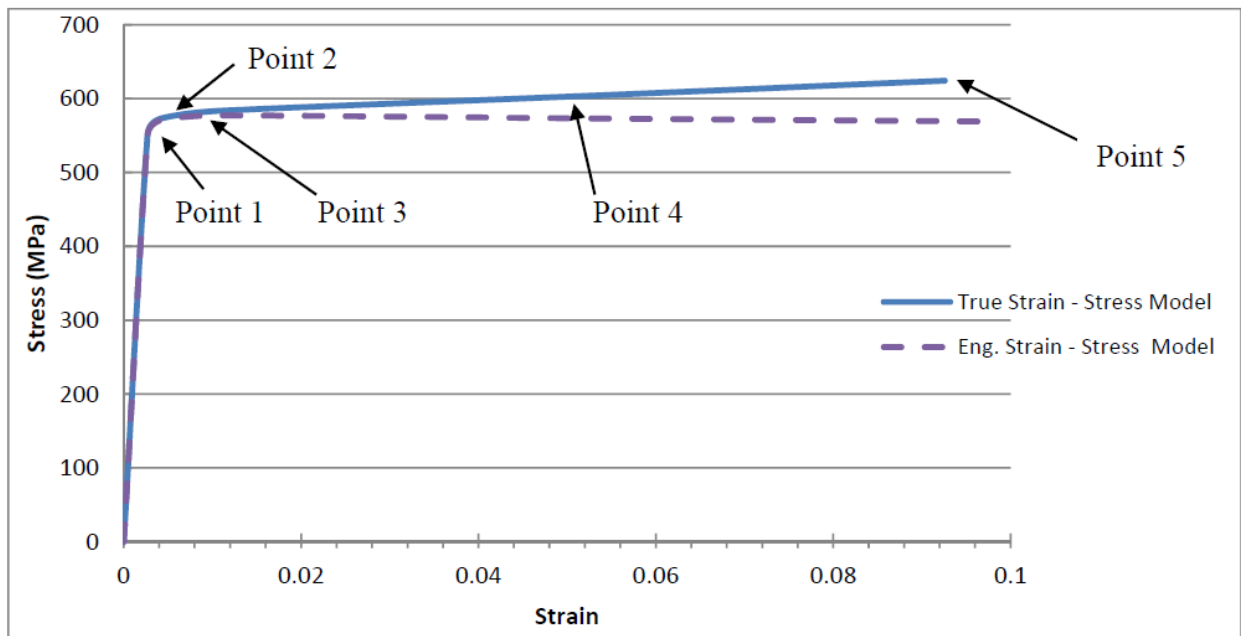
Figure 23: Comparison of true and engineering stress-strain for high strength steel
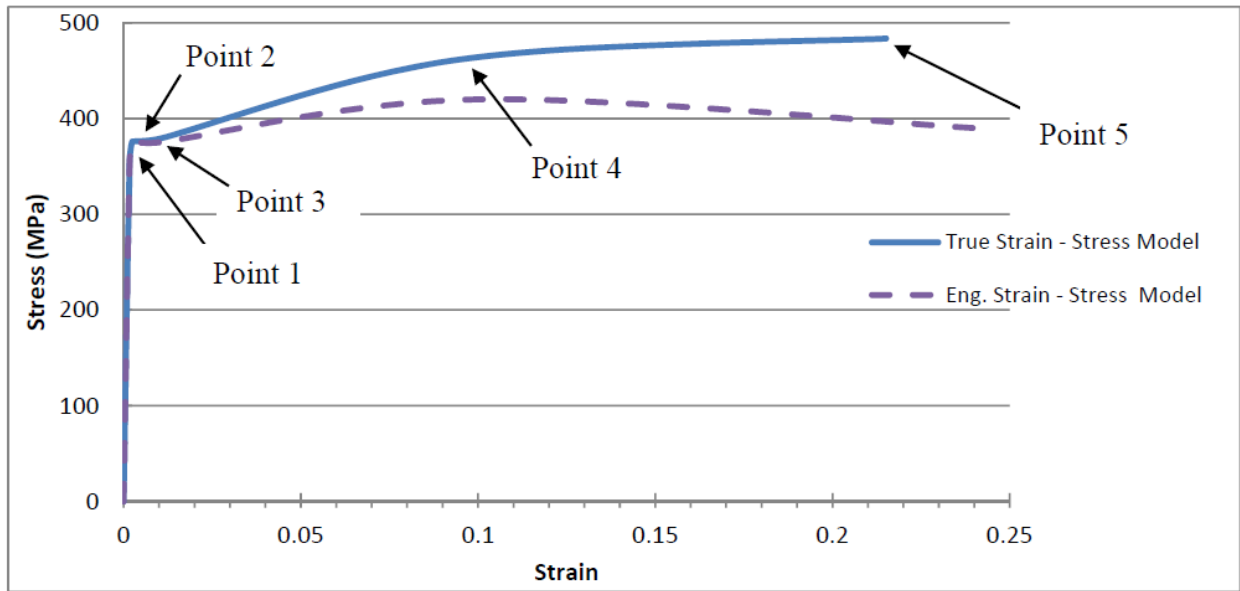
Figure 24: Comparison of true and engineering stress-strain for mild strength steel

The von-Mises yield surface criterion was utilized in ABAQUS/Explicit to specify the start of plastic flow in the state of multi axial stress. It was defined by giving the value of the uniaxial true stress as a function of uniaxial equivalent plastic strain at five points.

The summary of the results from the tensile coupon tests which were incorporated in the finite element model are presented in Table 3.2. True stress-plastic strain based on tensile coupon test results for ABAQUS model

Steel type	True stress & Plastic strain	Point 1 (yield)	Point 2	Point 3	Point 4	Point 5 (rupture)
High strength steel Fy = 552 Mpa E = 202,940 Mpa	True stress (MPa)	553.5	572.3	582.8	603.7	624.2
	Plastic strain	0.0	0.001184	0.007090	0.048682	0.089516
Mild strength steel Fy = 354 Mpa E = 206,980 Mpa	True stress (MPa)	354.6	375.9	378.8	462.0	483.6
	Plastic strain	0.0	0.000685	0.008125	0.093084	0.212781
F_y = Yield strength of profiled steel sheet; and E = Modulus of elasticity						

Table 3.2: True stress-plastic strain based on tensile coupon test results for ABAQUS model

3.3 RECORD SELECTION AND SCALING ACCORDING TO THE EUROCODE-8

3.3.1 STANDARD DESIGN SPECTRUM

Based on Eurocode-8 Part 1 [48], the elastic response spectrum, Sa (T), can be defined by Eq. (3.8).

$$(3.8) \qquad S_a(T) = \begin{cases} a_g S[1 + (\eta 2.5 - 1)] & 0 \leq T \leq T_B \\ a_g S \eta 2.5 & T_B \leq T \leq T_B \\ a_g S \eta 2.5 \left[\dfrac{T_C}{T}\right] & T_C \leq T \leq T_D \\ a_g S \eta 2.5 \left[\dfrac{T_C T_D}{T^2}\right] & T_D \leq T \leq 4s \end{cases}$$

Where T stands for the vibration period of a linear SDOF system; S is the soil factor; T_B , T_C are the limiting periods of the constant spectral acceleration branch; T_D is the value defining the beginning of the constant displacement response range of the spectrum; η is the damping correction factor with a reference value of $\eta = 1$ for 5% viscous damping;

a_g is the design ground acceleration on type A ground which is defined according to seismic hazard level of the site. In this study, a_g a is chosen as 0.35g.

The values of the periods T_B , T_C and T_D and of the soil factor S describing the shape of the elastic response spectrum depend upon the ground type. In Table 3.3, the specific values That determine the spectral shapes for type 1 spectra have been listed and the resulting spectra, normalized by a_g , plotted in Figure. 25.

Ground type	S	T_B	T_C	T_D
A	1.0	0.15	0.4	2.0
B	1.2	0.15	0.5	2.0
C	1.15	0.2	0.6	2.0
D	1.35	0.2	0.8	2.0
E	1.4	0.15	0.5	2.0

Table 3.3: Values of the parameters describing the recommended Type 1 spectral shape according to EC8
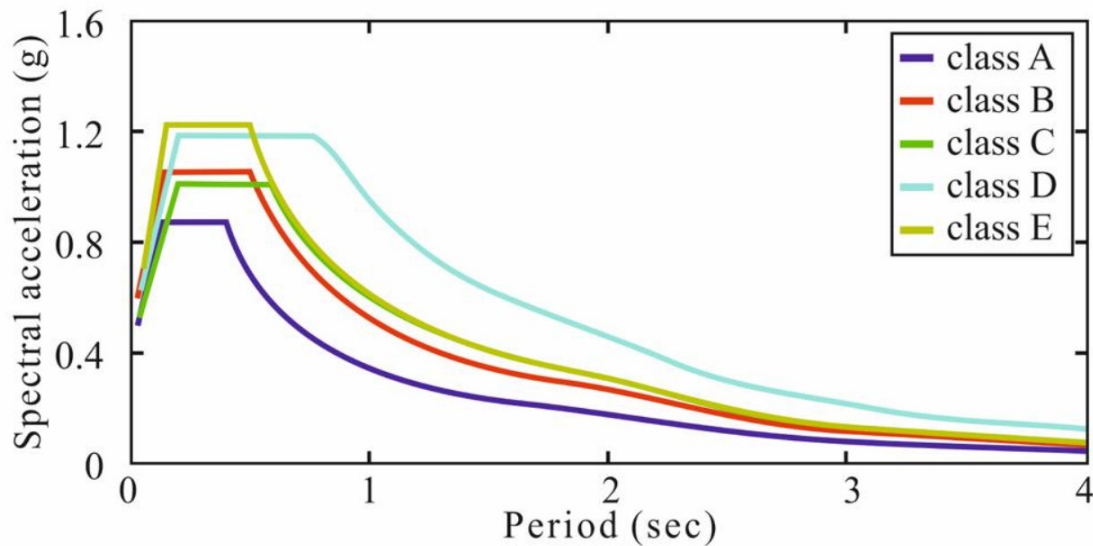
Figure 25: Elastic response spectra for different site soil classes, based on the EC8

3.3.2 Selection and Scaling Process Based on Eurocode-8

According to Eurocode-8 Part 1[48], which concerns buildings, the set of accelerograms, regardless if they are natural, artificial and simulated, should match the following criteria [48]:

a) a minimum of 3 accelerograms should be used.

b) the mean of the zero-period spectral response acceleration values (calculated from the individual time histories) should not be smaller than the value of $a_g\ S$ for the site in question.

c) in the range of periods between 0.2T and 2T, where T is the fundamental period of the structure in the direction where the accelerogram will be applied; no value of the mean 5% damping elastic spectrum, calculated from all time histories, should be less than 90% of the corresponding value of the 5% damping elastic response spectrum.

As well, the code permits the consideration of the mean effect on the structure, rather than the maximum, if at least seven non-linear time history analysis are performed. In the case of spatial structures, the seismic motion shall consist of three simultaneously acting accelerograms representing the three spatial components of the shaking. However, the vertical component of the seismic action should be taken into account only in special cases, as long span elements, not applying to most common structures [49]. Because of that, sets for analysis of joint spatial structures are made up of 14 records. The code also specifies that the same accelerograms may not be used concurrently along both horizontal directions, but it does not clear up the selection and scaling process for this instance.

Eurocode-8 Part 2 [50], which concerns bridges, states the requirements for the horizontal seismic input for dynamic analysis which are somehow similar to those for buildings. In this Part, time history analysis is permitted when at least three pairs of horizontal accelerograms are used. The selection and scaling process can be summarized as follows [50]:

a) For each earthquake record, the SRSS spectrum shall be established by taking the square root of the sum of squares of the 5% damped spectra of each two horizontal components.

b) The SRSS spectra shall be scaled and averaged so that the mean-scaled spectrum is not lower than 1.3 times the 5% damped elastic spectrum of the design seismic action, in the period range between 0.2T and 1.5T, where T is the natural period of the fundamental mode of the structure.

The selection and scaling process performed based on EC8 Part 1. Three pairs of records are selected. Then the horizontal components of each record are scaled with same scale factor. Selected records summarized in Table 3.4.

Record	Direction	Earthquake Magnitude	Distance (km)	DT (sec)	PGA (cm/sec^2)	PGV (cm/sec)	PGD (cm)
Imperial Valley, 1940, El Centro	X	6.9	10	0.02	452.03	62.40	27.73
Imperial Valley, 1940, El Centro	Y	6.9	10	0.02	662.88	59.89	14.28
Loma Prieta, 1989, Gilroy	X	7	12	0.02	652.49	79.14	28.30
Loma Prieta, 1989, Gilroy	Y	7	12	0.02	950.93	56.02	16.45
Northridge, 1994, Sylmar	X	6.7	6.4	0.02	558.43	80.19	17.33
Northridge, 1994, Sylmar	Y	6.7	6.4	0.02	801.44	118.93	26.90

Table 3.4: Selected Records

Figures 26 to 31 shows horizontal components of each record (orthogonal directions).
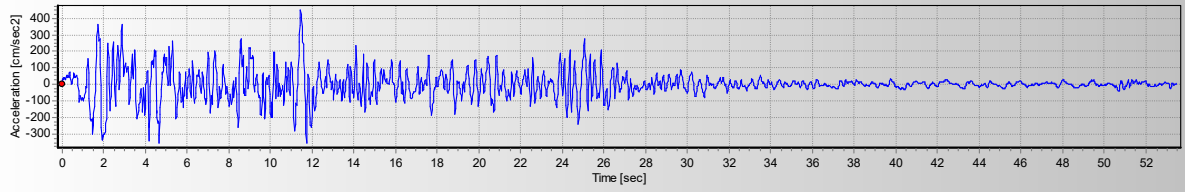
Figure 26: Elcentro record, x direction
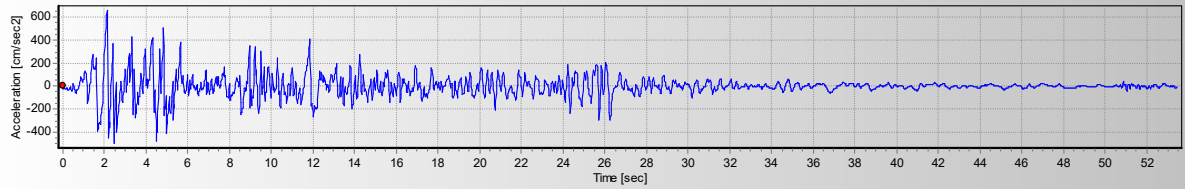
Figure 27: Elcentro record, y direction
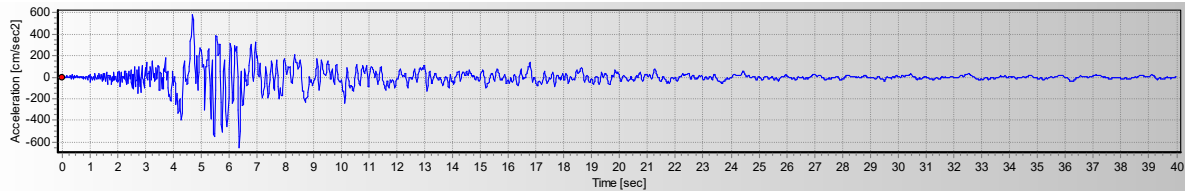
Figure 28: Loma Prieta record, x direction
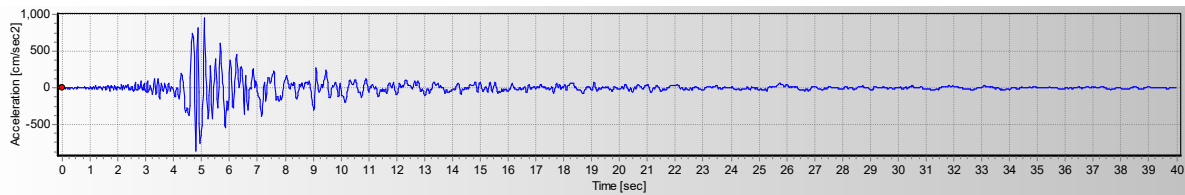
Figure 29: Loma Prieta record, y direction
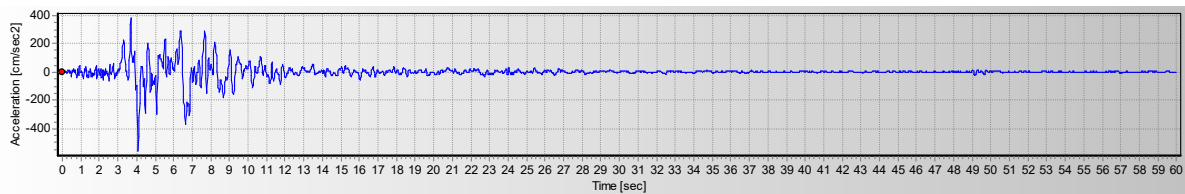
Figure 30: Northridge record, x direction
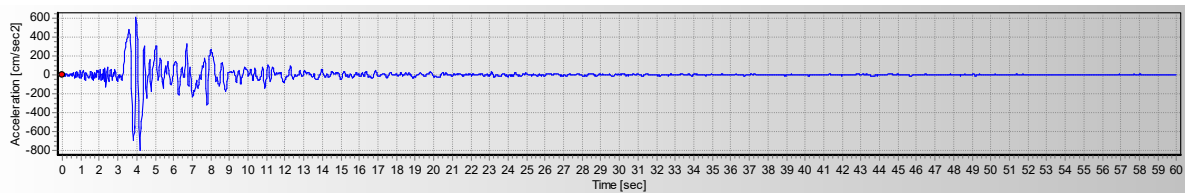
Figure 31: Northridge record, y direction

The scaling process performed based on EC8 Part 1, shows in Figure 32 with 5% viscous damping, Type 1 ground type B, importance class II, Earthquake were scaled to 0.35g.
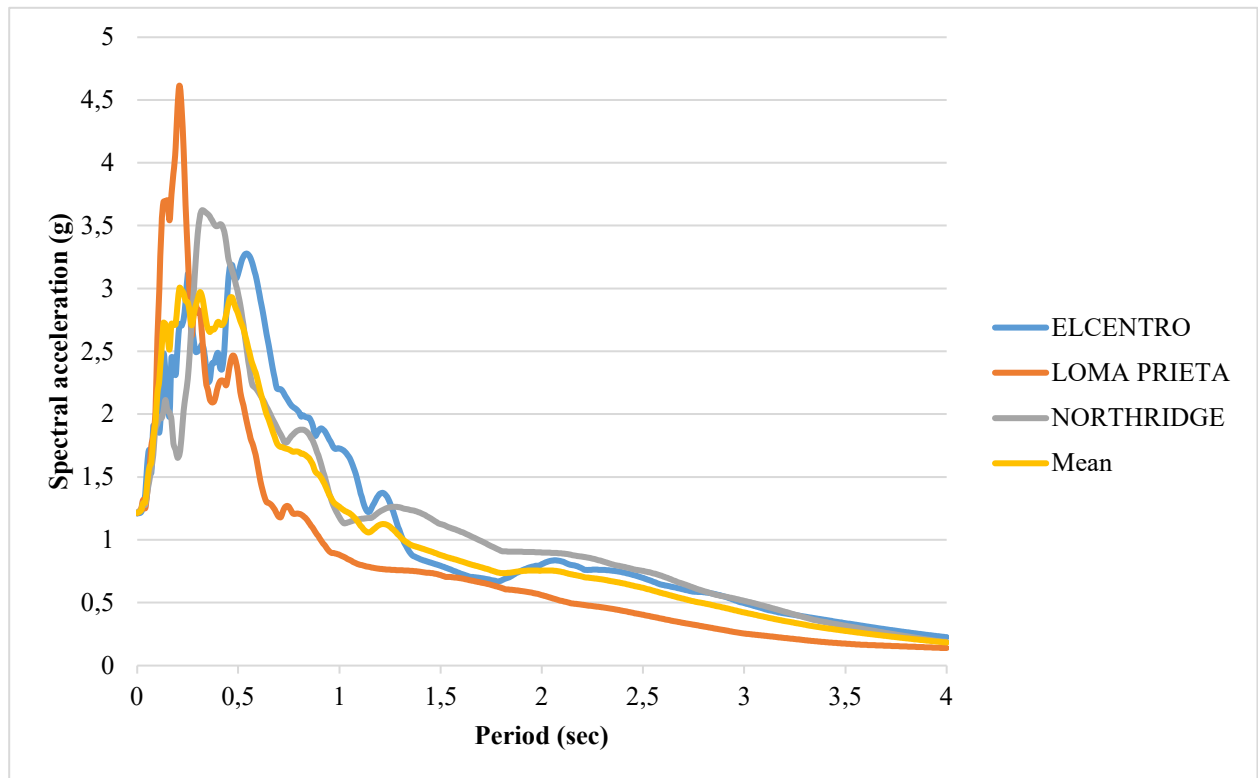
Figure 32: Ground motion spectra

3.4 Description of The FE Model

3.4.1 VERIFICATION

FEM is a numerical solution method. In finite element method, the geometric model devided into smaller components called elements and analysis based on the elements of division were done on model. Each element is made of nodes which input, and output values assigned to them. Each element is presented with a shape function. This function can be a linear function or nonlinear (quadratic or above). When analyzing a model with finite element method, a large number of equations must be solved; Therefore user must be able to see it properly according to the type of issue, degrees of freedom, boundary conditions, initial conditions, loads and etc., geometric model divided into a number of elements or the so-called mesh. To investigate the behavior of composite steel shear walls, a suitable mathematical model is required. According to features that have finite element method to solve complex problems; in this study, finite element method is used for Verification.

Here we try to simulate the results of a laboratory experiment with program ABAQUS. This test program consists of 2 parts. In Parts 1 and 2 7 to 8 copies were tested.

The samples in phase-I included five- CSPSW specimens with pinned beam-column connections, one specimen with rigid moment frame, one specimen with SPSW and the last one with CSPSW with fixed beam–column connections. All of the specimens in phase-I were built with 1:4 scale, the specimens in phase-II comprise four 1:3 scale single-bay three-storey and 1:4 scale single-bay one-storey frames. All the specimen in phase-II were CSPSW, Figure 33. Before testing, all models were analyzed by push-over analysis to evaluate yield displacement and the gap size around the RC panel.
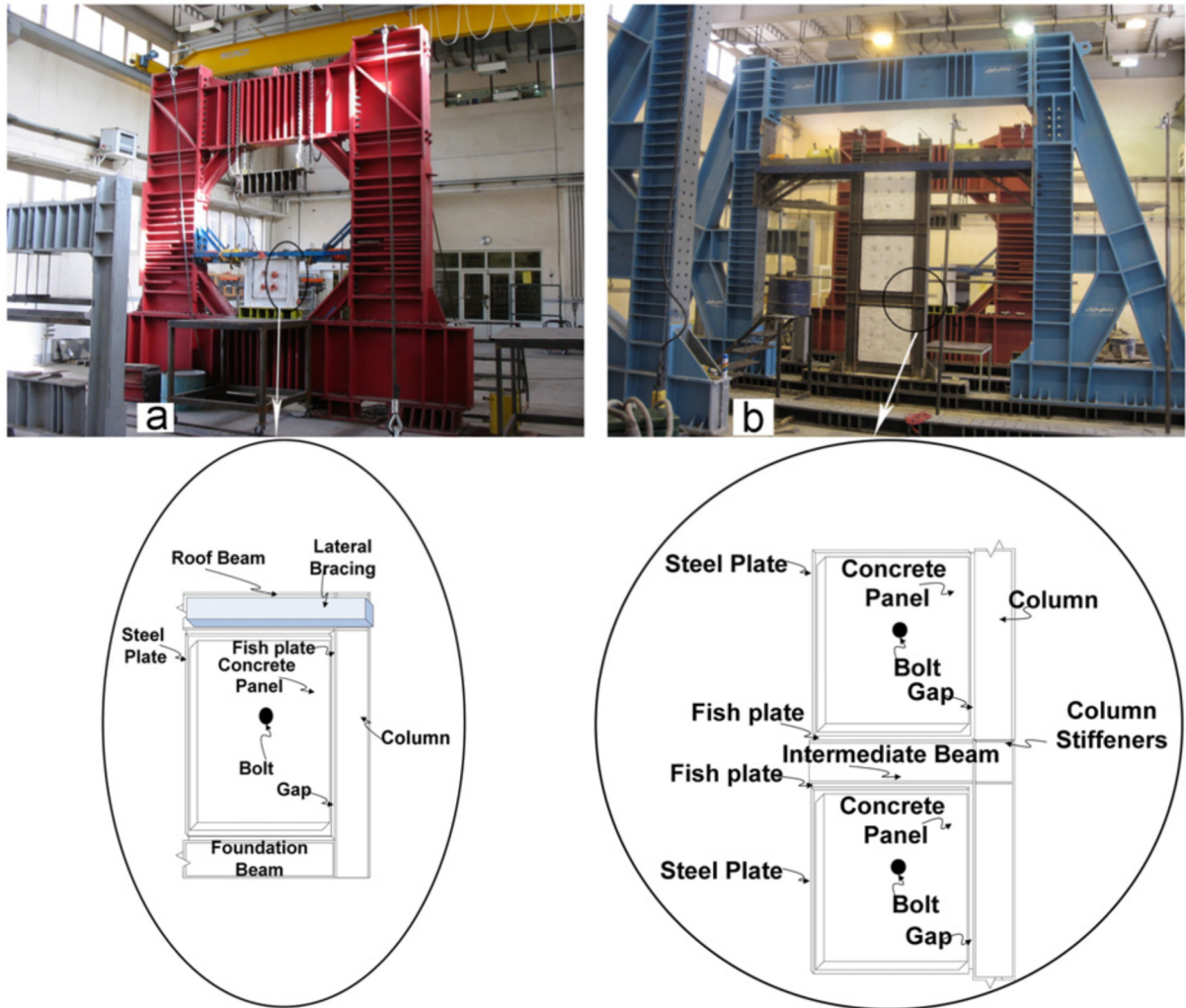
Figure 33: (a) Setup experimental of one-storey specimens and (b) setup experimental of three-storey specimens [51]

Figure. 34 shows a schematic view of the experimental setup. Model details and their characteristics are described in Table 3.5. The main components of the test's setup included: reaction frame, H-shape beam, lateral bracing, actuators and specimen. In order to secure the specimen to the strong floor during the test, it was attached to a strong H-shape beam, which was bolted to the strong floor by high strength bolts. The beam and column were connected directly by the groove welding. The steel plate was welded continuously to the fish plate, which in turn was welded continuously to the boundary frame. Fish plate connection, which was used for the connection of infill plates to the inside flanges of boundary frame in the test specimens, was designed based on an infill plate shear capacity. [51]. The bolts and reinforcing bars were brought to corresponding locations when the steel components were joined Next, the concrete slab produced by fine aggregate material is poured onto the steel plate.
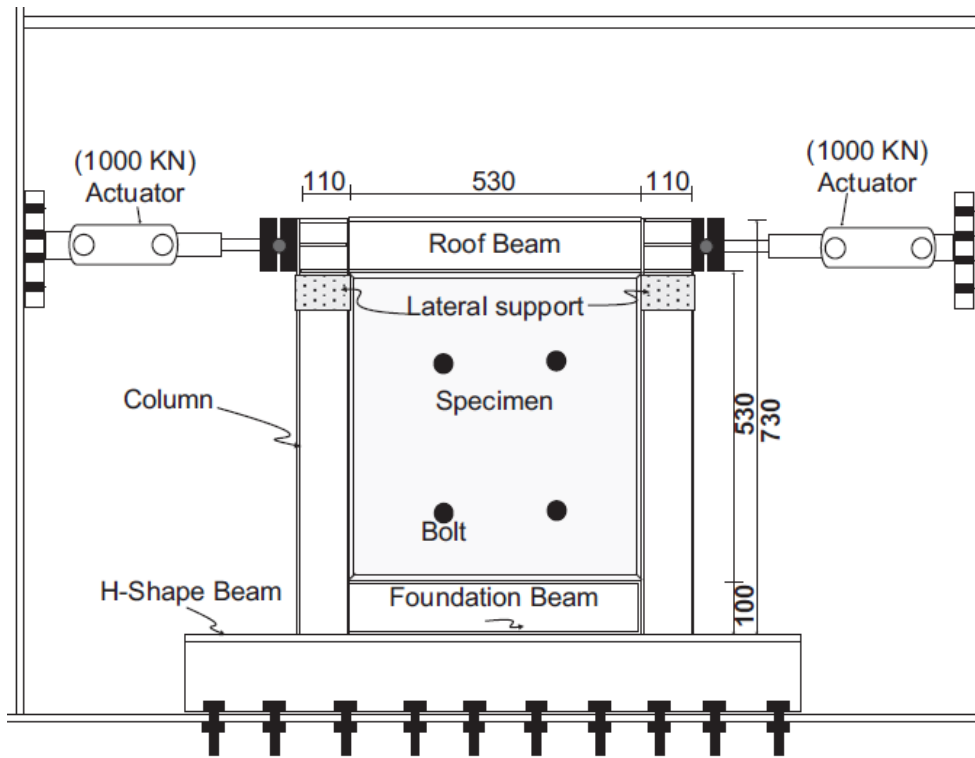
Figure 34: General setup of the one-storey test [51]

The steel plate functions as a formwork for the concrete wall in the time of the concrete casting. In this model, IPE100+2Pl100*5 section has been used for columns and IPE100 section have been for beams. In this case, steel wall plate thickness of 2 mm was used for modeling plate. Concrete elastic modulus of 210,000 MPa and maximum compressive stress of 79 MPa is considered. Steel mechanical properties are shown in Table 3.6.

Columns (mm)	2IPE100+2Pl100*5
Foundation beam (mm)	2IPE100
Roof beam (mm)	2IPE100
Steel wall plate thickness (mm)	2
Fish plate (mm)	40*5
Number of bolts	4
Bolt diameter (mm)	6
Type of bolt	10.9
Rebar diameter (mm)	3
Reinforcement ratio	1%
Concrete thickness (mm)	30
Free space around concrete (gap) (mm)	11.25

Table 3.5: Model details [51]

Section type	Yield stress F_y (MPa)	Ultimate strength F_u (MPa)
IPE100 beam Flange	308	479
IPE100 beam web	285	446
Steel Plate	268	415
Rebar and Connector	336	492

Table 3.6: Steel properties. [51]

To connect the boundary frame to each other in the five hinged specimens, half-flange of an IPE160 was cut-out at the end of the columns. Small triangular steel plates are welded in order to reduce sudden tearing of the steel plate at the corners Figures 36 – 37 – 38.
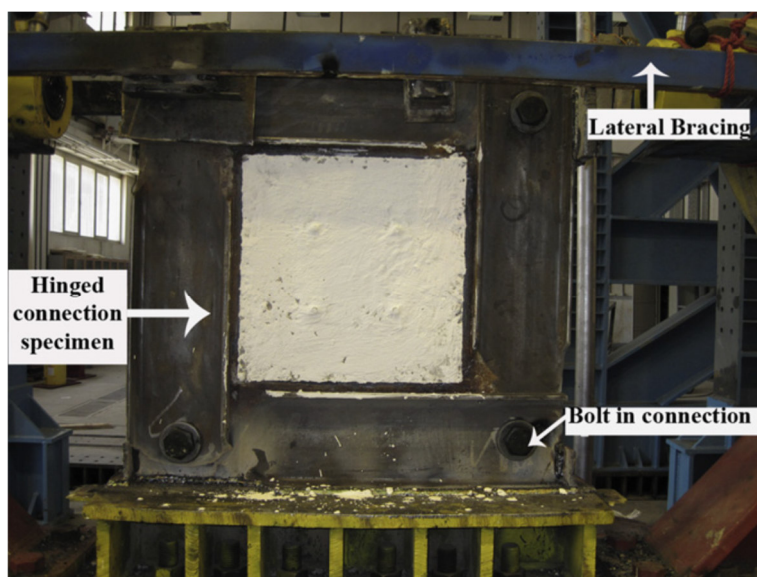
Figure 35: Hinged-connection specimen with four bolts

The specimens' height was short, so they were under pure shear approximately. The important factors including shear strength, yield and ultimate displacement, initial stiffness and ductility are given in Table 3.7 [51].

Specimen	Yield point			Maximum		Ductility	Total energy dissipation (kN m)	FE estimation
	Py (kN)	δ_y (mm)	Initial stiffness (kN/mm)	Pmax (kN)	δ_{max} (mm)	$\mu_{max}=\delta_{max}/\delta_y$ (mm)		δ_y (mm)
CS	390	4,6	85	585	26	5,65	260	6,3

Table 3.7: Behavioural characteristics of the tested specimens in Phase-I. [51]

Here we try to simulate the results of a laboratory experiment with the program ABAQUS this model consists of Steel and concrete. The steel parts to be merged to make the pieces stick together, and as a piece of memory we used it for the steel frame. But we used Tie to attach the concrete to the steel plate That is, it does not allow the junction to be moved. To attach the frame to the ground, we fixed one side of the frame completely, which is the same as the ground connection.
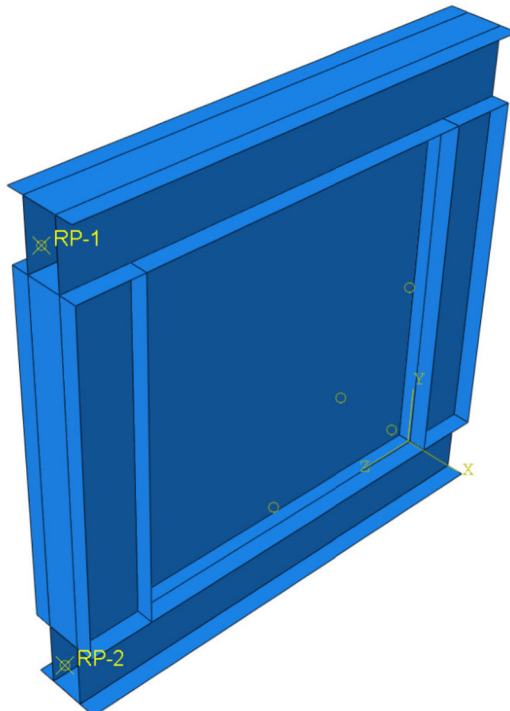
Coumns (mm)	2IPE 100
Beam (mm)	2IPE 100
Conserte thickness (mm)	15 mm
Steel Wall thickness (mm)	2 mm
Rebar diamete (mm)	3 mm

Figure 36: Shows our model with ABAQUS that corresponds to all laboratory test properties
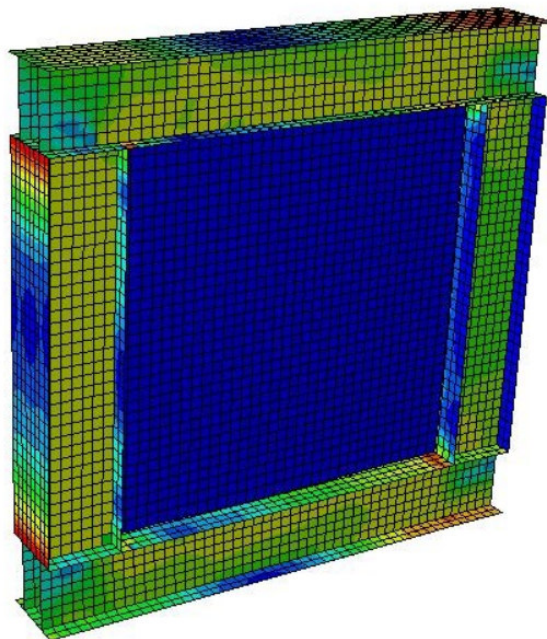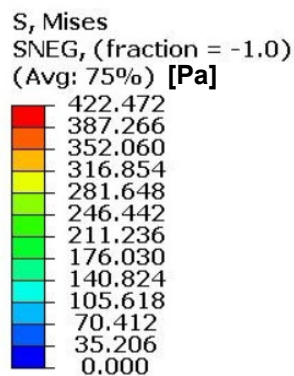
Figure 37: Mises tension

Columns
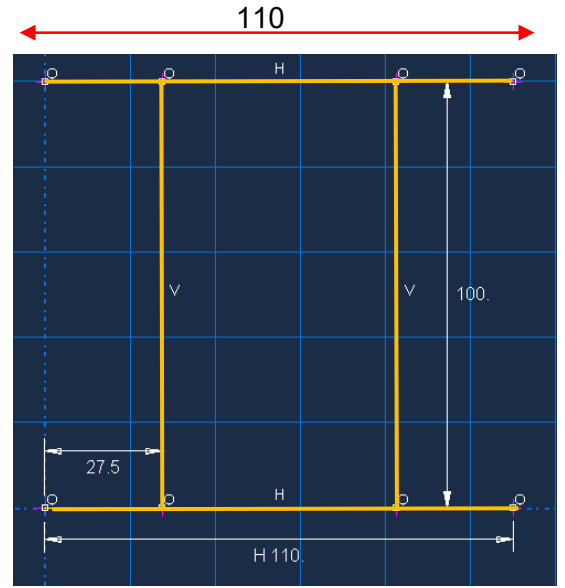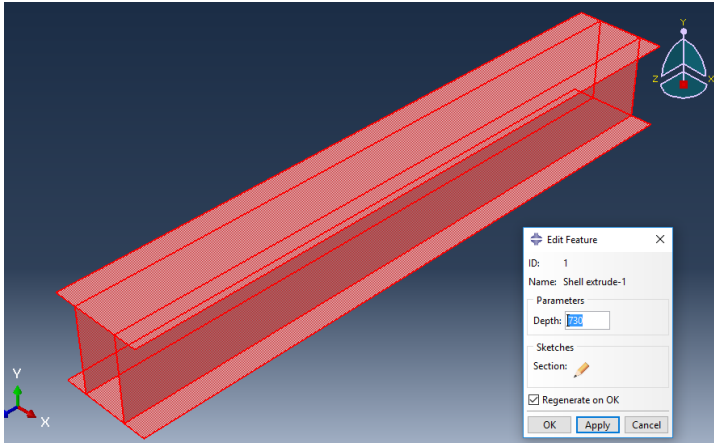
Steel Plate
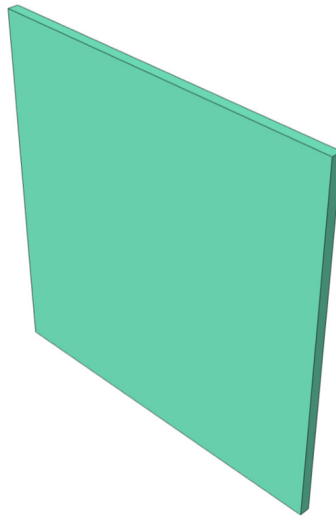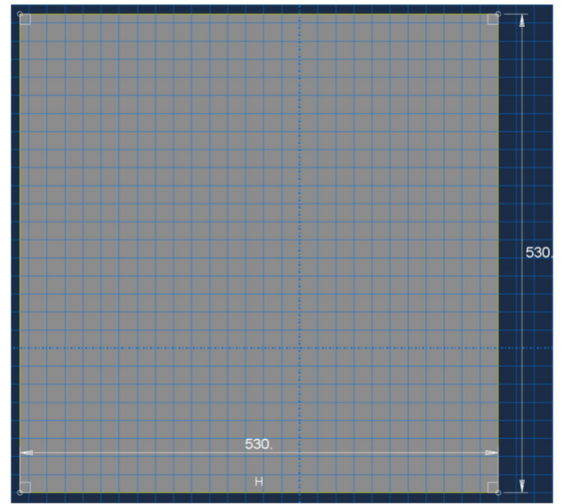
Concrete
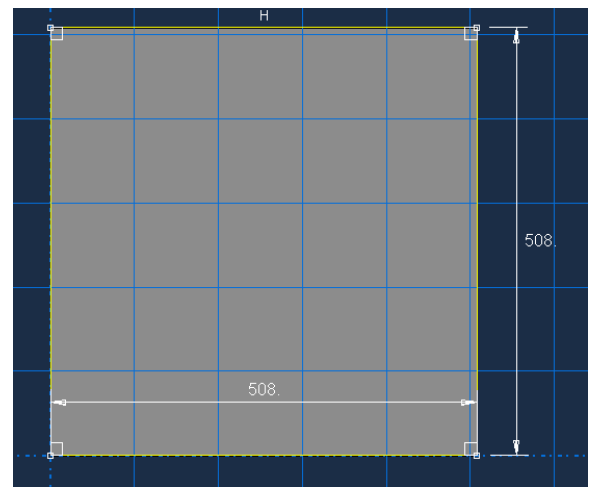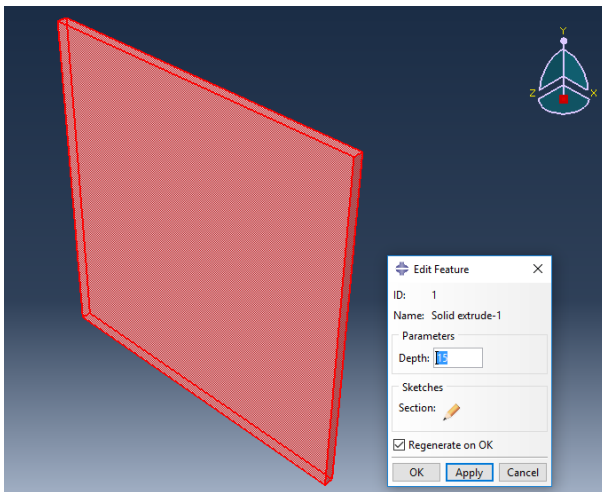
Figure 38: Section type our model with ABAQUS

Figure 39 shows the hysteresis loop curve for experimental sample and Figure 40 shows, the hysteresis loop curve for numerical model. As can be seen, the numerical model is good agreement with experimental sample.
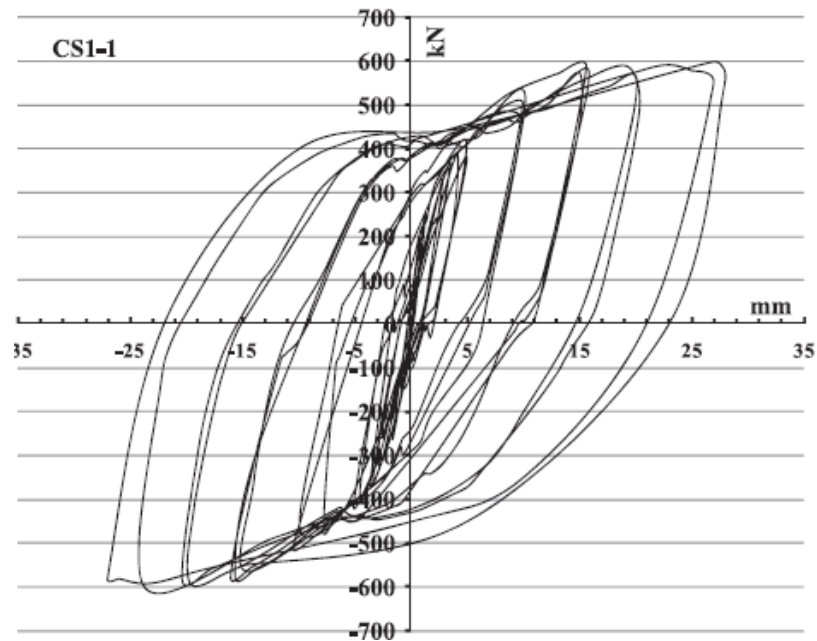
Figure 39: Lateral load vs. displacement (hysteresis loop) of the one-storey specimens [51]
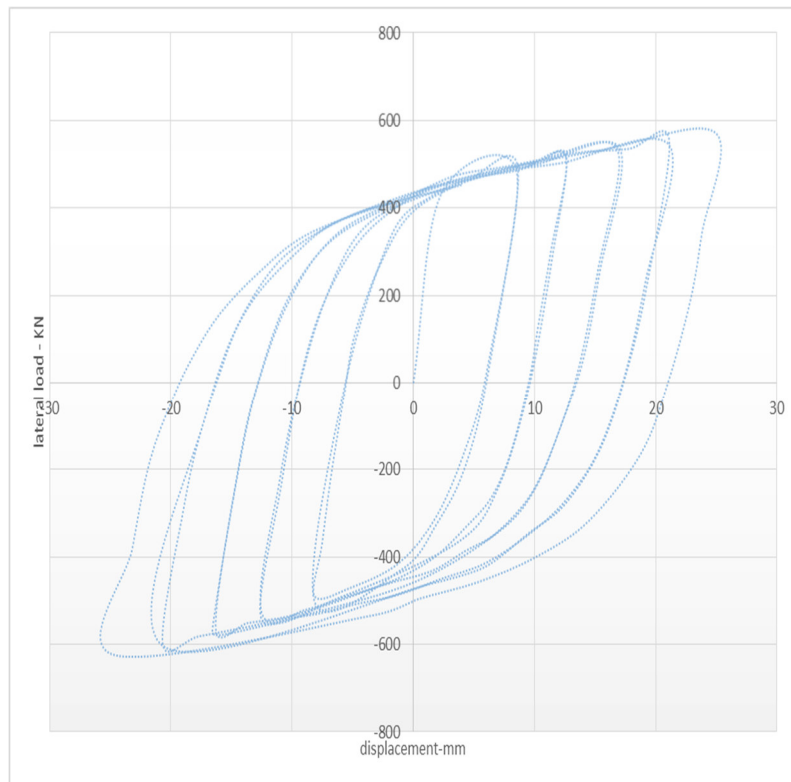
Figure 40: Hysteresis loop of the model simulated in ABAQUS

3.4.2 Model Specification

Two three-storey and five-storey frames was designed with the EC. Each frame consists of three span. Shear wall located at the mid span. Two wall specimens were designed, having an encased steel X-brace and V brace. The two specimens had identical geometry. Each wall was 3000 mm tall. A flanged wall section was intentionally used to ensure that the walls fail in shear mode. The web wall majorly resisted the in-plane shear, while two flange walls majorly resisted the overturning moment. Figures. 40 shows three or five -storey frame simulated in ABAQUS. In part 4 are outlines the detail of the finite element model developed to predict the behavior of the shear wall under impact loading.to be found
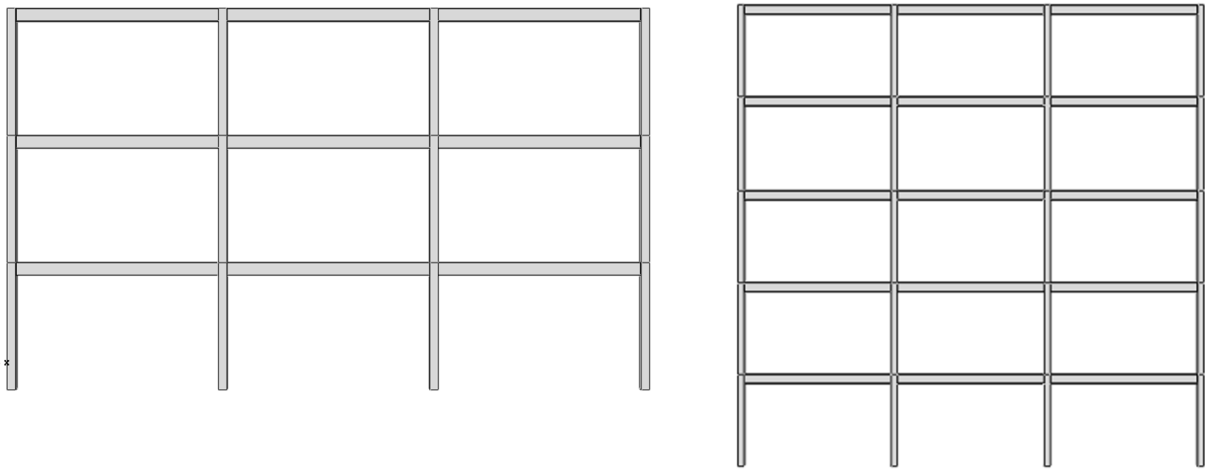
Figure 41: Three- five storey frame

4. MODELING IN ABAQUS

4.1 INTRODUTION

Earthquake is one of the most destructive factors of many building structures in different parts of the world. This phenomenon causes irreparable loses to life and property each year. However, the amount of these loses can be significantly reduced by rebuilding the building structure. This has led many researchers to perform many studies on the seismic vulnerability of structures caused by destructive earthquakes. No study has investigated the impact of using three types of braces: V, X and shear walls together and this issue that the use of which braces reinforces the structure against earthquake vibrations. That is why this study will examine the effect of these reinforcements under different earthquakes.

In this thesis, the structure of 3 and 5-storey buildings under the influence of various earthquakes, are examined using sequential accelerograms installed in the areas ELCENTRO, LOMA PRIETA and NORTHRIDGE. Then two types of V and X braces and a shear wall are used to retrofit the building and prevent the damage the plastic zone.

4.2 1940 EL CENTRO Earthquake

The 1940 El Centro earthquake (or 1940 Imperial Valley earthquake) occurred at 21:35Pacific Standard Time on May 18 (05:35 UTC on May 19) in the Imperial Valley in southeastern Southern California near the international border of the United States and Mexico. It had a moment magnitude of 6.9 and a maximum perceived intensity of X (Extreme) on the Mercalli intensity scale. It was the first major earthquake to be recorded by a strong-motion seismograph located next to a fault rupture. The earthquake was characterized as a typical moderate-sized destructive event with a complex energy release signature. It was the strongest recorded earthquake to hit the Imperial Valley, and caused widespread damage to irrigation systems and led to the deaths of nine people.[52]

Figure 42: Collapsed buildings in Imperial, California, in which four people died [52]

4.3 1994 NORTHRIDGE Earthquake

The 1994 Northridge earthquake was happened on January 17 1994 at 4:30:55a.m.PST in the San Fernando Valley region of the County of Los Angeles Its epicenter was in Reseda, a neighborhood in the north-central Valley. The quake had a duration of approximately 10–20 seconds, and its peak ground acceleration of 1.8g(16.7 m/s2) was the highest ever instrumentally recorded in an urban area in North America. Strong ground motion was felt as far away as Las Vegas, Nevada, about 220 miles (360 km) from the epicenter. The velocity at the Rinaldi Receiving Station was 183 cm/s (4.09 mph or 6.59 km/h), the fastest ever recorded.

Two 6.0 Mw aftershocks followed, the first about one minute after the initial event and the second approximately 11 hours later, the strongest of several thousand aftershocks in all. The death toll was 57, with more than 8,700 injured. In addition, property damage was estimated to be between $13 and $50 billion, making it one of the costliest natural disasters in U.S. history.[53]

Figure 43: Kaiser Permanente building [53]

4.4   1989 LOMA PRIETA Earthquake

The 1989 Loma Prieta earthquake occurred in Northern California on October 17 at 5:04 p.m.local time (1989-10-18 00:04 UTC). The shock was centered in Park approximately 10 mi (16 km) northeast of Santa Cruz on a section of the San Andreas Fault System and was named for the nearby Loma Prieta Peak in the Santa Cruz Mountains. With a moment magnitude of 6.9 and a maximum Mercalli intensity of IX (Violent), the shock was responsible for 63 deaths and 3,757 injuries. The Loma Prieta segment of the San Andreas Fault System had been relatively inactive since the 1906 San Francisco earthquake (to the degree that it was designated a seismic gap) until two moderate foreshocks occurred in June 1988 and again in August 1989.[54]

Figure 44: Image of collapsed double-decker freeway structure in Oakland, California [54]

4.5   3D Modeling of building structures

Wire elements are used to model building structures. Two-dimensional view of a three-storey building can be seen in Figure 45 and 46 Each storey is three meters high. Also, in this figure, the three-dimensional view of the building is shown in as normal and with two modes of brace and shear wall. The same sizes and dimensions are used to construct a five-storey building. Figure 47 shows a 5-storey building structure.
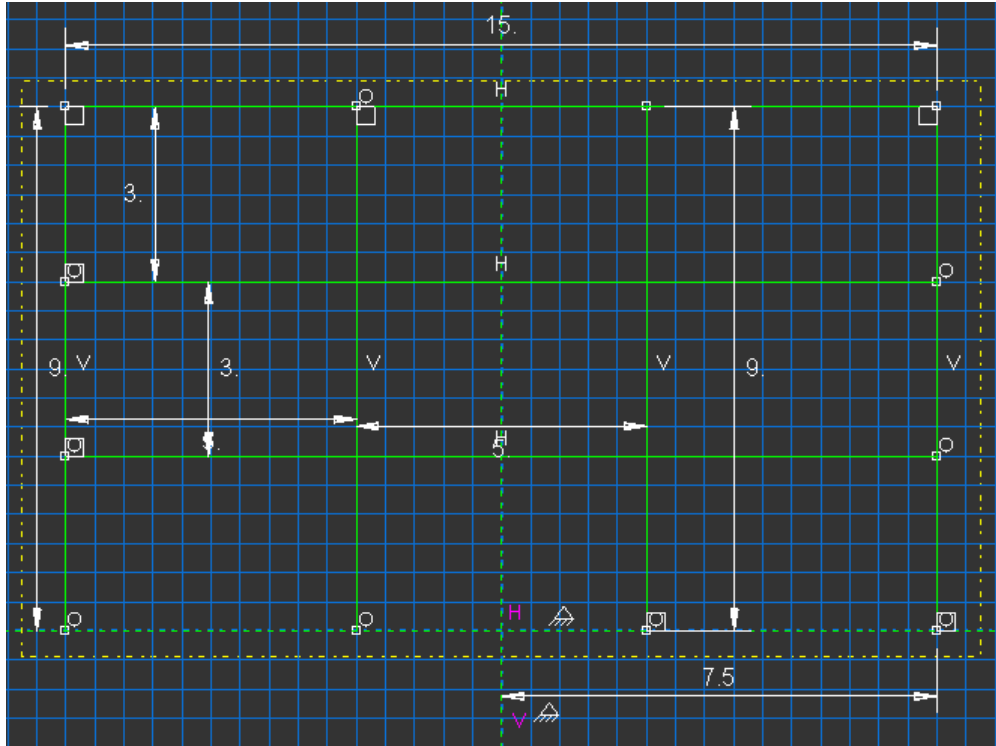
Figure 45: Dimensions and sizes used to model three-storey building
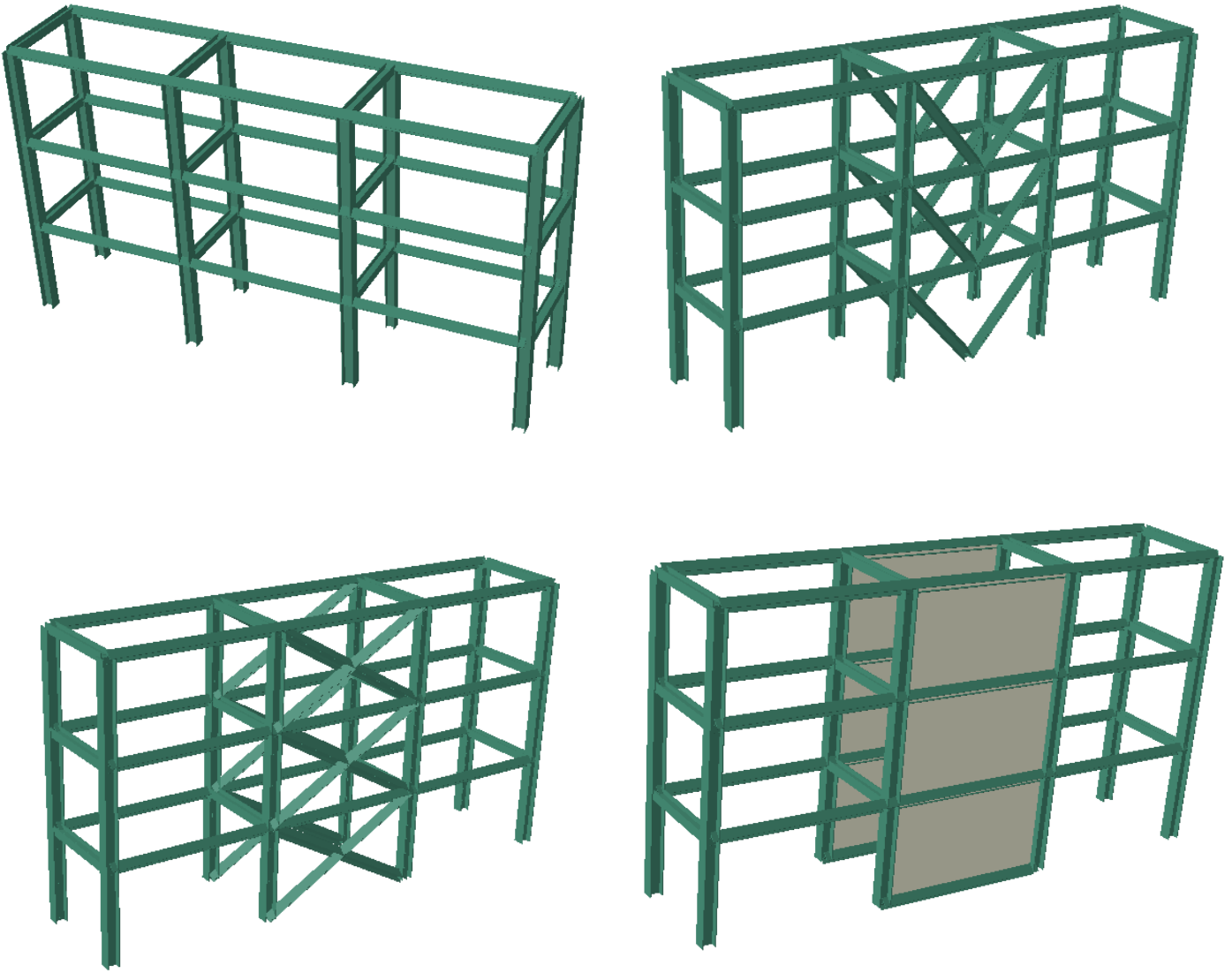
Figure 46: Dimensions and sizes used to model three-storey building
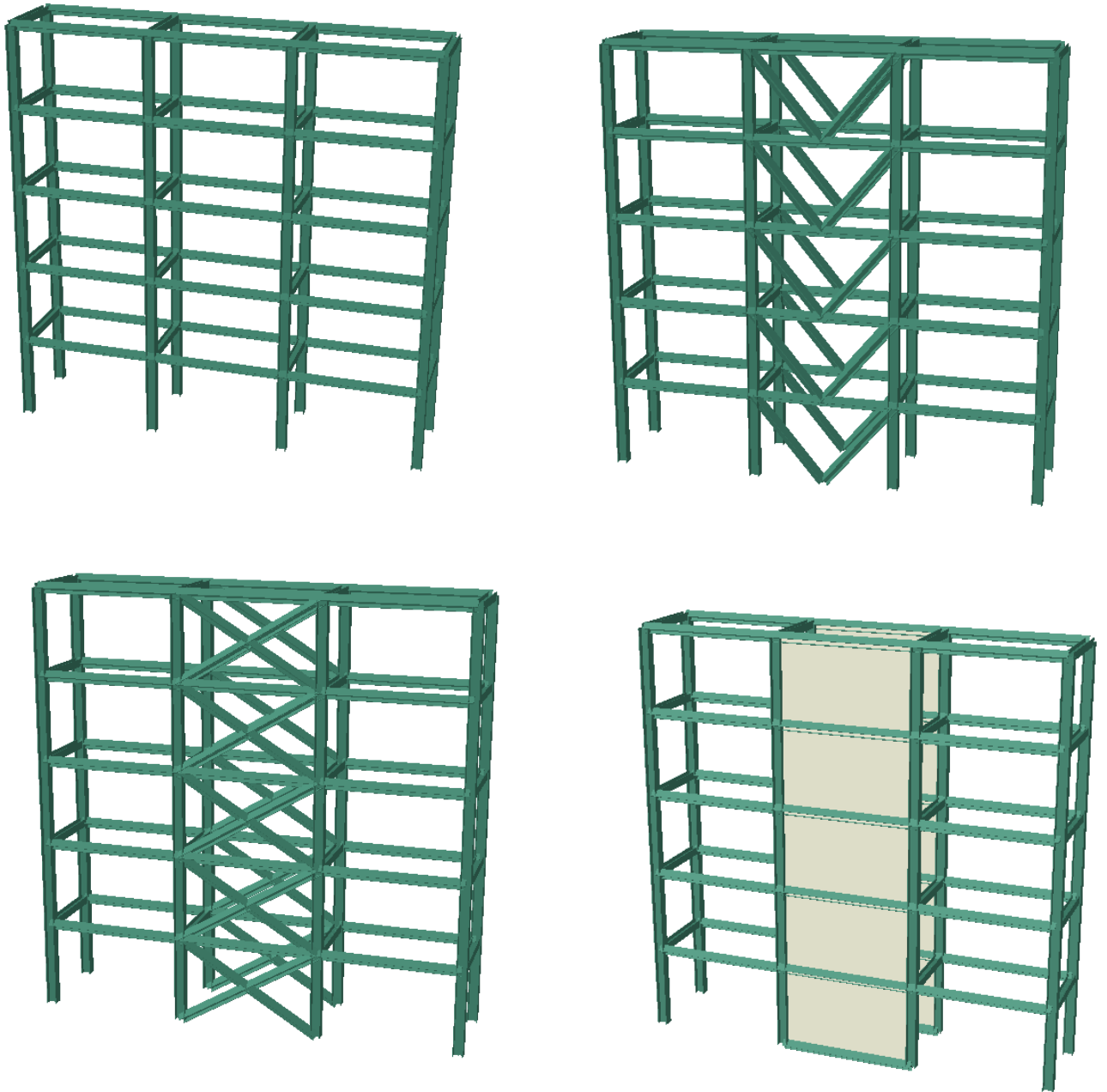
Figure 47: Three-dimensional model of five-storey building

in Abaqus, there are three ways to apply ground foundation:

1- Place a plate under the structure and move it to the middle of this page. Place the panel at the base of the building.

2- Connect the uprights: in this case, all the stairs of the building are connected, and the movement is applied only to the center of the floor of the building. As follows Figure 48.
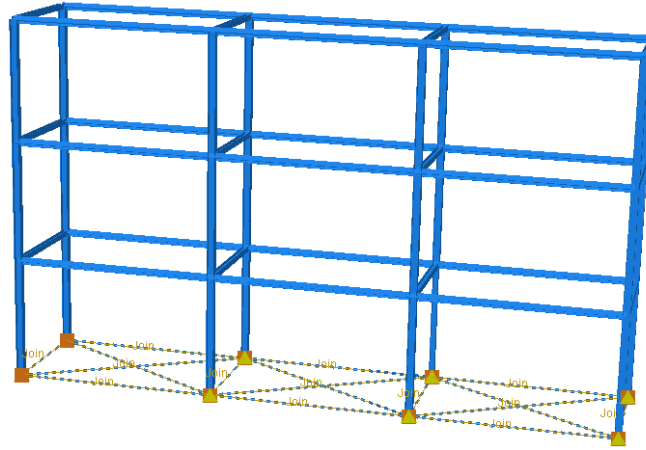
Figure 48: Ground foundation with Connect the uprights

3- the shift can be applied equally to all bases. About earthquakes applied to the foundations We actually apply the earth reaction to the foundations of the building here the earth is eliminated and only the earth reaction which is applied to the base the same times the seismometers register This case study was used in this study.

As follows Figure 49.
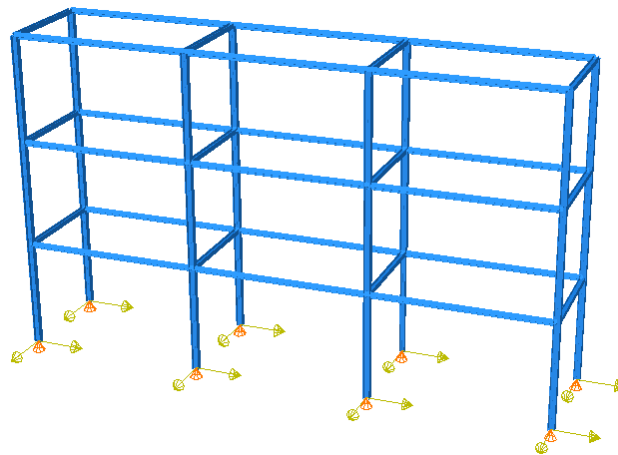
Figure 49: Ground foundation with apply equally to all bases (Columns)

to connect the profiles with each other we use in our Models tie constraint ties two separate surfaces together so that there is no relative motion between them. This type of constraint allows you to fuse together two regions even though the meshes created on the surfaces of the regions may be dissimilar. meaning Abacus generally welds these parts together itself it does not allow the junction to move.

4.6 Profiles and mechanical properties used

our models consist of two types of profiles. One type of profile was used for building columns and the other type for horizontal beams and building reinforcements. IPB180 profiles were used for columns and IPB140 profiles for horizontal ones. In order to define the mechanical properties of the building structure, steel with the following specifications is used.

Steel mechanical properties with regard to true stress and strain	
Density	8050
Elastic modulus	210 GPa
Poisson's ratio	0.3

Table 4.1: Table of the material used specifications

4.7 Load and boundary conditions

Following the complete modeling of three and five-storey buildings in Abaqus software, it is now time to apply the load and boundary conditions to the building. To this end, the acceleration recorded by the earthquake accelerometer sensors in the EL CENTRO LOMA PRIETA and NORTHRIDGE areas is applied to the building foundation. These accelerometers have recorded the accelerations applied in the directions x and y. In Figure 50, the acceleration applied in the directions x and y for the EL CENTRO area are shown.
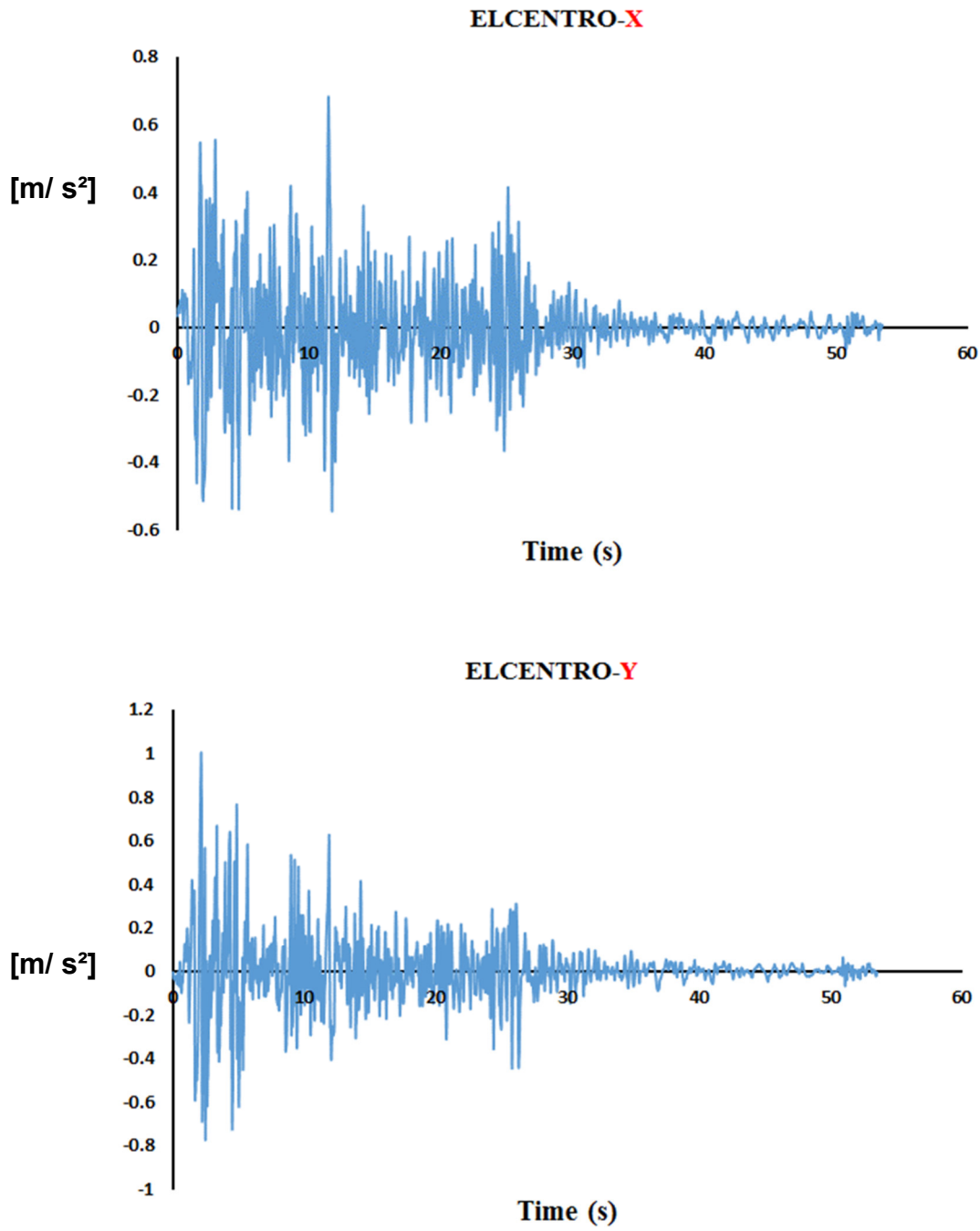
Figure 50: The earthquake applied in directions x and y to the building foundation for the Elcentro area

4.8 Finite Element analysis of three-storey building

4.8.1 EL CENTRO AREA

In the figures below, the stress contours for the three-storey building are shown, when the accelerogram is used in the El Centro area. As is evident, the building is not damaged by applying this earthquake to the structure, but a lot of force and pressure are applied to the all building Columns. By applying reinforcement to the structure of the building, the stress value is regularly reduced. In fact, by applying the V-shaped reinforcement to the structure, the stress is significantly reduced compared to the normal mode, and by applying X-shaped reinforcement, this stress will be less than that of the V-shaped reinforcement. Finally, by applying the shear wall to the structure, the stress value reaches its lowest extent, and much less stress is applied to the structure of the building than the two V and X-shaped reinforcement modes.
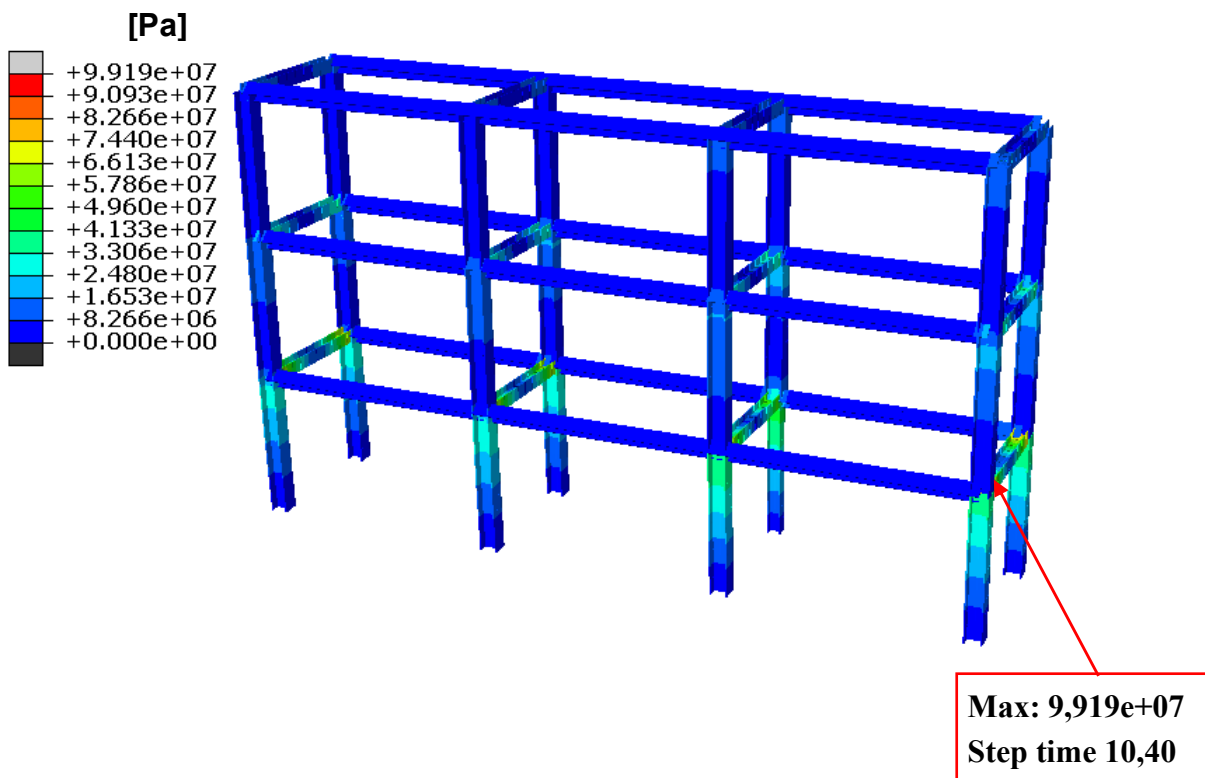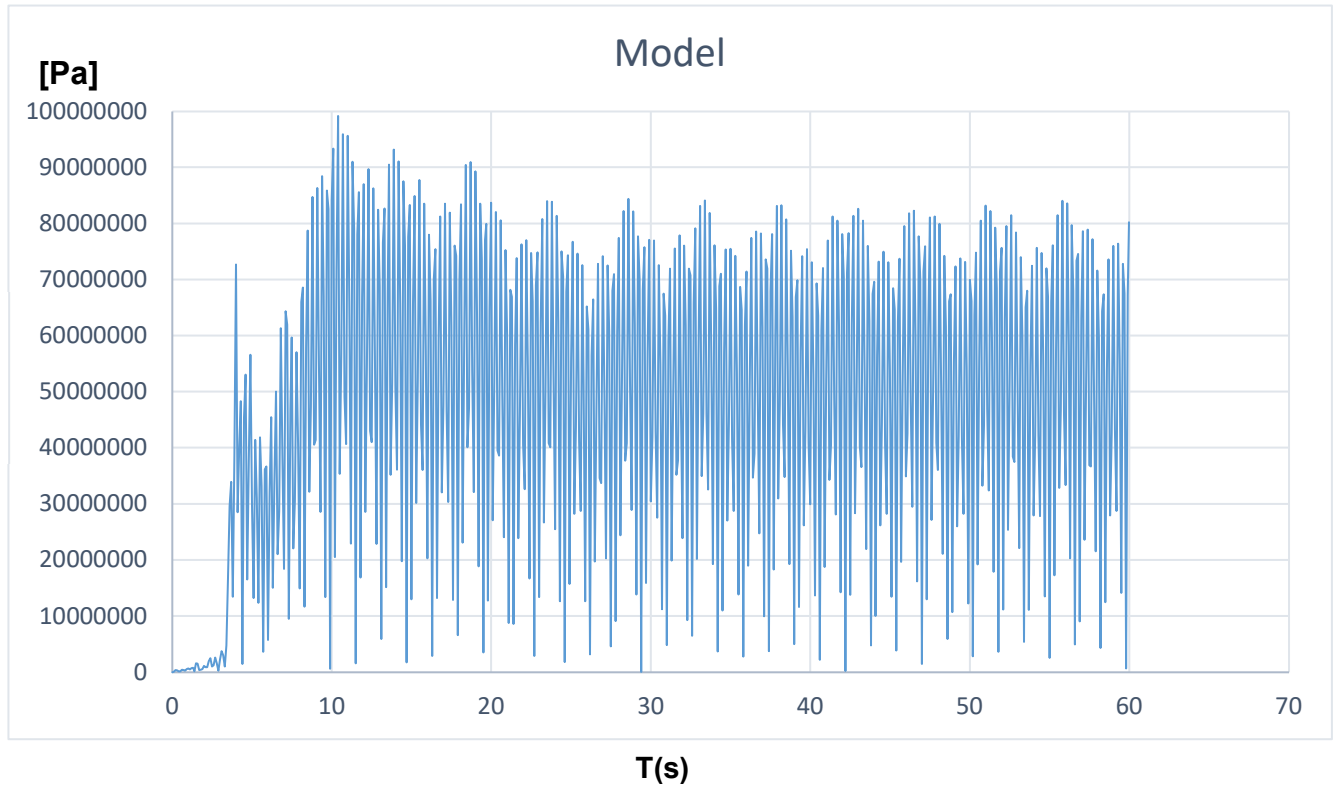
- **Building normal Model**
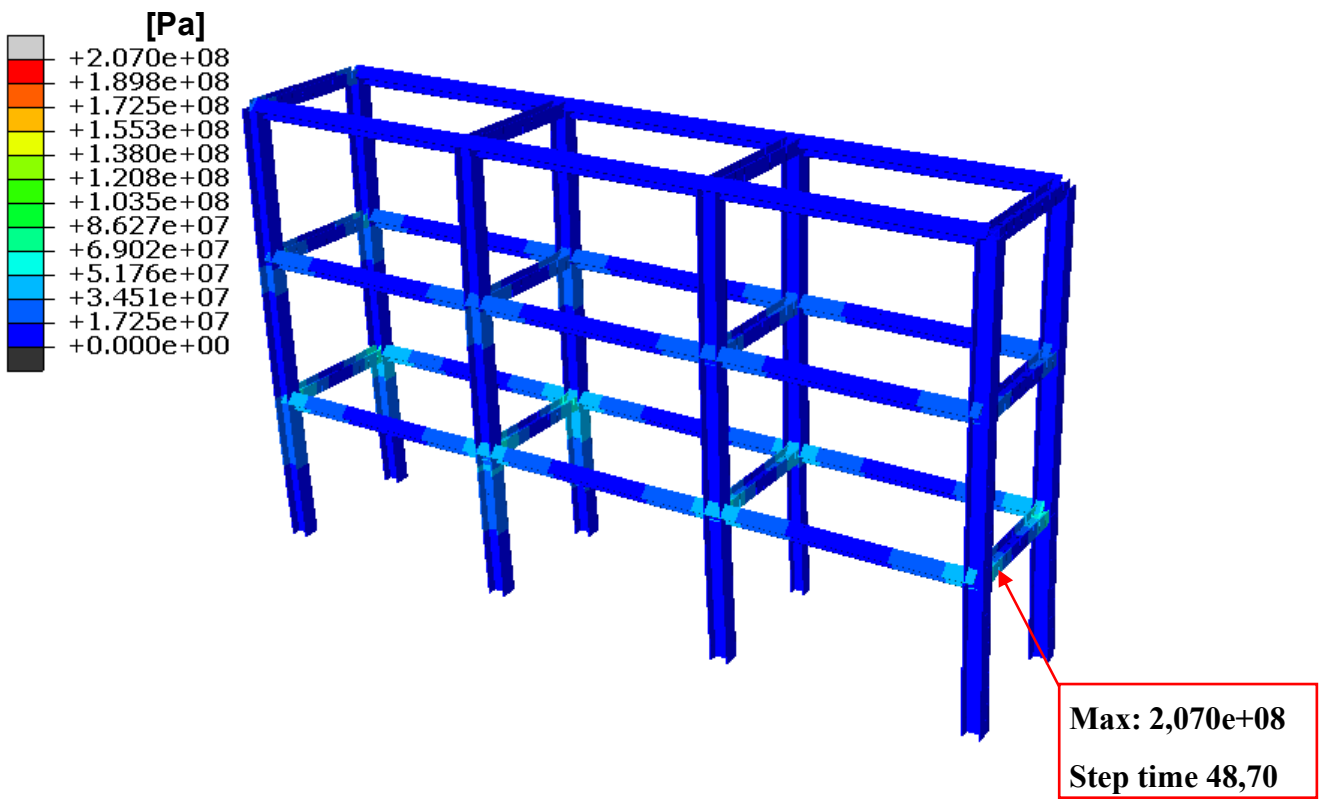
Figure 51: Stress contour for three-storey building in normal model
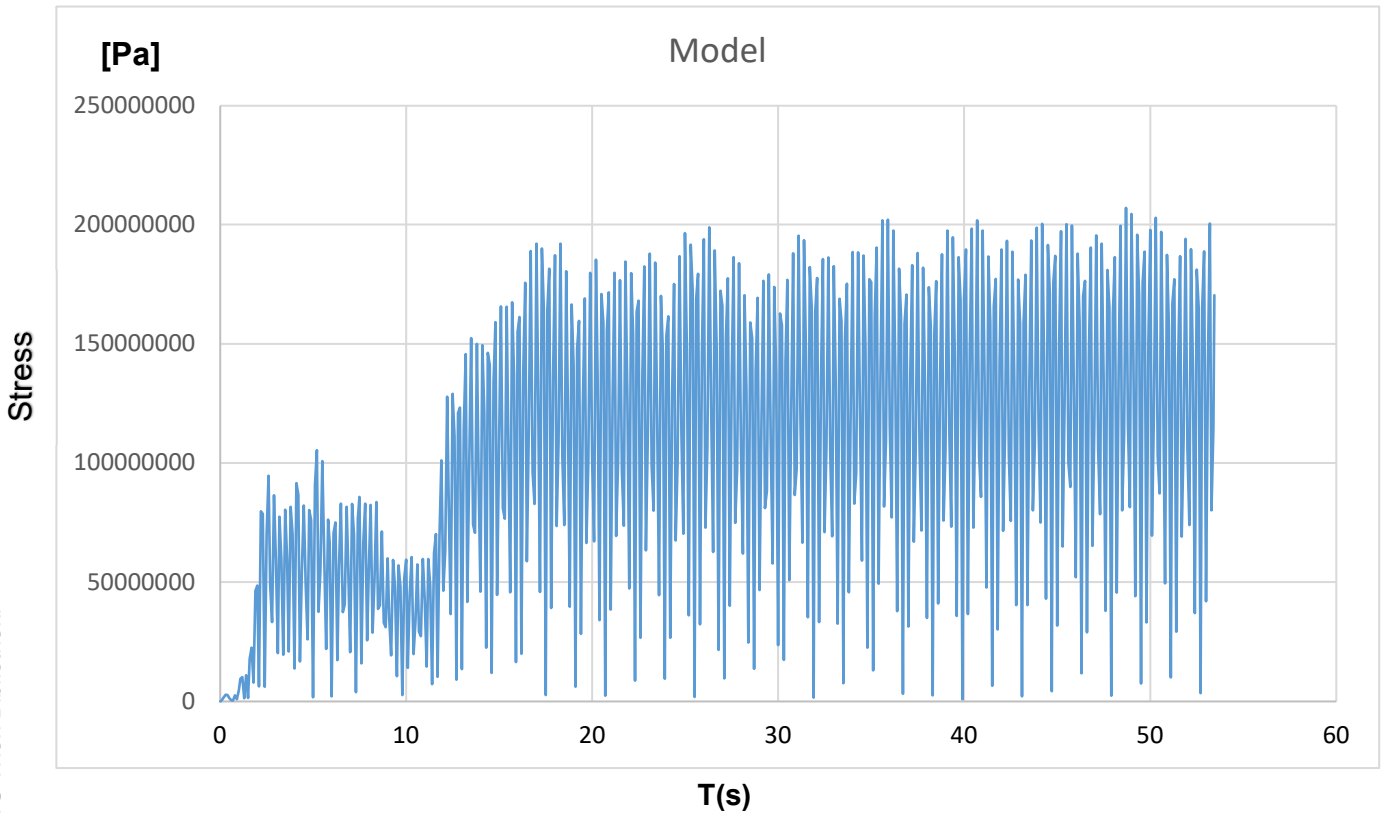
Figure 52: The total stress time course for those nodes in which the maximum values in normal model

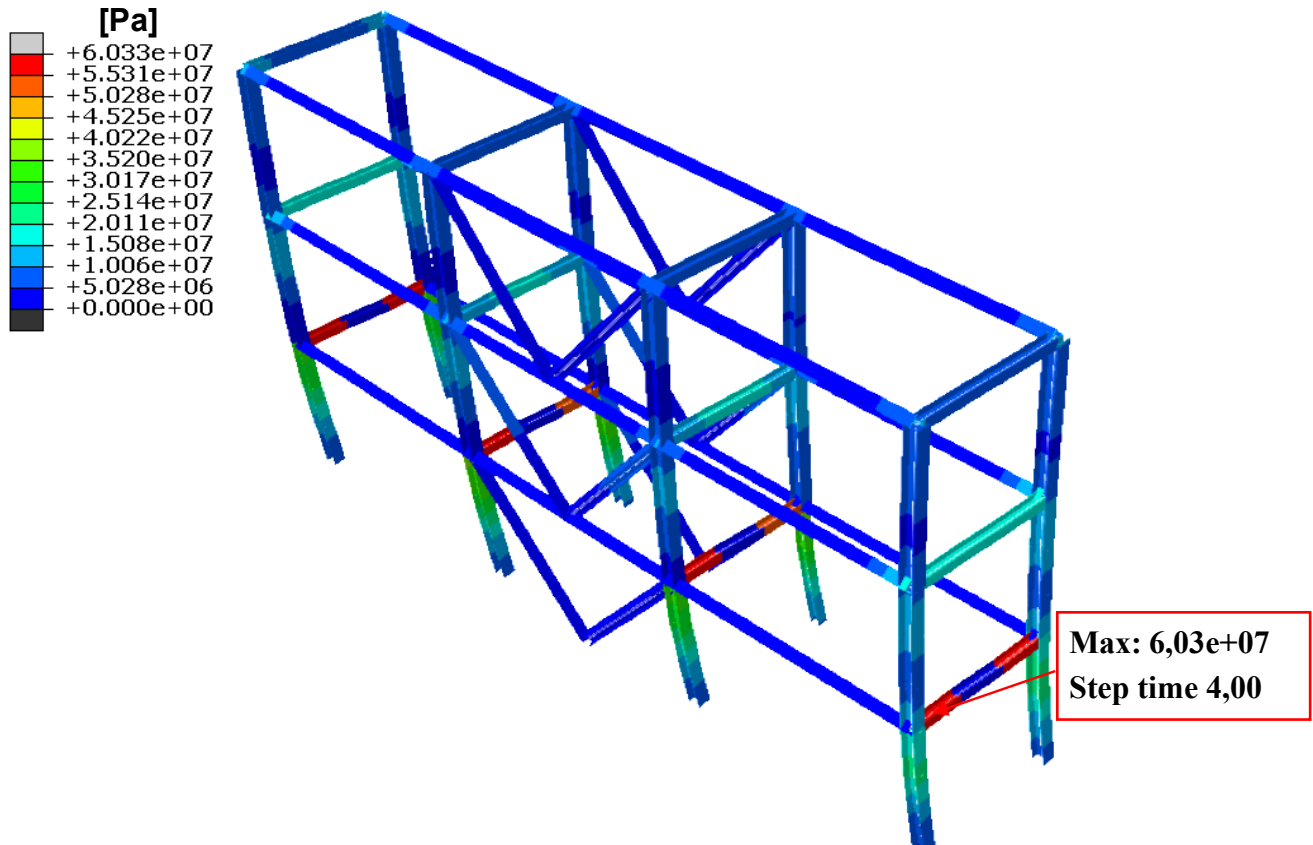- **Building with V-shaped reinforcements**
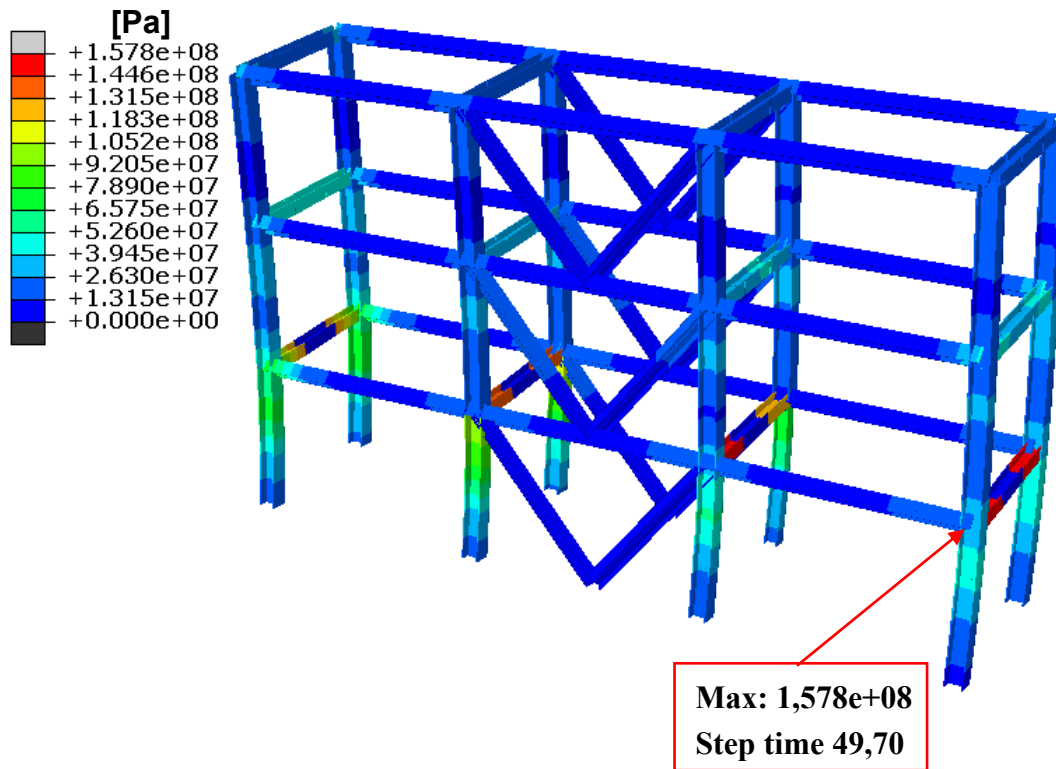
Figure 53: Stress contour for three-storey building with V-shaped reinforcements
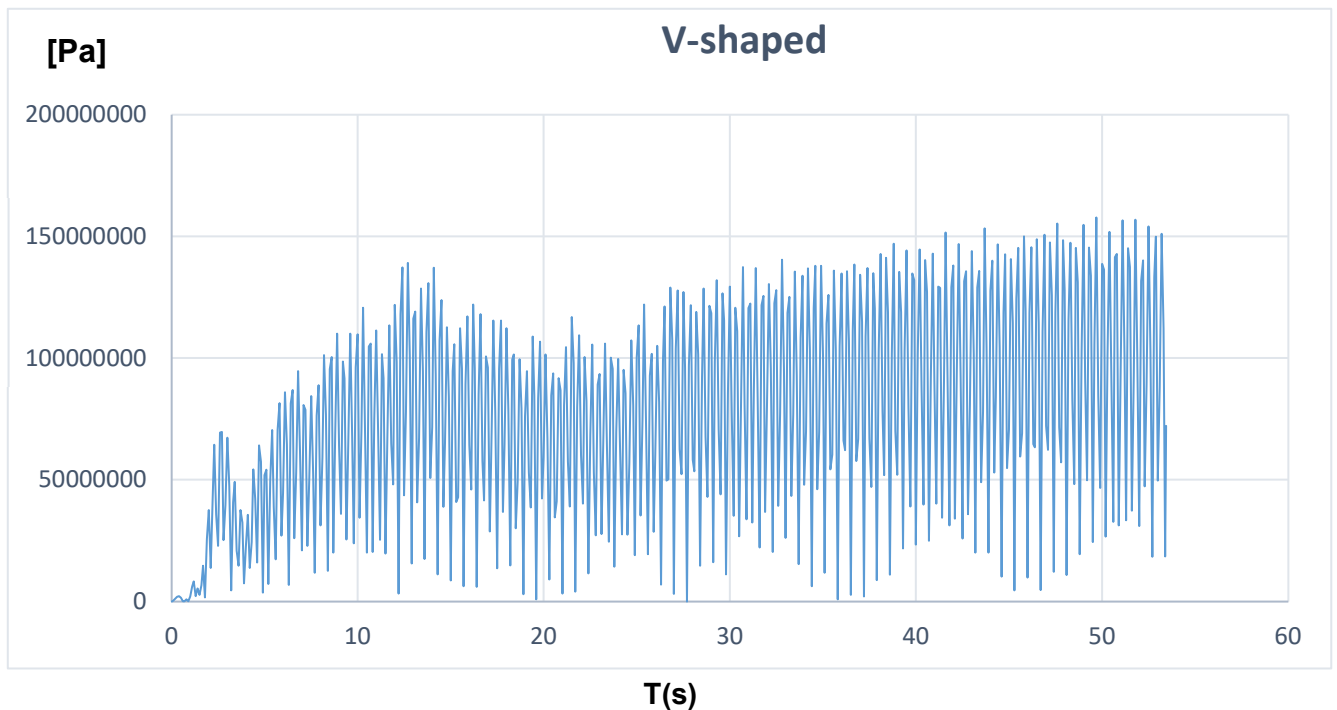
Figure 54: The total stress time course for those nodes in which the maximum values in model with V-shaped reinforcements

- **Building with X-shaped reinforcements**

[Pa]
+7.382e+07
+6.767e+07
+6.152e+07
+5.537e+07
+4.921e+07
+4.306e+07
+3.691e+07
+3.076e+07
+2.461e+07
+1.846e+07
+1.230e+07
+6.152e+06
+0.000e+00

Max: 7,382e+07
Step time 2,70

Max: 7,382e+07
Step time 2,70
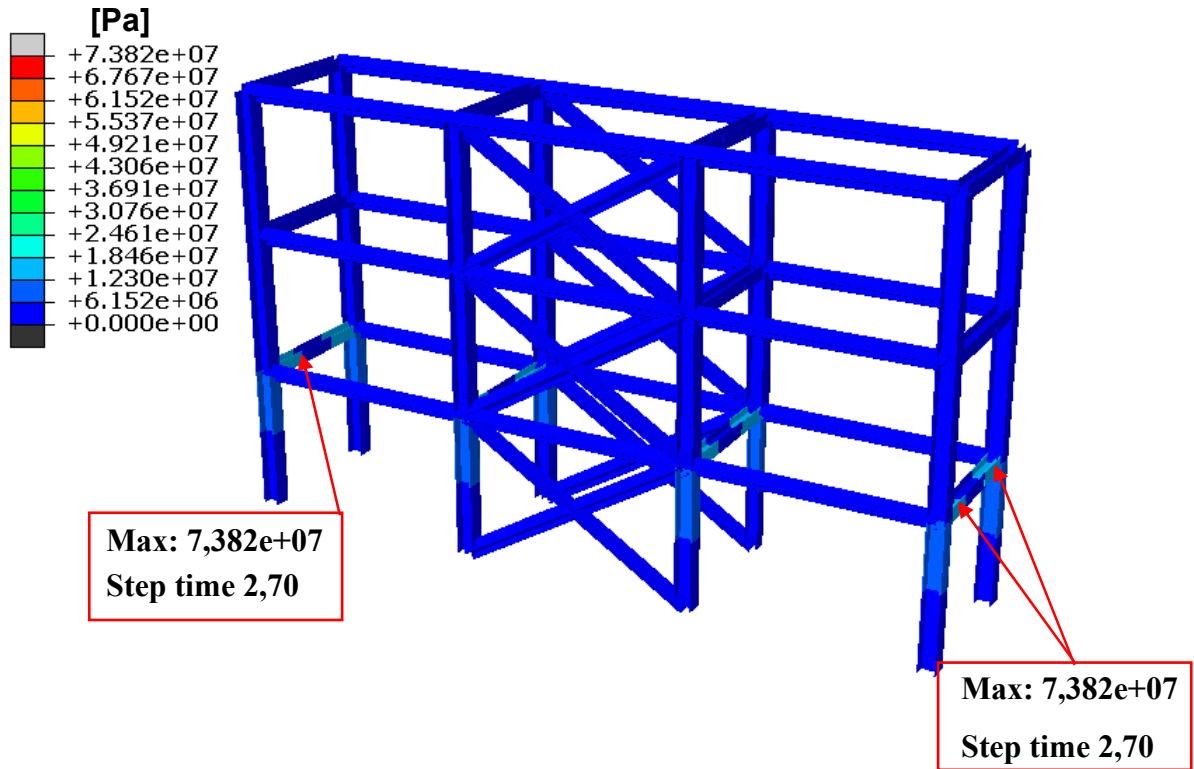
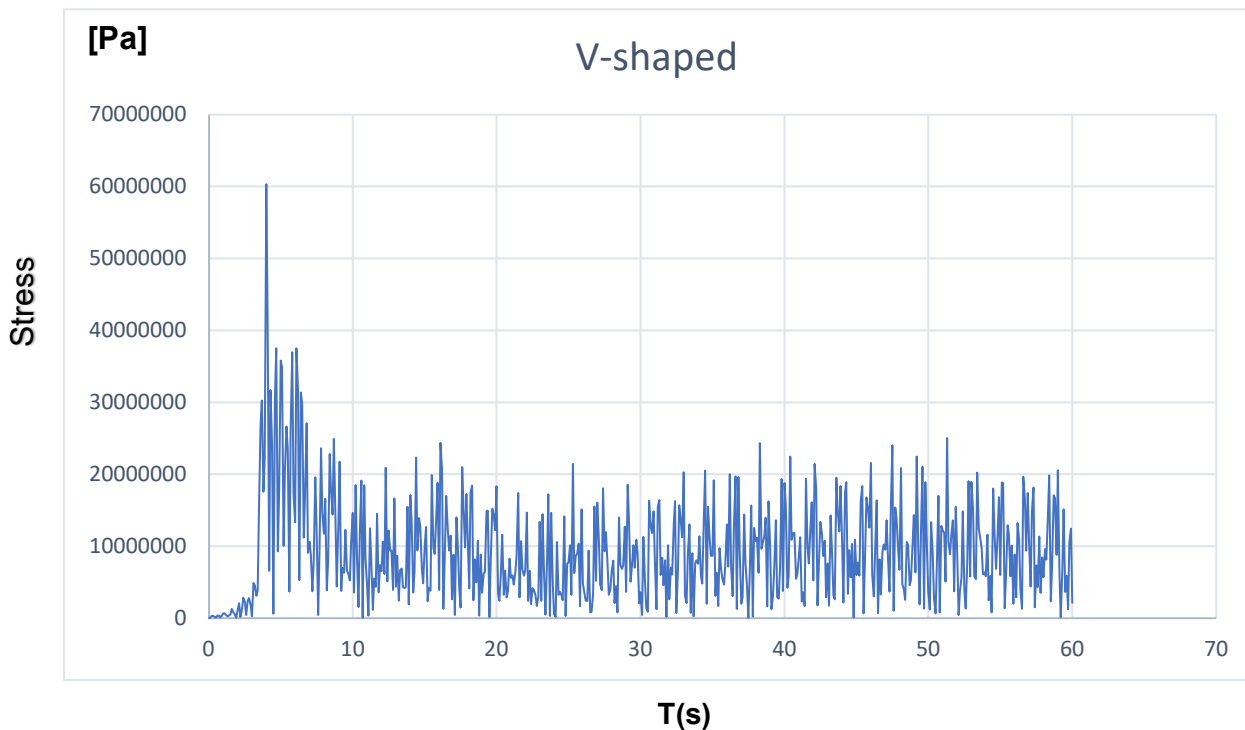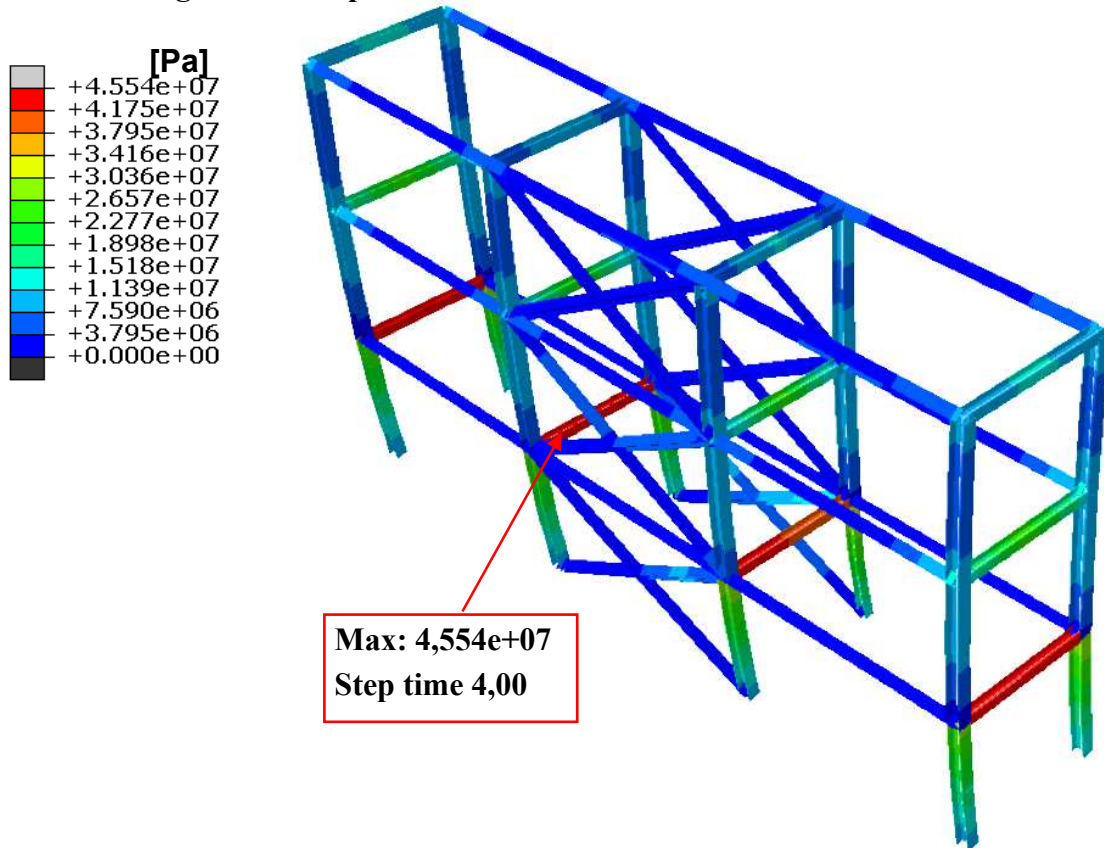**Figure 55: Stress contour for three-storey building with X-shaped reinforcements**
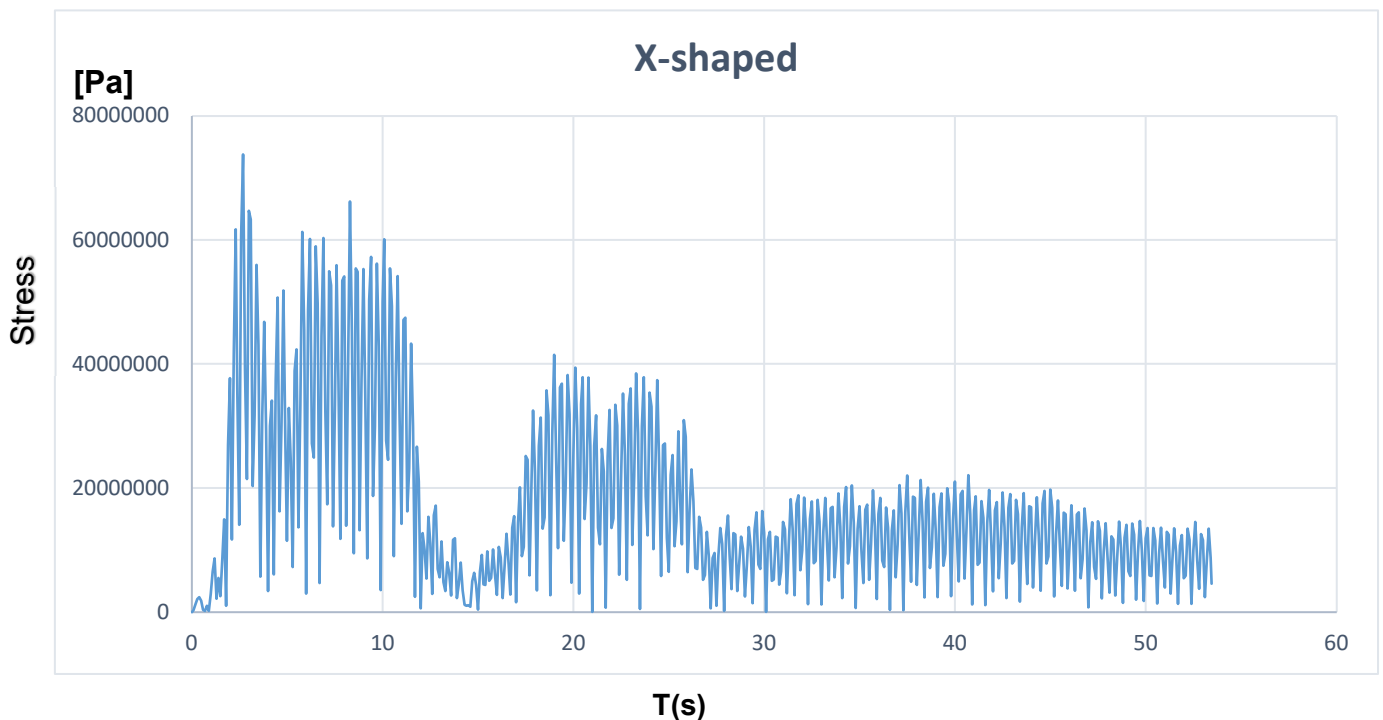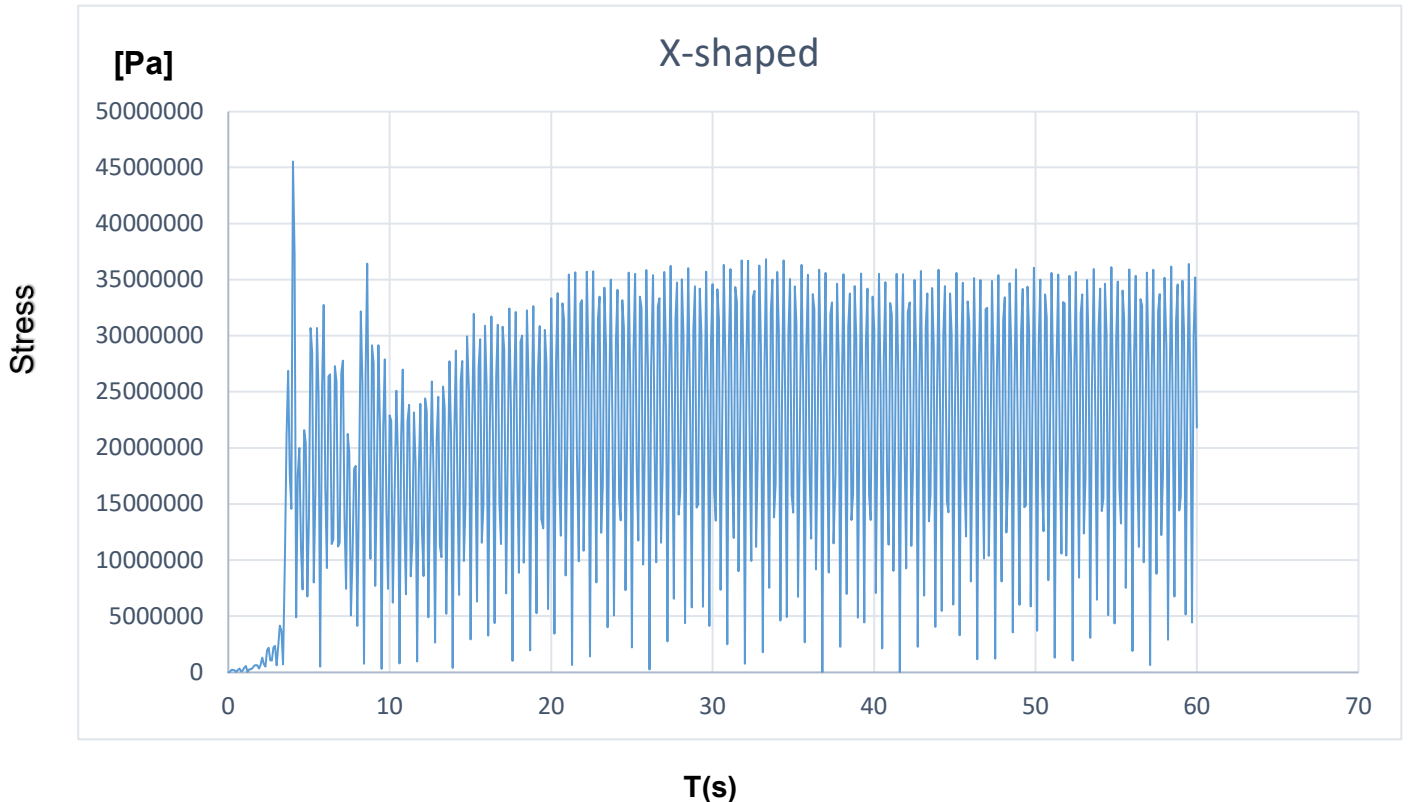

Figure 56: The total stress time course for those nodes in which the maximum values in model with X-shaped reinforcements
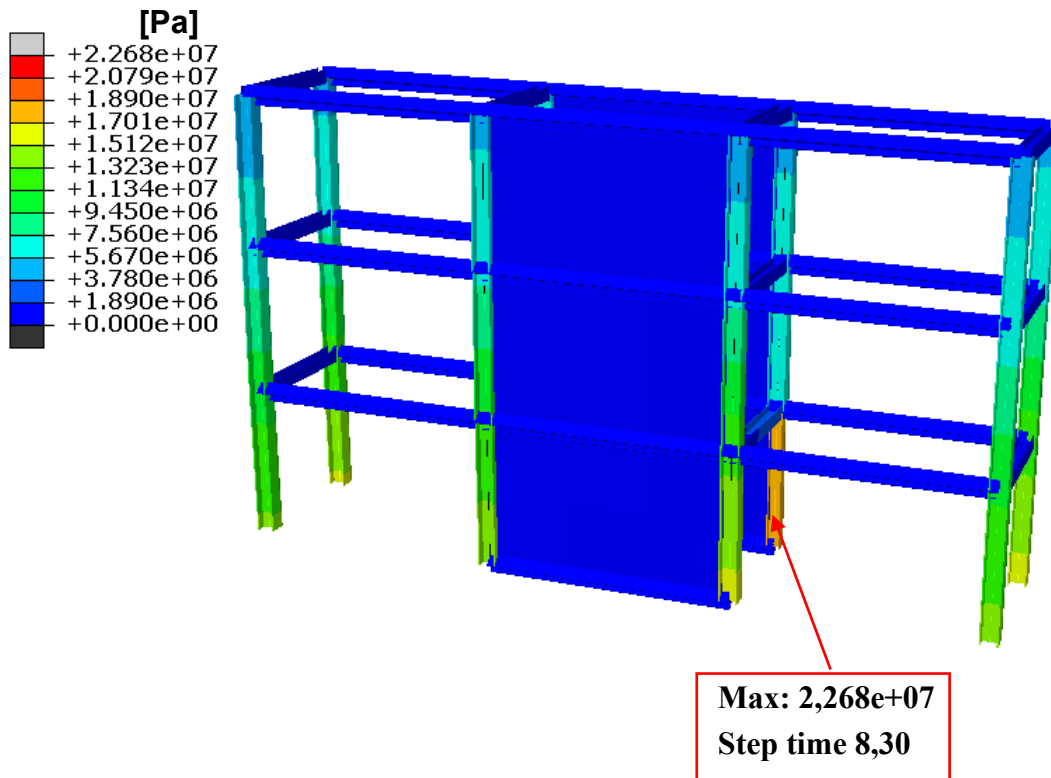
- **Building with shear wall**
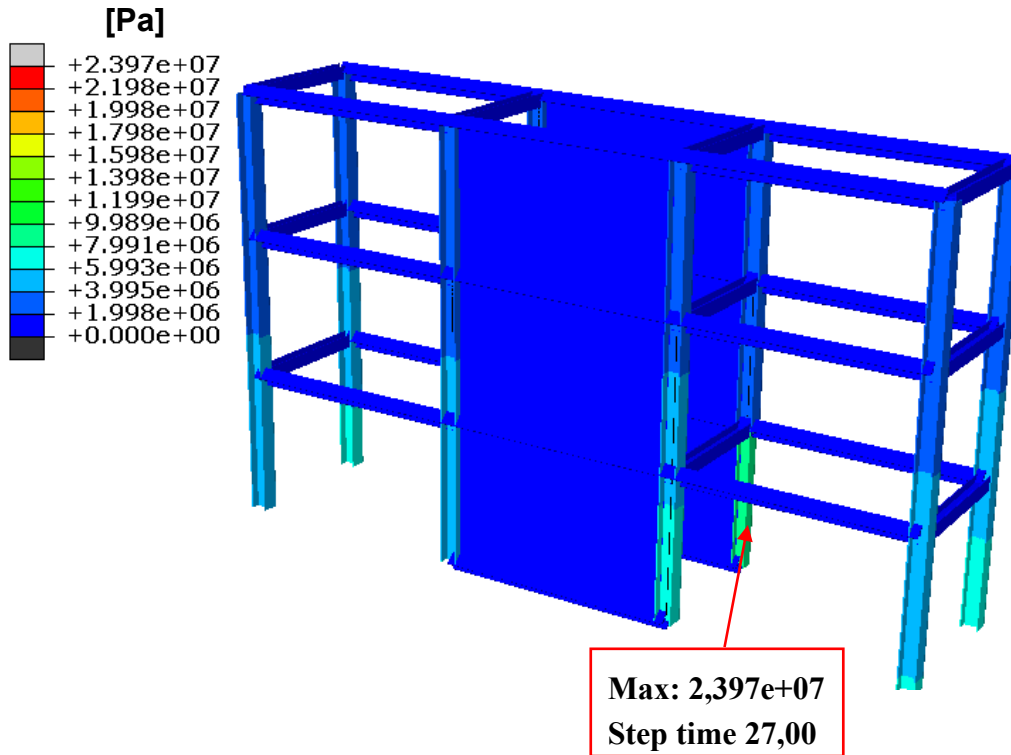
Figure 57: Comparison of stress results for three-storey building with shear wall
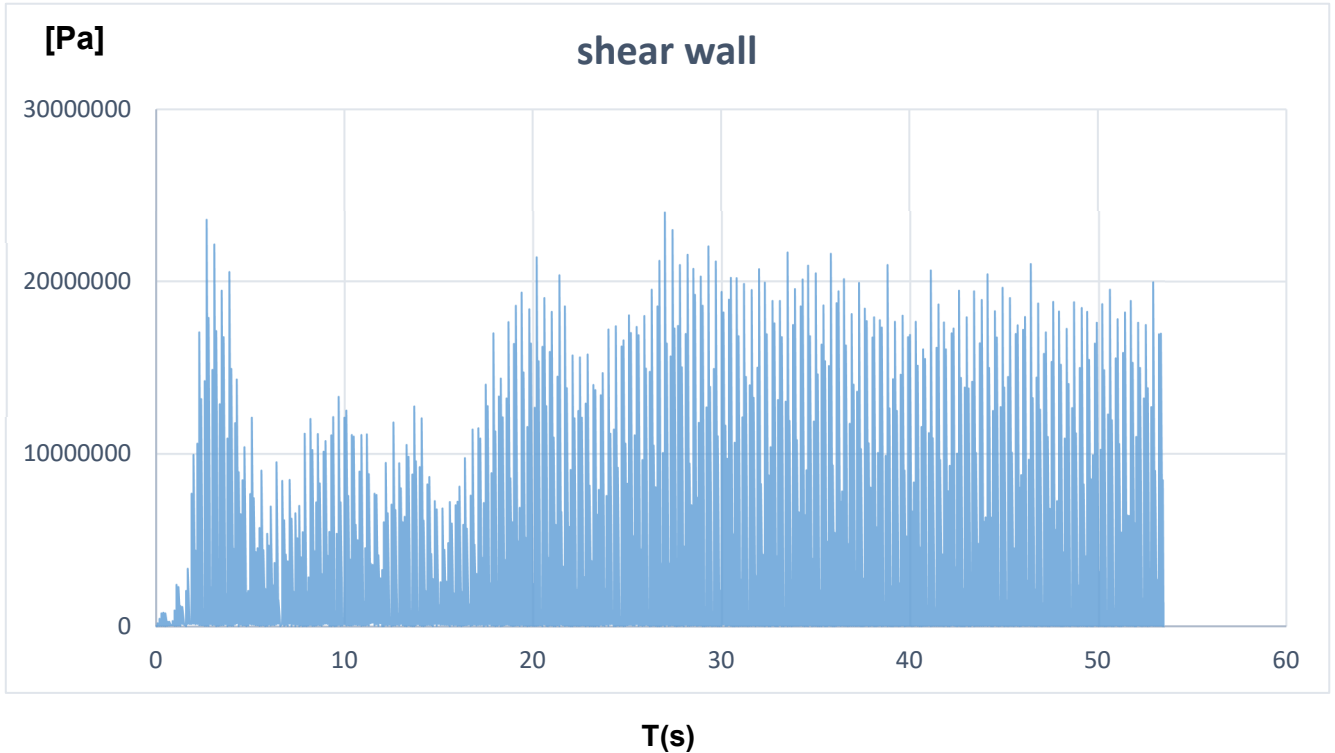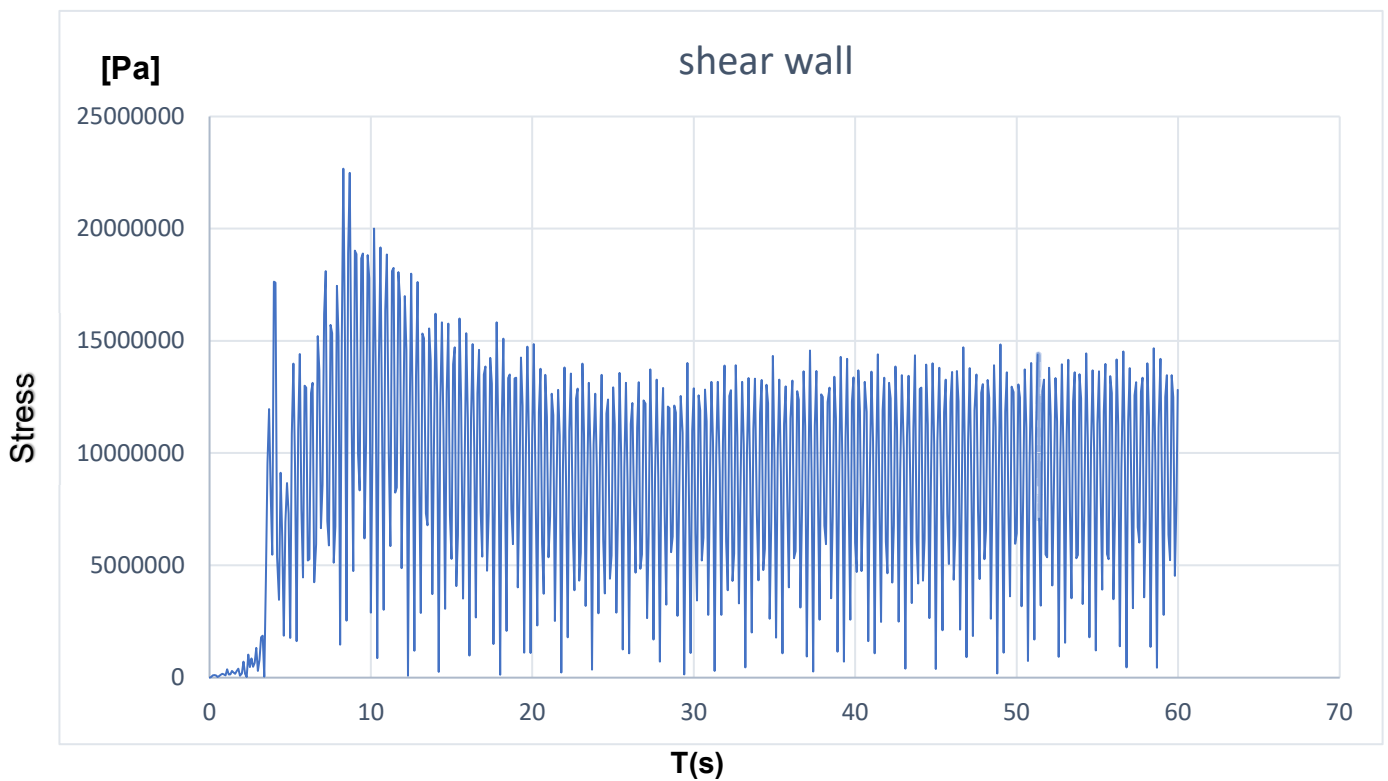

Figure 58: The total stress time course for those nodes in which the maximum values in model with shear wall

4.8.1.1 Comparison of stress results for three-storey building in the El Centro area

The maximum stresses applied to the building structure are presented in the table below. As it is obvious, the stress value decreases as a result of improvement of building reinforcements. This means that the structure needs more intense pressures and vibration so that it can enter the plastic zone and thus fracture zone. For modeling this structure, steel with a yield stress of 345 MPa has been used. If the structure is without any reinforcement, the building only needs 138 MPa to enter the plastic deformation zone, but if a shear wall is used, this difference reaches 321 MPa.

Stress (Mpa)	Building type
207	Building normal Model
157.8	Building with V-shaped reinforcement
73.82	Building with X-shaped reinforcement
23.97	Building with shear wall

Table 4.2: Table of Comparison of stress results

4.8.2   **LOMA PRIETA AREA**

In the figures below, the stress contours for the three-storey building are shown, when the accelerogram is used in the Loma Prieta Area. As is evident, the building is not damaged by applying this earthquake to the structure, but a lot of force and pressure are applied to the building foundations. By applying reinforcement to the structure of the building, the stress value is regularly reduced. In fact, by applying the V-shaped reinforcement to the structure, the stress is significantly reduced compared to the normal mode, and by applying X-shaped reinforcement, this stress will be less than that of the V-shaped reinforcement. Finally, by applying the shear wall to the structure, the stress value reaches its lowest extent, and much less stress is applied to the structure of the building than the two V and X-shaped reinforcement modes.

- **Building normal mode**
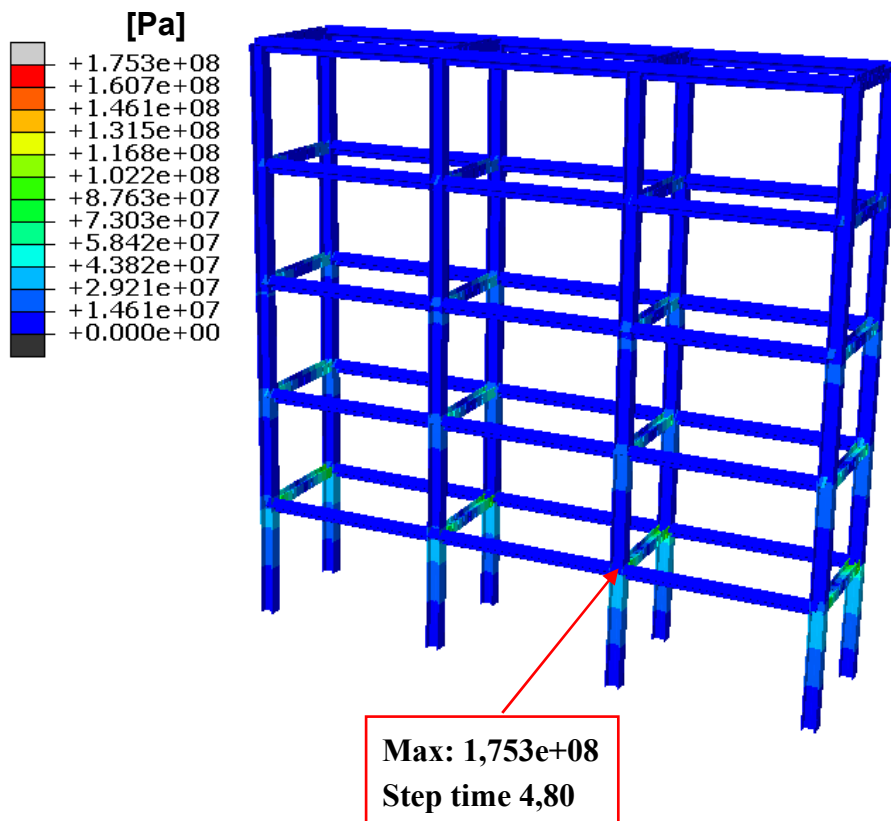

Figure 59: Stress contour for three-storey building in normal model
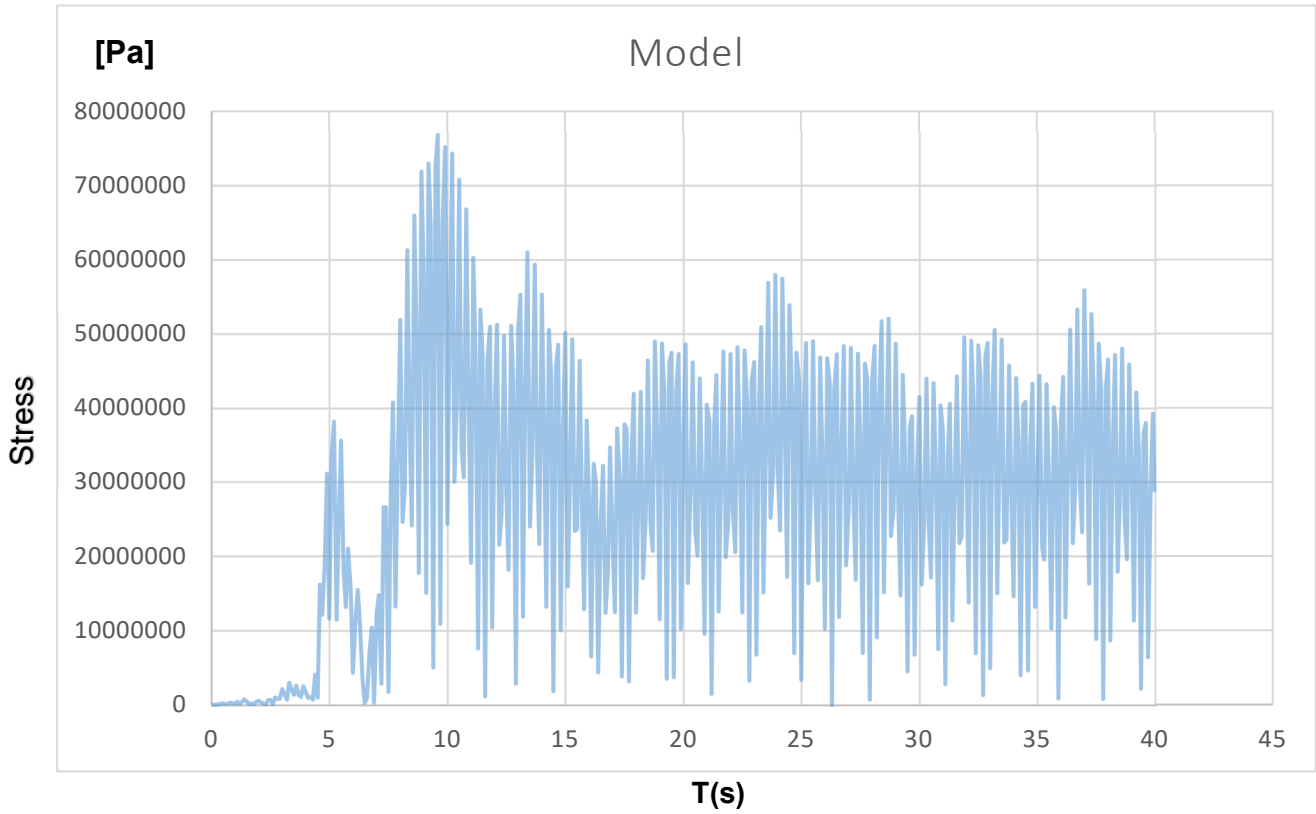
Figure 60: The total stress time course for those nodes in which the maximum values in normal model

- **Building with V-shaped reinforcements**

Max: 6,715e+07
Step time 20,80
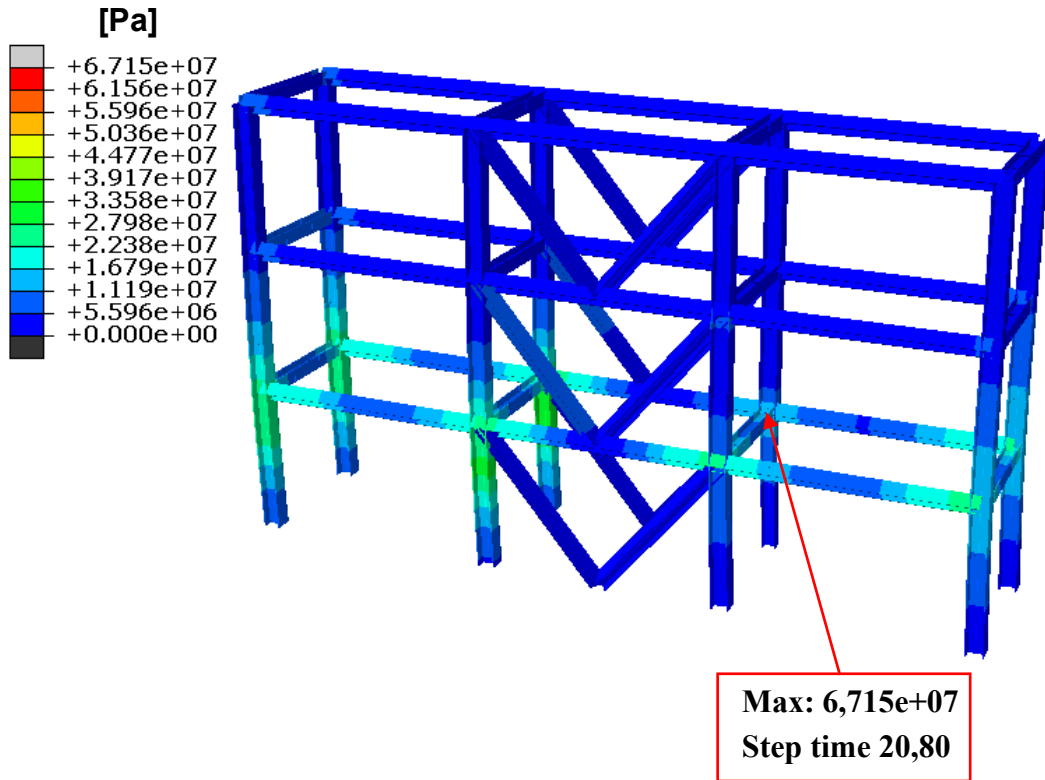
Figure 61: Stress contour for three-storey building and V-shaped reinforcements
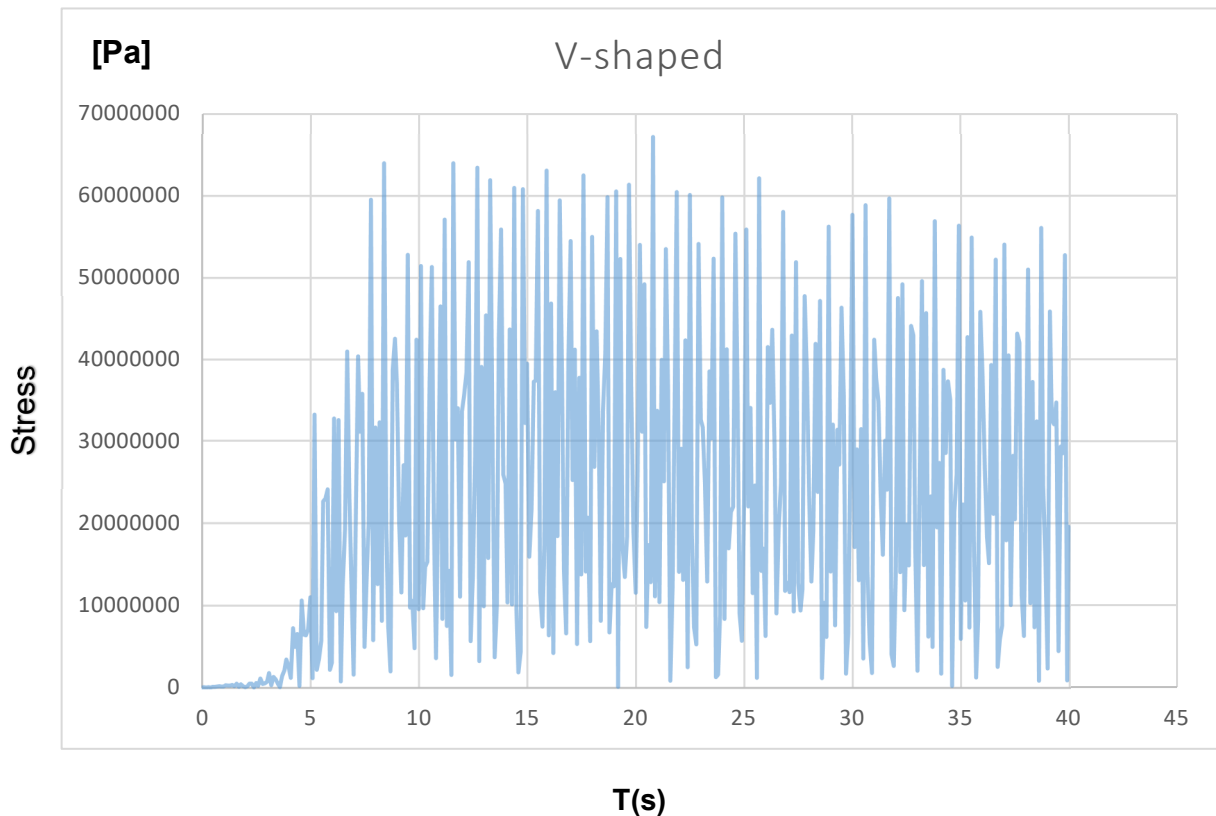
T(s)
Figure 62: The total stress time course for those nodes in which the maximum values in model with V-shaped reinforcements

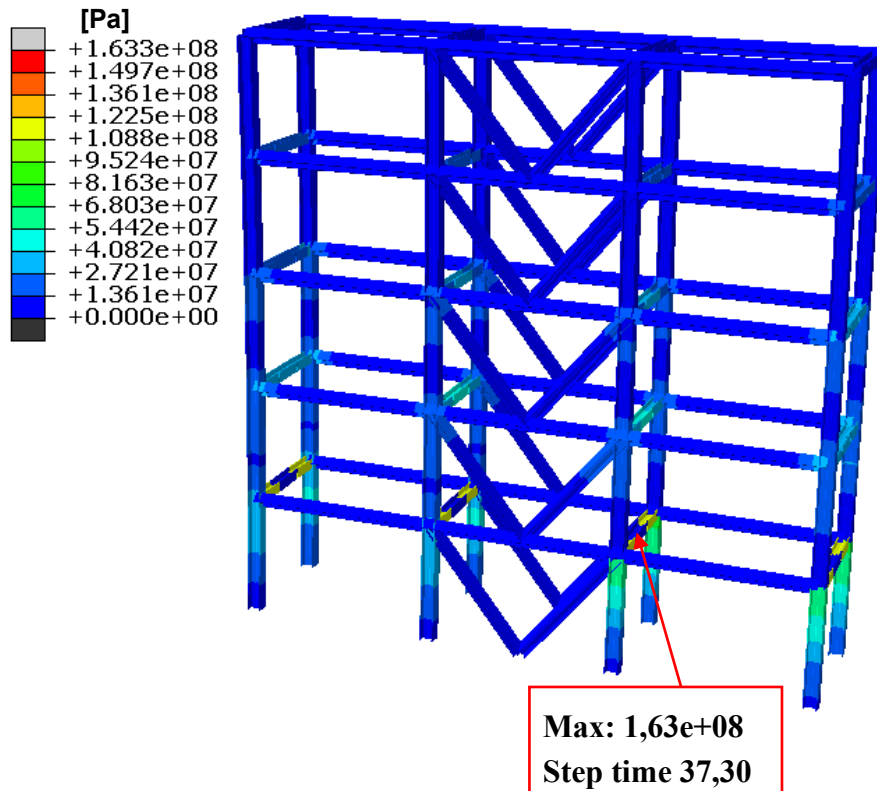- **Building with X-shaped reinforcements**
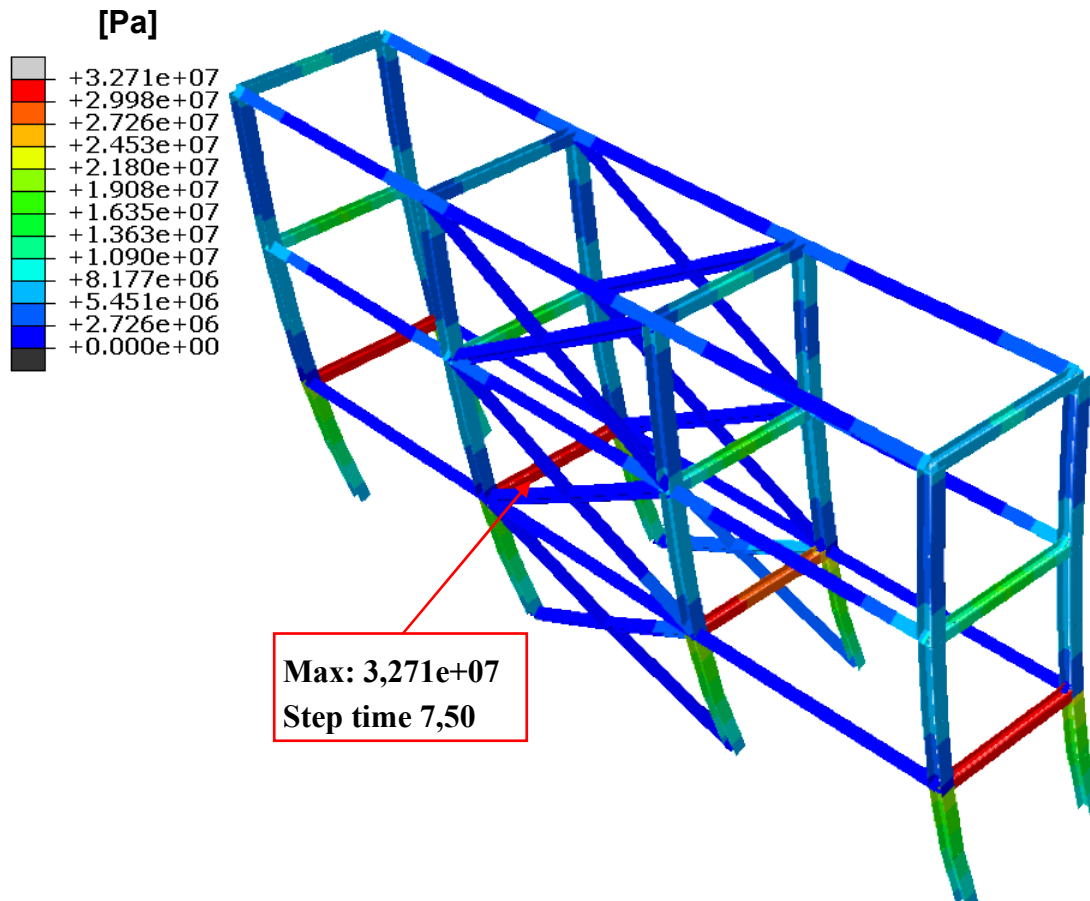
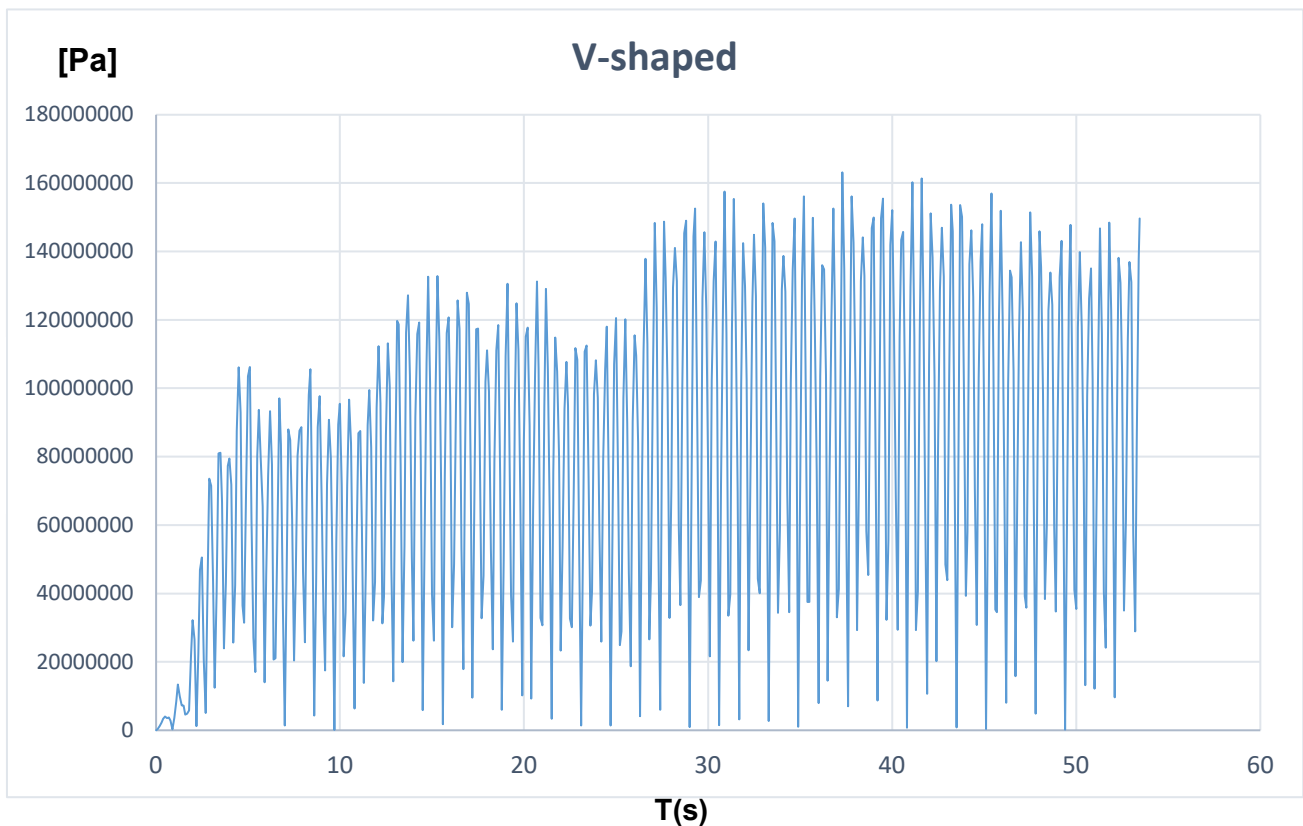**Figure 63: Stress contour for three-storey building and X-shaped reinforcements**
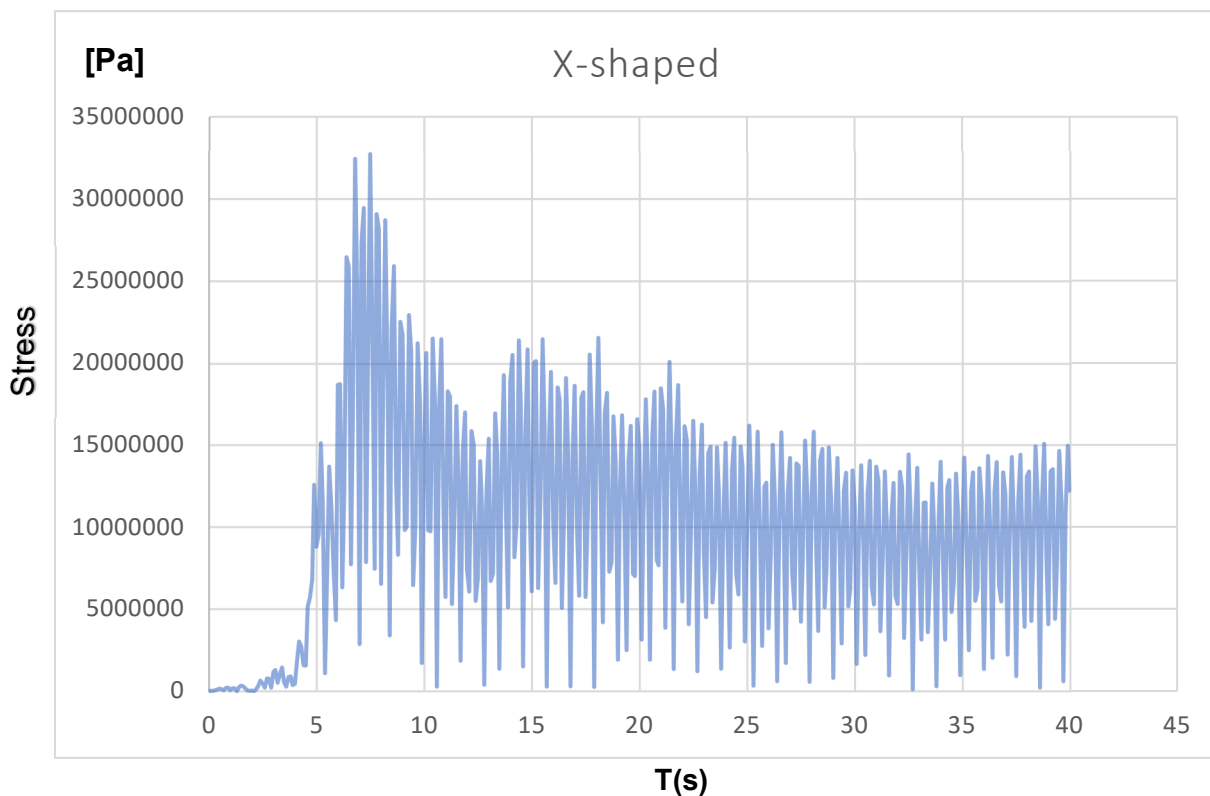
Figure 64: The total stress time course for those nodes in which the maximum values in model with X-shaped reinforcements

- **Building with shear walls**
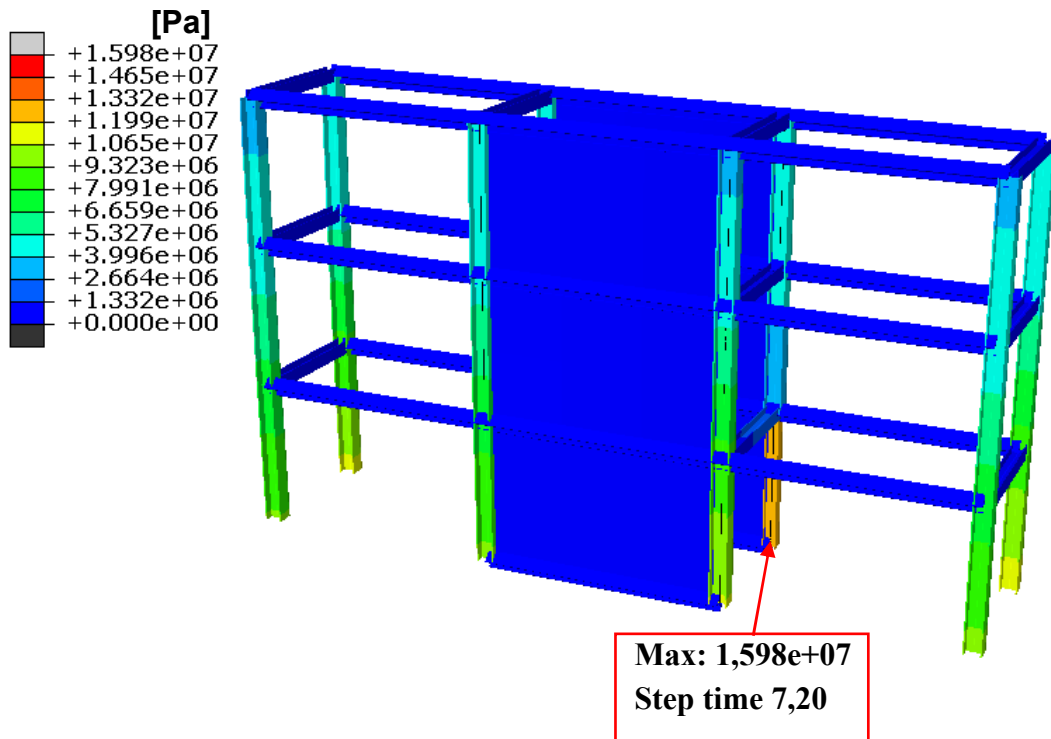
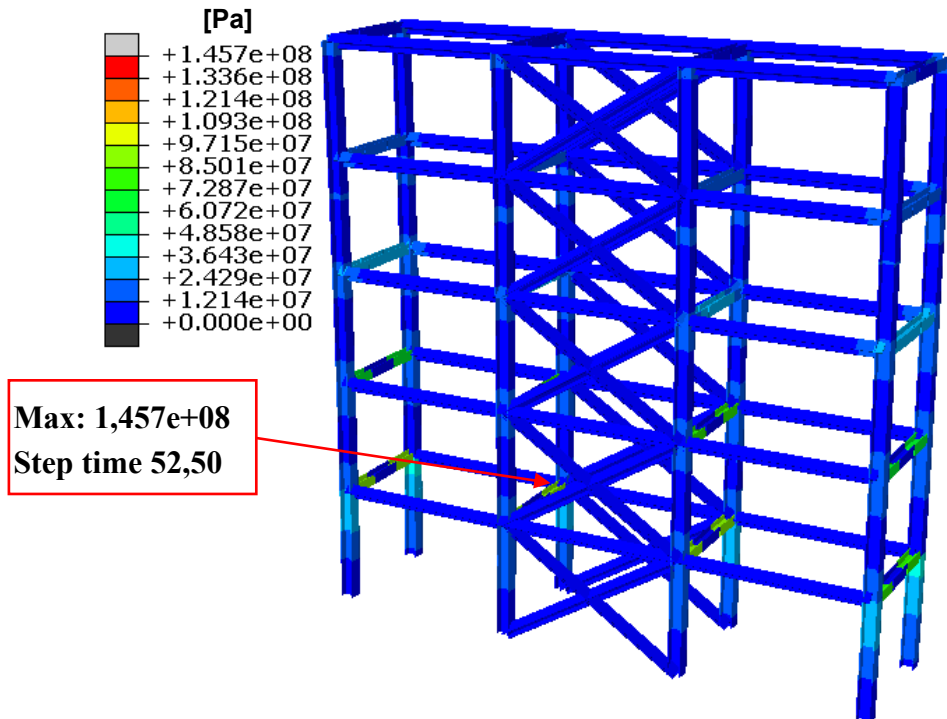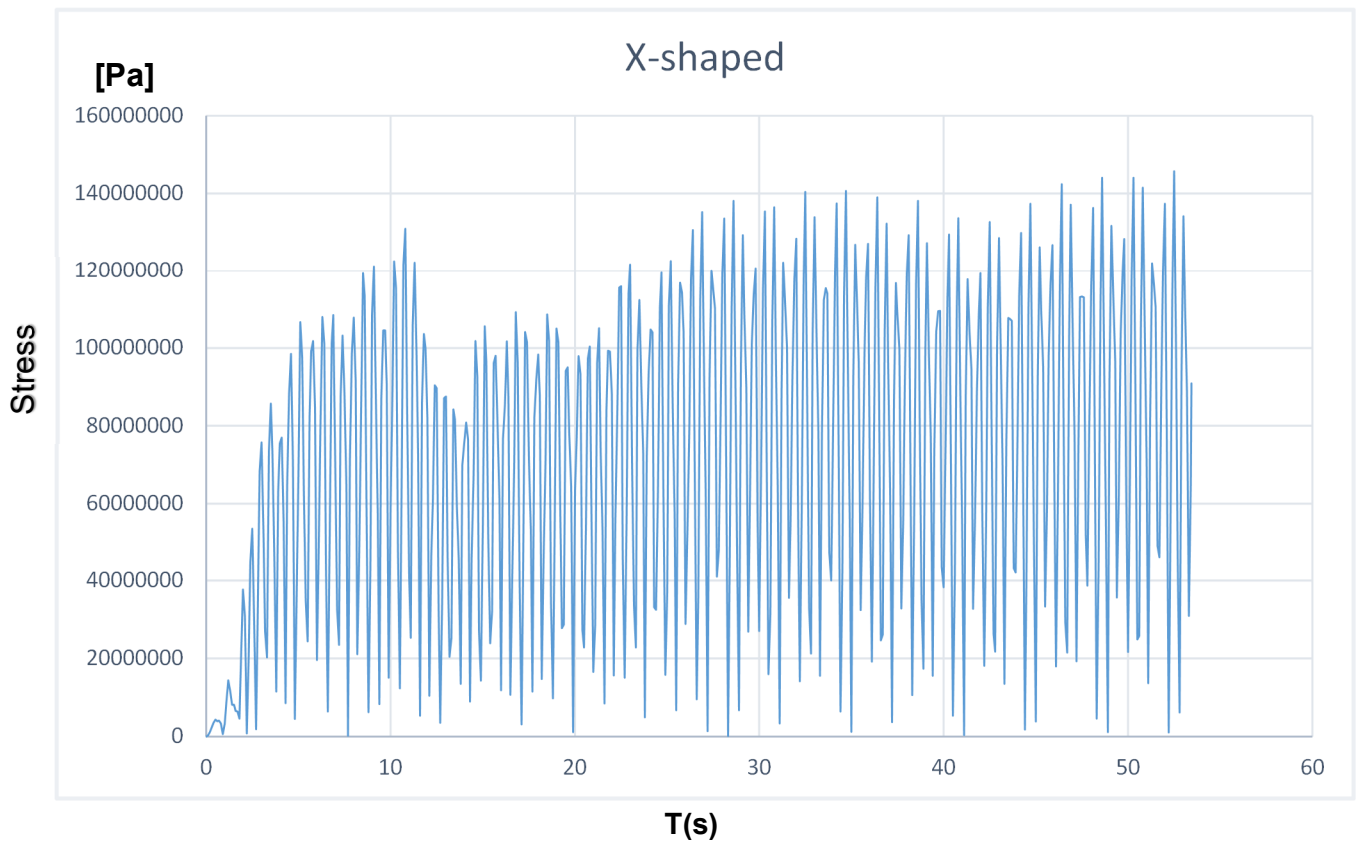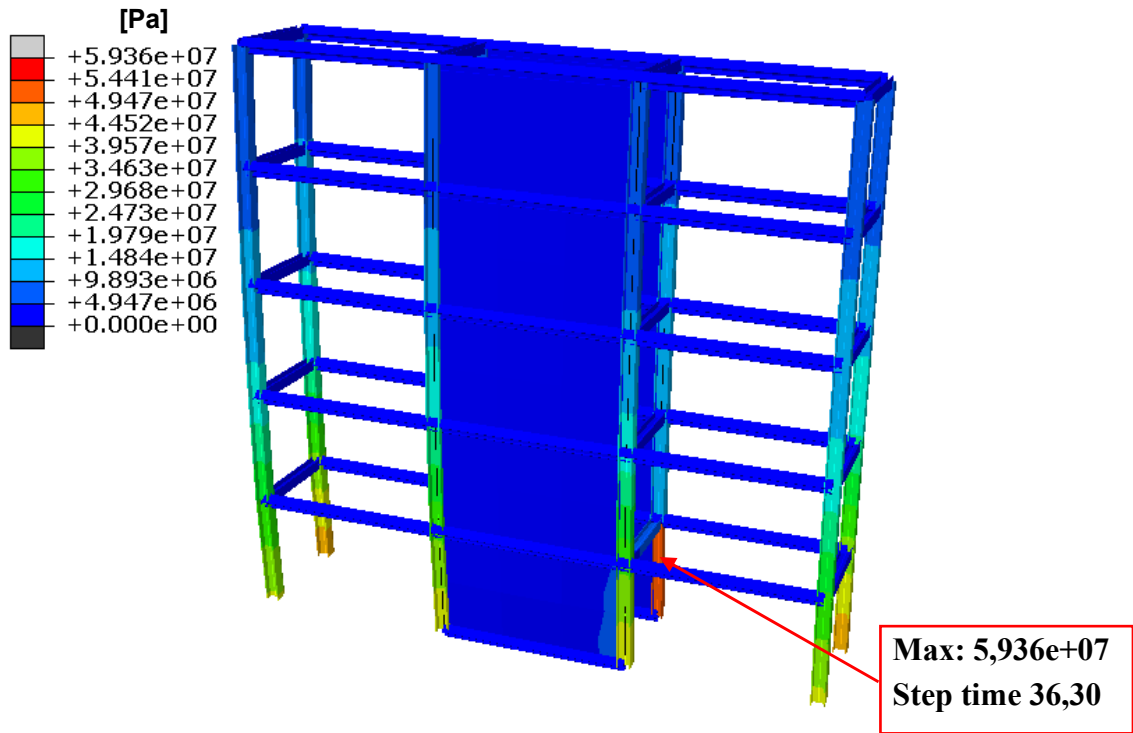**Figure 65: Stress contour for three-storey building with shear wall**
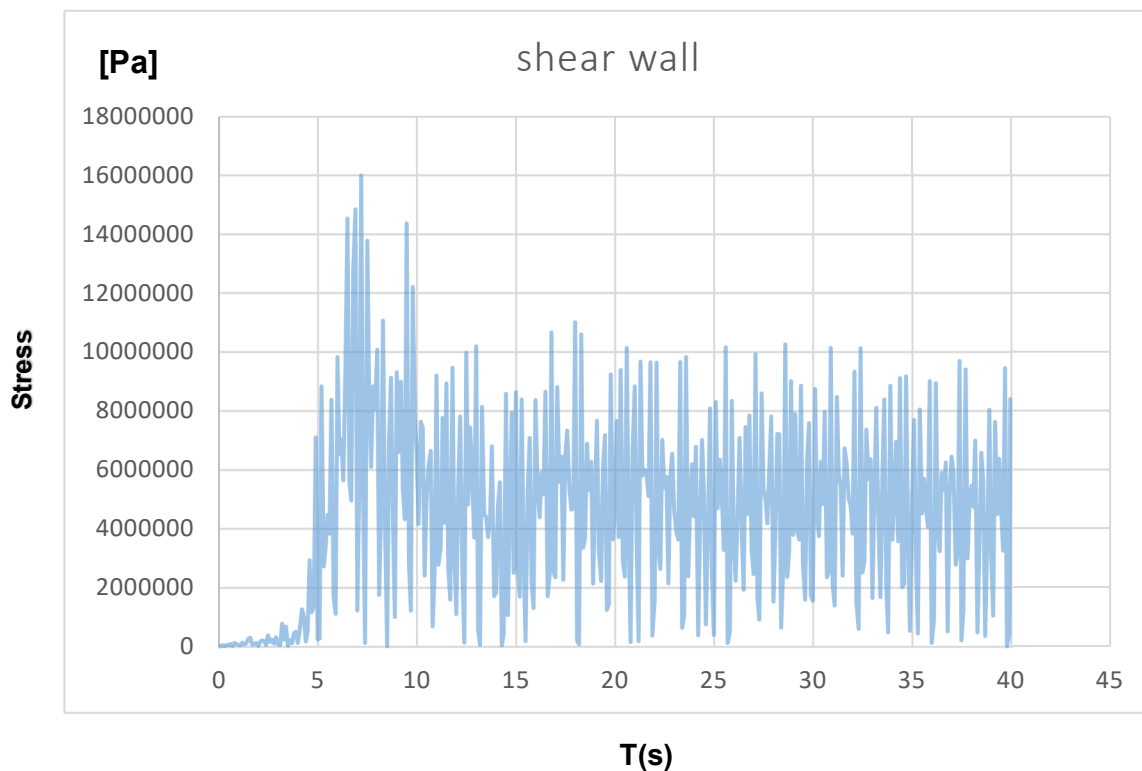
Figure 66: The total stress time course for those nodes in which the maximum values in model with shear wall

4.8.2.1 <u>Comparison of stress results for three-storey building in the Loma Prieta area</u>

The maximum stresses obtained for building structure in the event of vibrations applied in the Loma Prieta area are given in the table below. As it is obvious, in this case applying the reinforcement to the structure of the building will reduce the amount of stress and thus the structure remains healthy.

Stress (Mpa)	Building type
75.15	Building normal Model
67.15	Building with V-shaped reinforcement
32.71	Building with X-shaped reinforcement
15.98	Building with shear wall

Table 4.3: Table of Comparison of stress results

4.8.3 NORTHRIDGE AREA

In the figures below, the stress contours for the three-storey building are shown, when the accelerogram is used in the Northridge Area. As is evident, the building is not damaged by applying this earthquake to the structure, but a lot of force and pressure are applied to the building foundations. By applying reinforcement to the structure of the building, the stress value is regularly reduced. In fact, by applying the V-shaped reinforcement to the structure, the stress is significantly reduced compared to the normal mode, and by applying X-shaped reinforcement, this stress will be less than that of the V-shaped reinforcement. Finally, by applying the shear wall to the structure, the stress value reaches its lowest extent, and much less stress is applied to the structure of the building than the two V and X-shaped reinforcement modes.

- **Building normal mode**

Figure 67: Stress contour for three-storey building in normal model

Figure 68:The total stress time course for those nodes in which the maximum values in normal model

- **Building with V-shaped reinforcements**

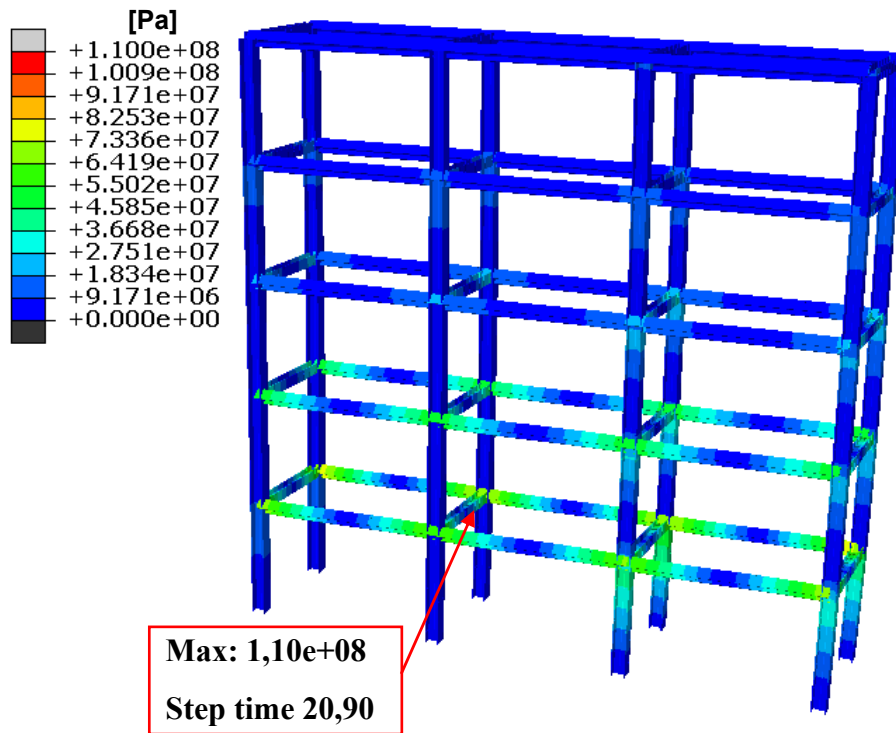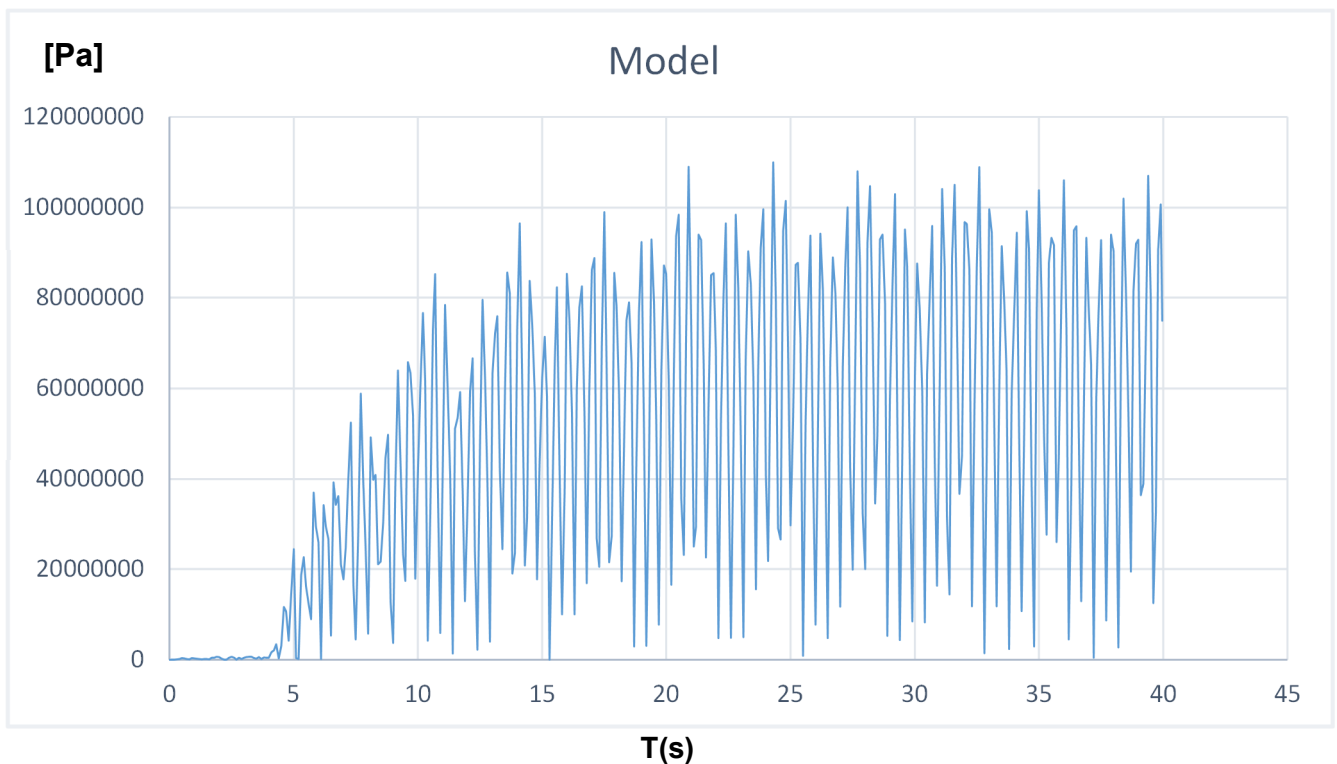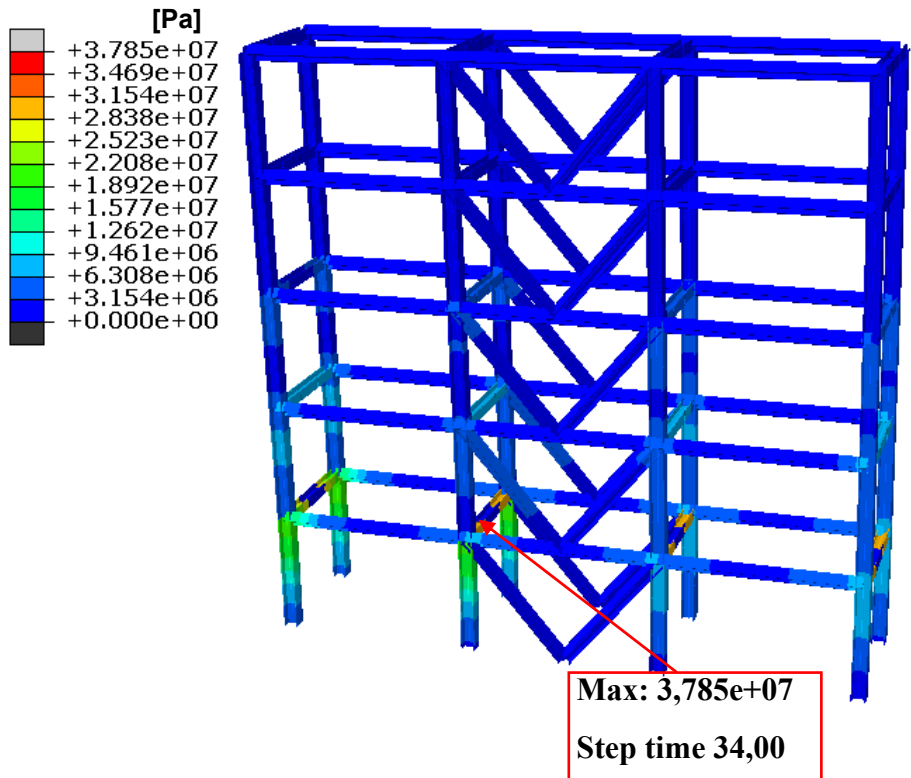**Figure 69: Stress contour for three-storey building and V-shaped reinforcements**
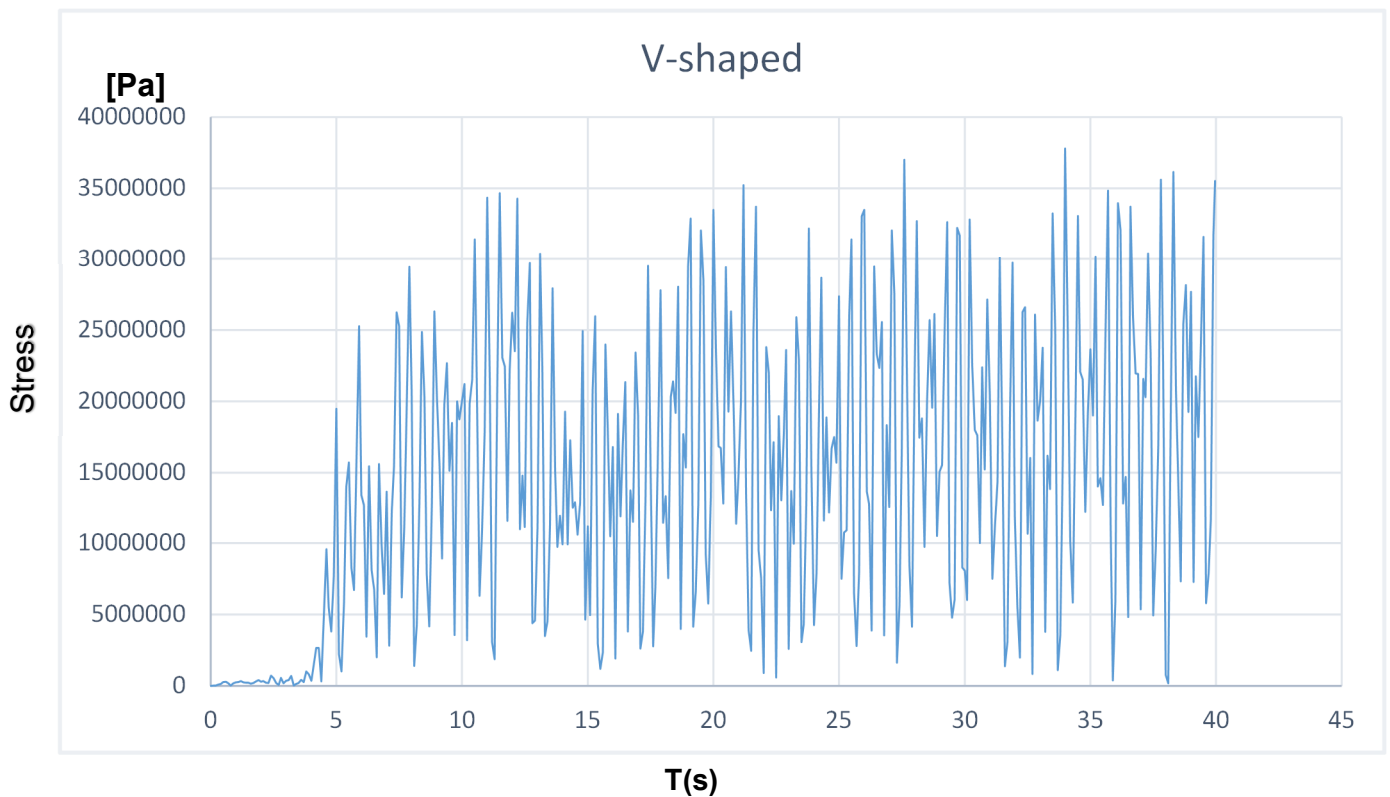

Figure 70: The total stress time course for those nodes in which the maximum values in model with V-shaped reinforcements

- **Building with X-shaped reinforcements**

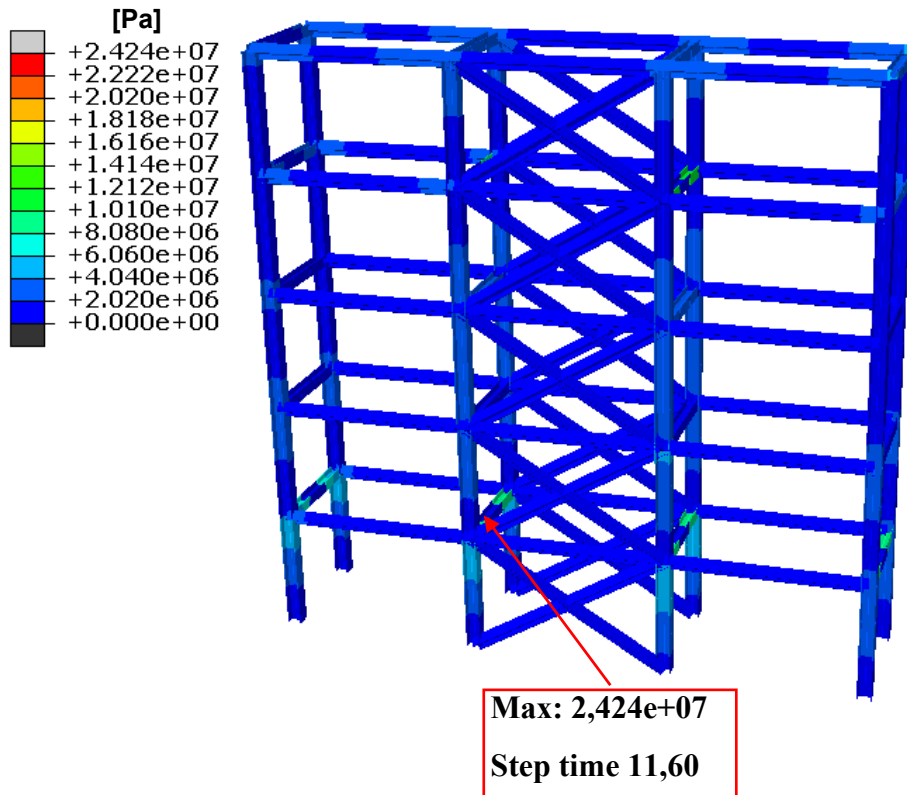**Max: 4,554e+07**
Step time 4,00

Figure 71: Stress contour for three-storey building and X-shaped reinforcements
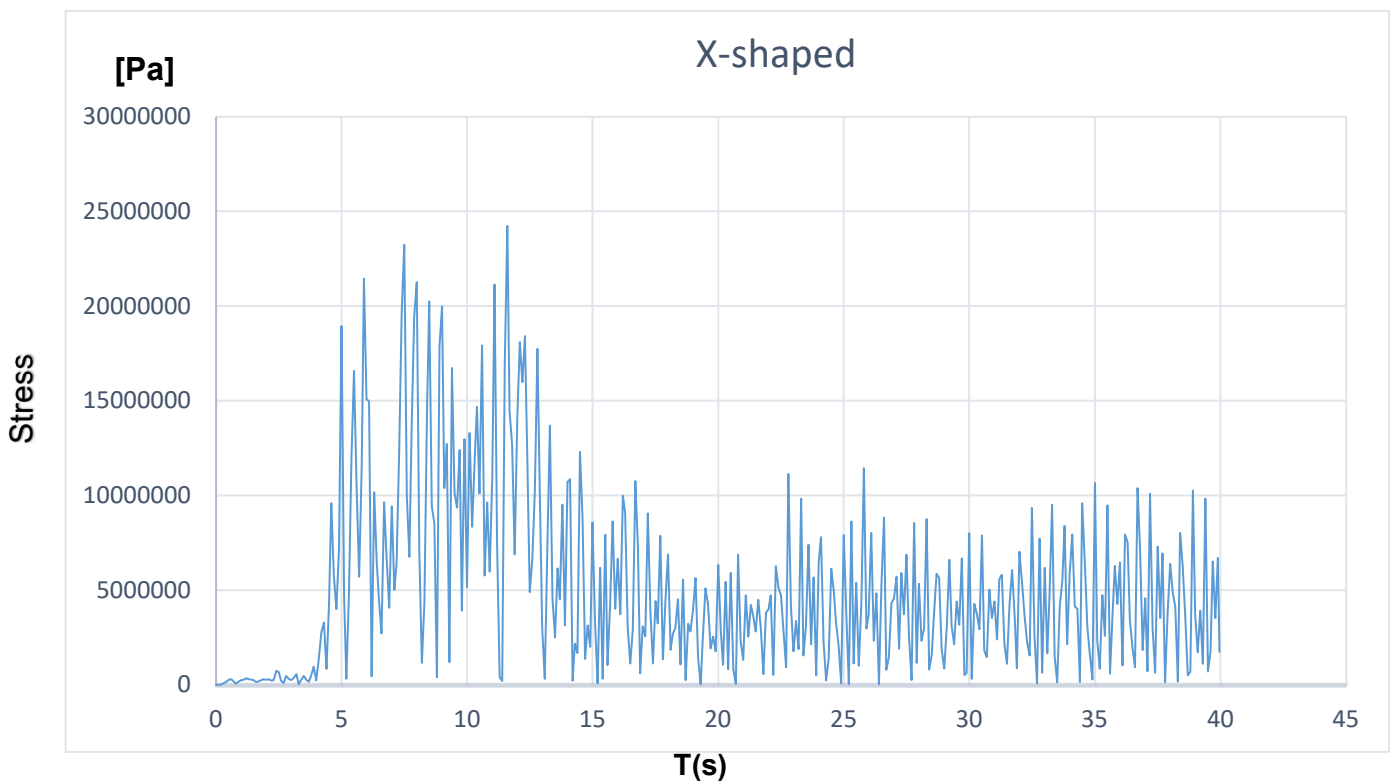

Figure 72: The total stress time course for those nodes in which the maximum values in

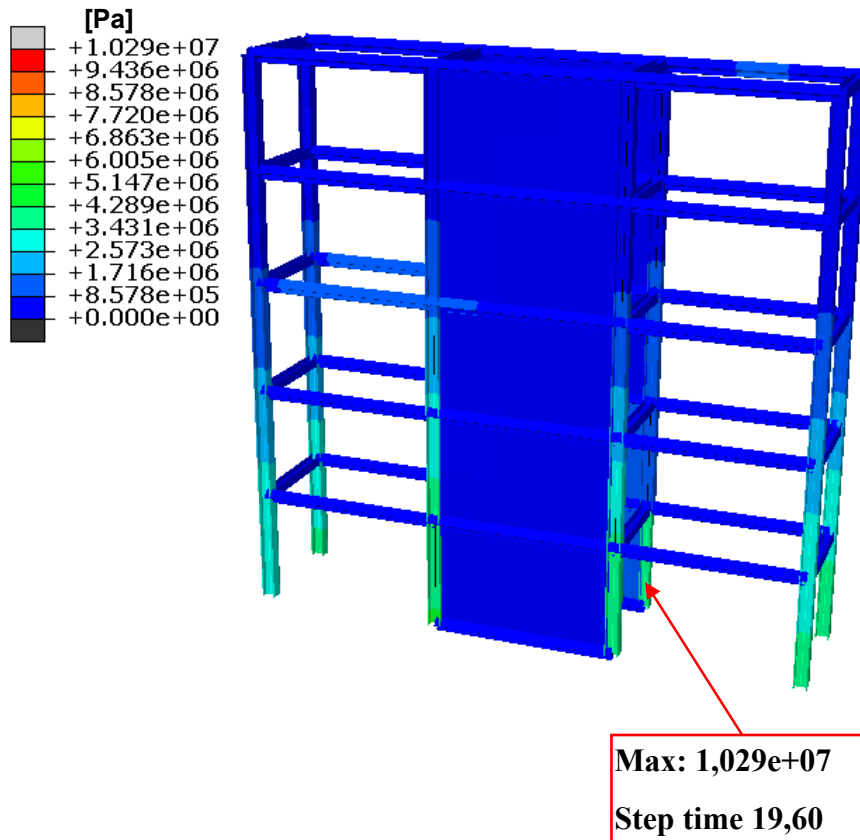**model with X-shaped reinforcements**

- **Building with shear wall**

Figure 73: Stress contour for three-storey building with shear wall

Figure 74: The total stress time course for those nodes in which the maximum values in model with shear wall

4.8.3.1 <u>Comparison of stress results for three-storey building in the Northridge area</u>

The maximum amount of stresses applied to the building structure is given in the table below. In this area, like the other two areas, the amount of stressed to the structure decreases regularly by improving the reinforcements.

Stress (Mpa)	Building type
99.19	Building normal Model
60,33	Building with V-shaped reinforcement
45.54	Building with X-shaped reinforcement
22.68	Building with shear wall

Table 4.4: Table of Comparison of stress results

4.8.4   General comparison for three-storey building

In the figure below, the maximum stresses applied to the building structure for the three areas (ELCENTRO, LOMA PRIETA and NORTHRIDGE) and for the four types of structures are depicted. As is seen in this figure, when the earthquake occurs in the EL CENTRO area, the stress is higher than the other two. This is due to the severity of the earthquake in the area. As it is clear from this diagram, by varying the reinforcement from V to X, and then to the shear wall, the applied stress in all three areas will be regularly reduced. This suggests that the use of a shear wall in the building structure has major impact on reducing the amount of stress applied to it.
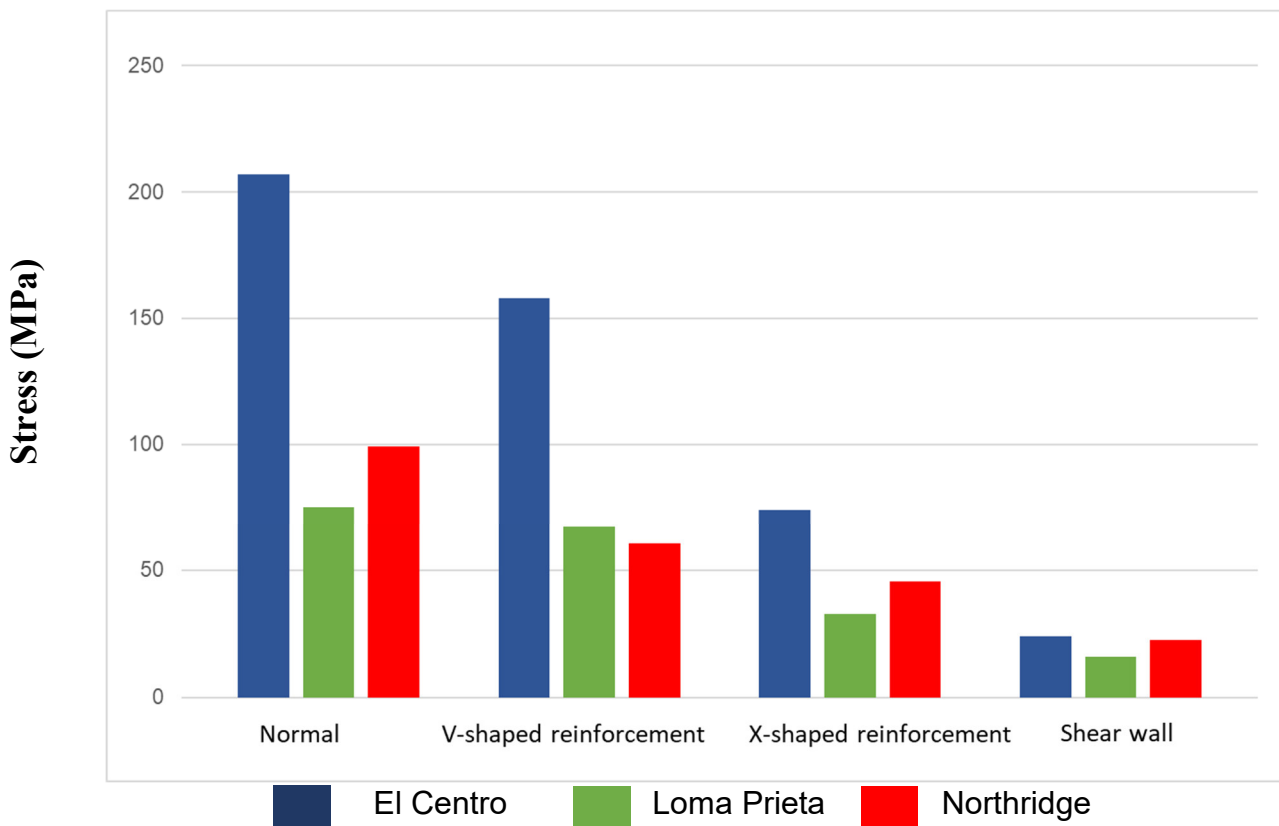
Figure 75: Comparing the results of the obtained stresses

4.9 Finite Element analysis of five-storey building

4.9.1 EL CENTRO AREA

All the steps taken for three-storey building were also taken for five-storey building. The results obtained for this building are given below.
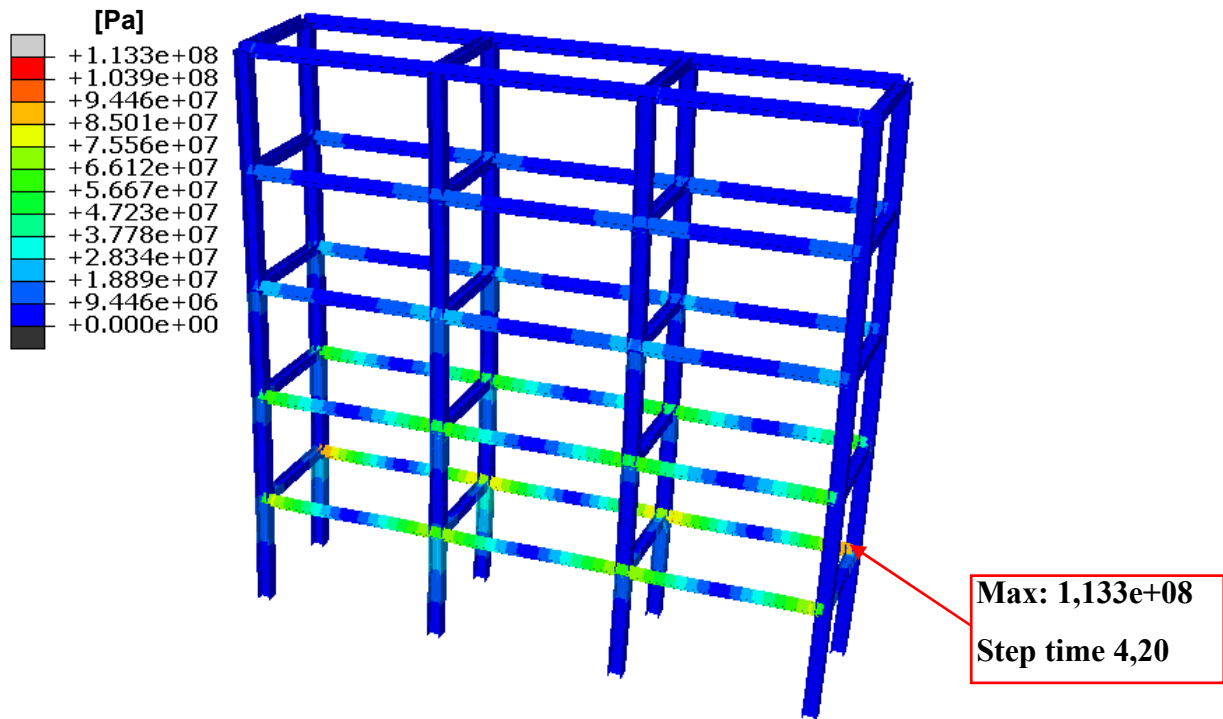
- **Building normal mode**

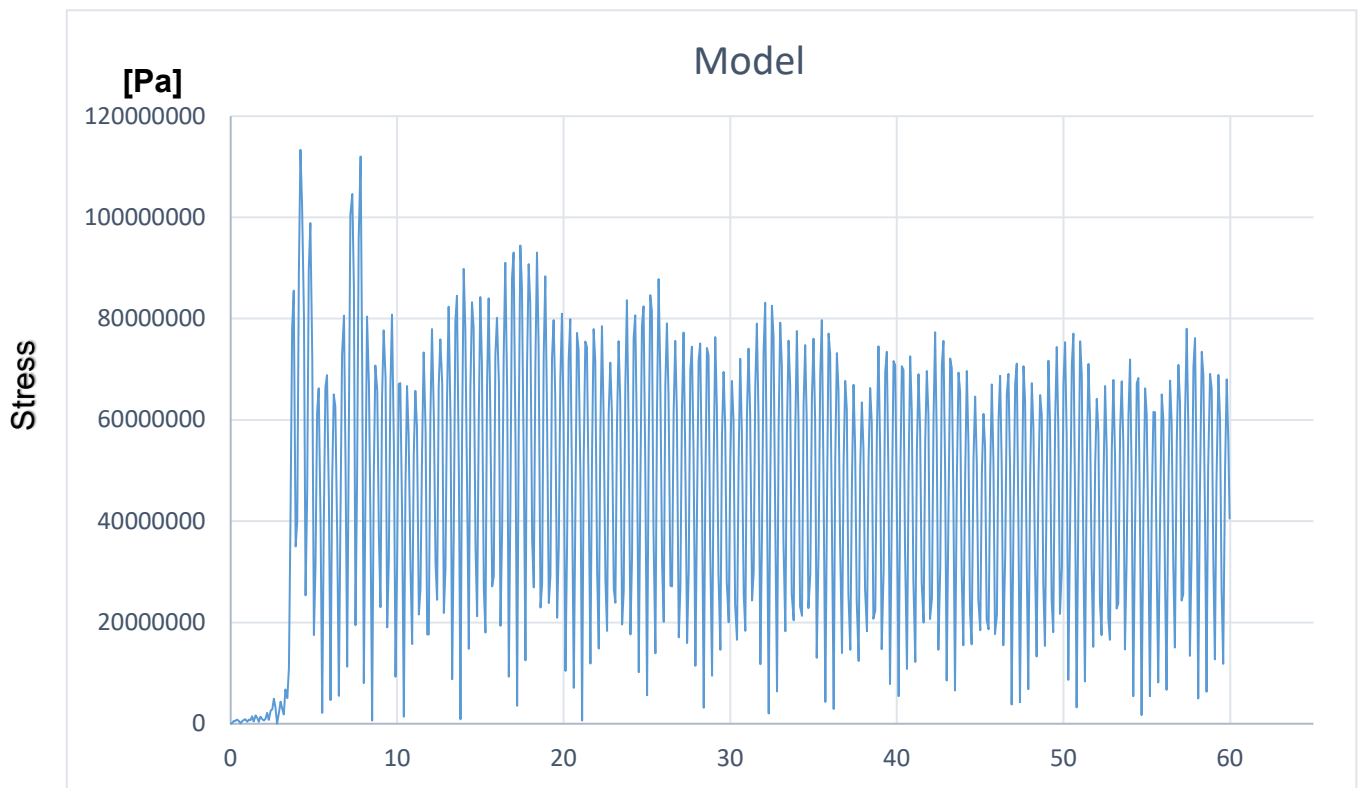**Figure 76: Stress contour for five-storey building in normal model**

Figure 77: The total stress time course for those nodes in which the maximum values in normal model

- **Building with V-shaped reinforcements**

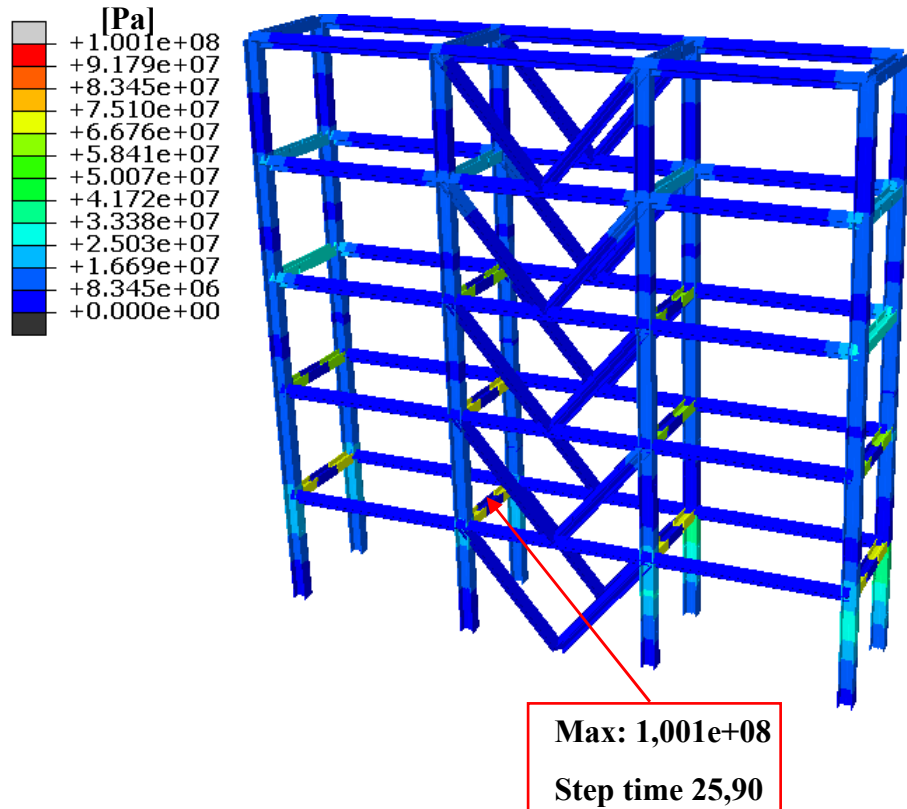Max: 1,63e+08
Step time 37,30

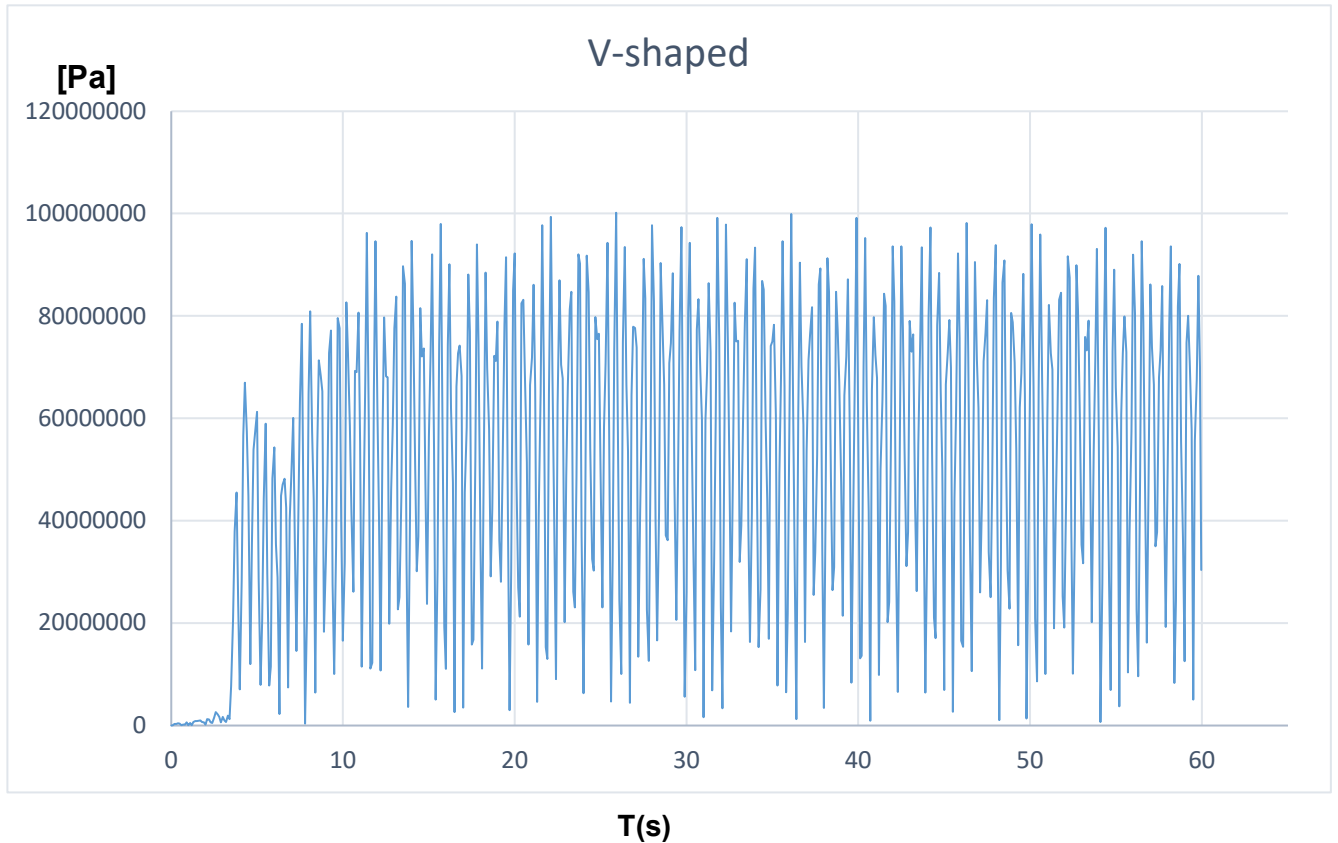**Figure 78: Stress contour for five-storey building with V-shaped reinforcements**

Figure 79: The total stress time course for those nodes in which the maximum values in model with V-shaped reinforcements
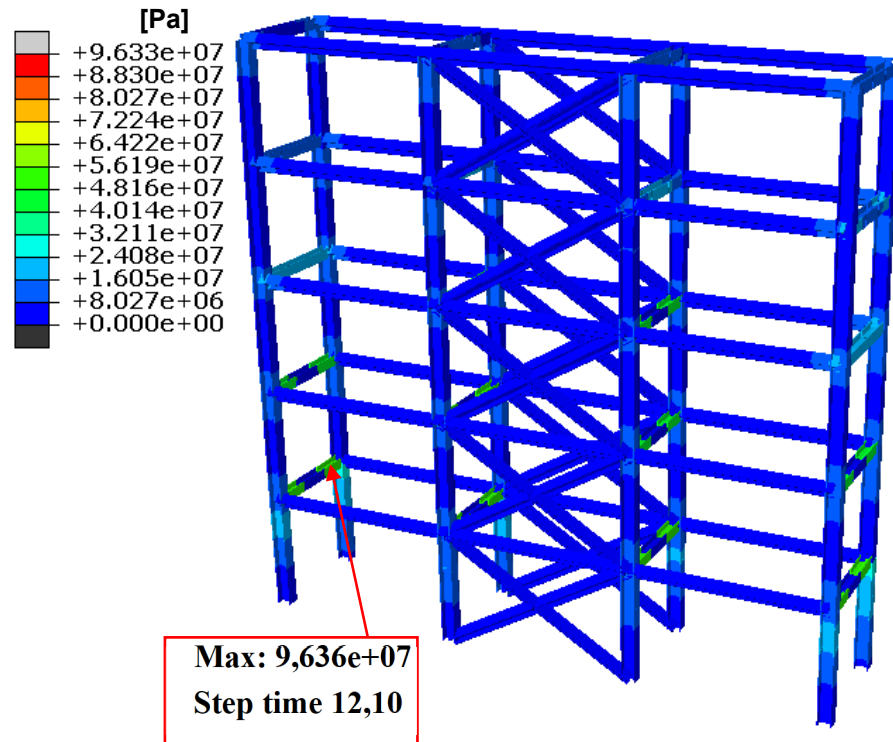
- **Building with X-shaped reinforcements**

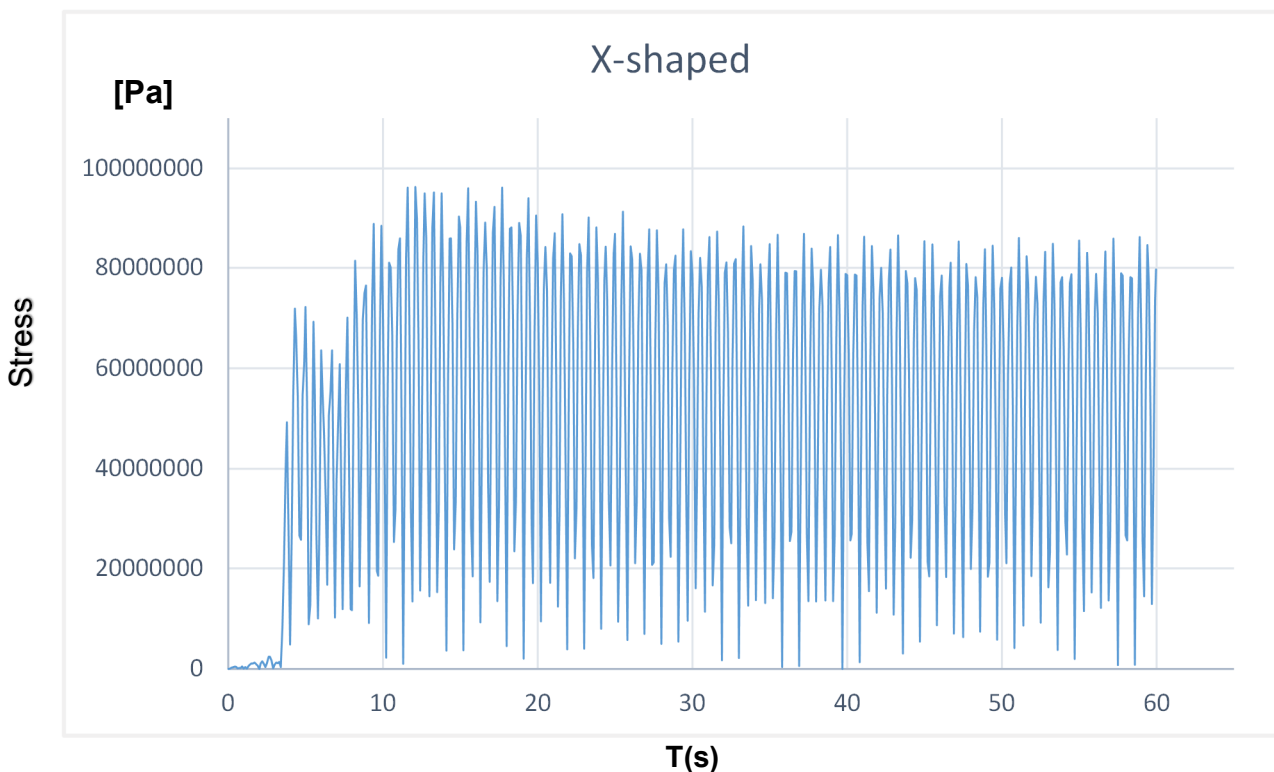**Figure 80: Stress contour for five-storey building with X-shaped reinforcements**

Figure 81: The total stress time course for those nodes in which the maximum values in model with X-shaped reinforcements

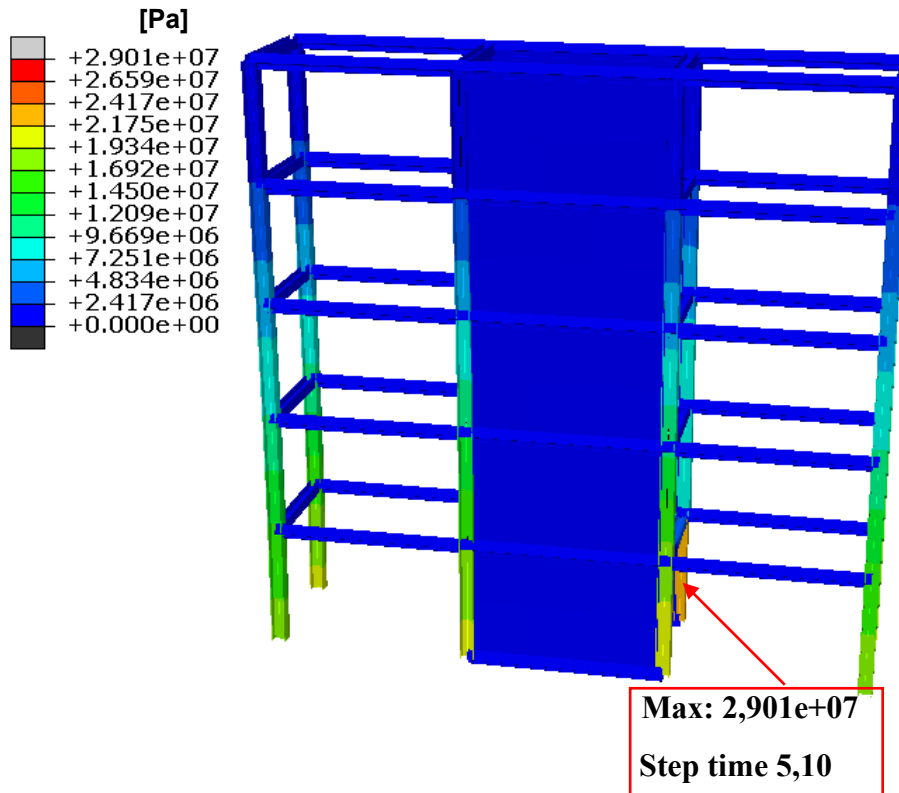- **Building with shear wall**

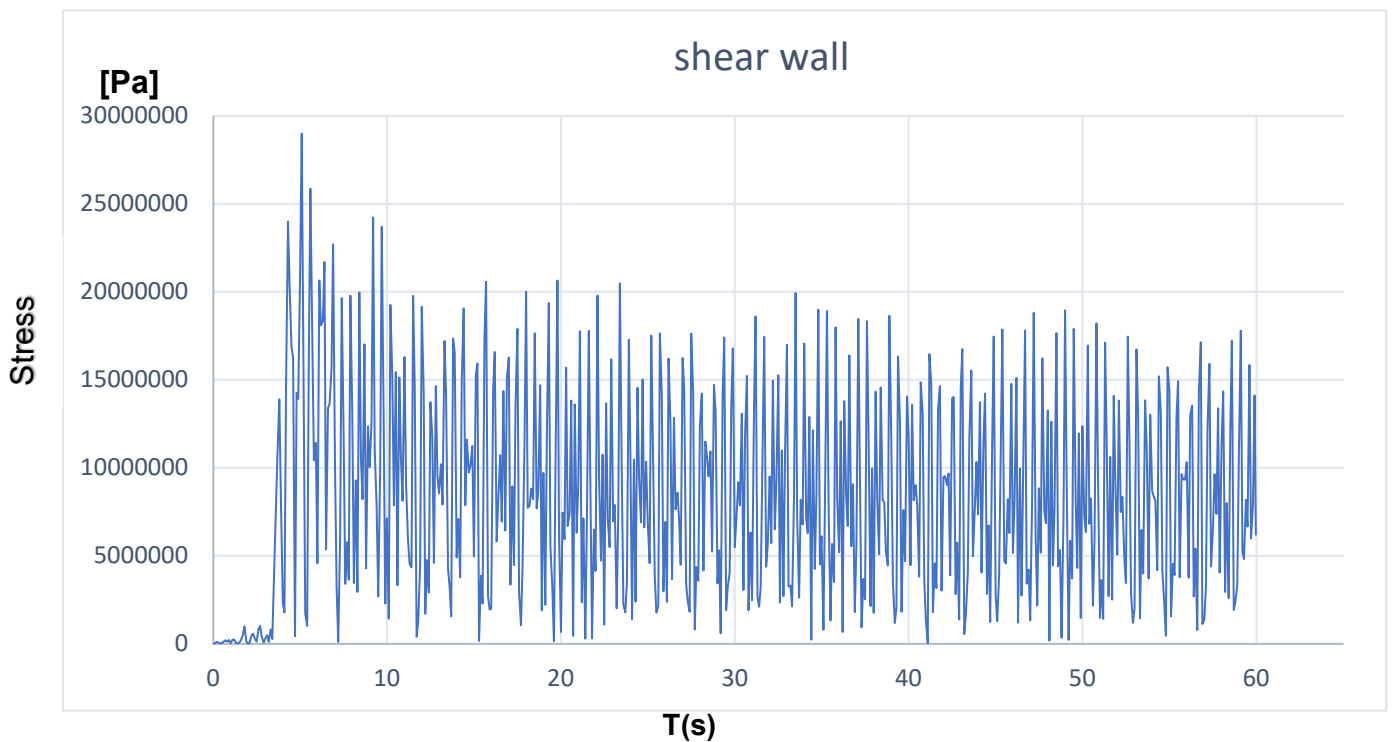**Figure 82: Stress contour for five-storey building with shear wall**
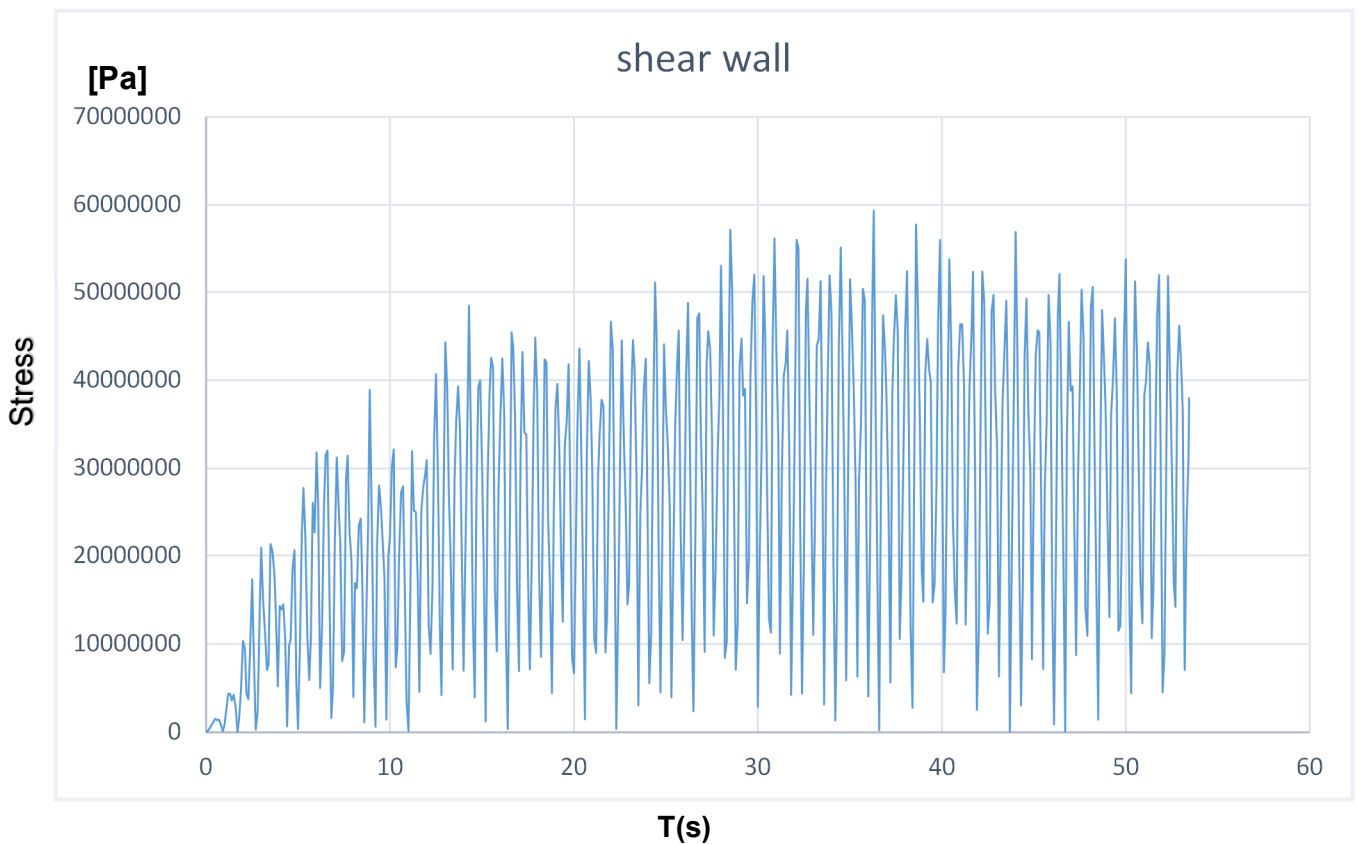
Figure 83: The total stress time course for those nodes in which the maximum values in model with shear wall

4.9.1.1 Comparison of stress results for five-storey building in the El Centro area

The maximum stresses applied to the structure of the five-storey building are given in the table below. As is clear, the amount of stress decreases regularly by changing the reinforcement of the building from the V to the shear wall.

Stress (Mpa)	Building type
175.30	Building normal Model
163.3	Building with V-shaped reinforcement
145.70	Building with X-shaped reinforcement
59.36	Building with shear wall

Table 4.5: Table of Comparison of stress results

4.9.2 LOMA PRIETA AREA

- **Building normal mode**

Max: 1,10e+08

Step time 20,90

Figure 84: Stress contour for five-storey building in normal model

Figure 85: The total stress time course for those nodes in which the maximum values in normal model

- **Building with V-shaped reinforcements**

Figure 86: Stress contour for five-storey building with V-shaped reinforcements

Figure 87: The total stress time course for those nodes in which the maximum values in model with V-shaped reinforcements

- **Building with X-shaped reinforcements**

Figure 88: Stress contour for five-storey building with X-shaped reinforcements

Figure 89: The total stress time course for those nodes in which the maximum values in model with X-shaped reinforcements

- **Building with shear wall**

Max: 1,029e+07

Step time 19,60

Figure 90: Stress contour for five-storey building with shear wall
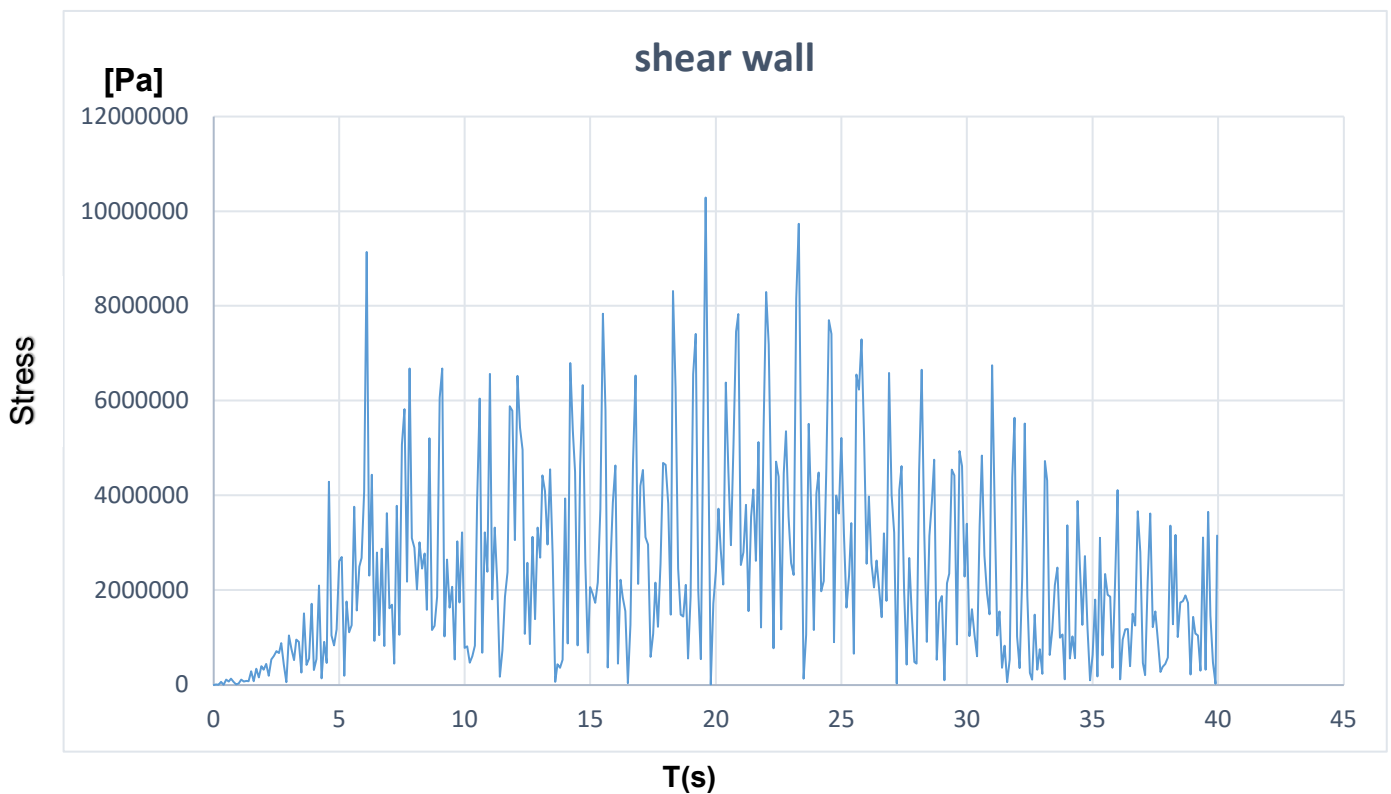
Figure 91: The total stress time course for those nodes in which the maximum values in

model with shear wall

4.9.2.1   <u>**Comparison of stress results for five-storey building in the Loma Prieta area**</u>

The maximum amount of stress applied to the structure of the five-storey building in the Loma Prieta area is given in the table below. As it is obvious, the amount of stress decreases regularly by changing the reinforcement from the V to the shear wall.

Stress (Mpa)	Building type
110	Building normal Model
37.85	Building with V-shaped reinforcement
24.24	Building with X-shaped reinforcement
10.29	Building with shear wall

Table 4.6: Table of Comparison of stress results

4.9.3 NORTHRIDGE AREA

- **Building normal mode**

Figure 92: Stress contour for five-storey building in normal model

Figure 93: The total stress time course for those nodes in which the maximum values in normal model

- **Building with V-shaped reinforcements**

Figure 94: Stress contour for five-storey building with V-shaped reinforcements

Figure 95: The total stress time course for those nodes in which the maximum values in model with V-shaped reinforcements

Left margin text (rotated):

- **Building with X-shaped reinforcements**

[Pa]
+9.633e+07
+8.830e+07
+8.027e+07
+7.224e+07
+6.422e+07
+5.619e+07
+4.816e+07
+4.014e+07
+3.211e+07
+2.408e+07
+1.605e+07
+8.027e+06
+0.000e+00

Max: 9,636e+07
Step time 12,10

Figure 96: Stress contour for five-storey building with X-shaped reinforcements

Figure 97: The total stress time course for those nodes in which the maximum values in model X-shaped reinforcements

- **Building with shear wall**

Figure 98: Stress contour for five-storey building with shear wall

Figure 99: The total stress time course for those nodes in which the maximum values in

model with shear wall

4.9.3.1 Comparison of stress results for five-storey building in the Northridge area

In the following, the maximum amount of stresses applied to the structure of the five-storey building are provided. The amount of stress reaches its lowest value, when the shear wall is used in the building structure. However, the use of X-shaped reinforcements will result in a further reduction in the stress value than to the V-shaped reinforcements.

Stress (Mpa)	Building type
113,3	Building normal Model
100	Building with V-shaped reinforcement
96.33	Building with X-shaped reinforcement
29.01	Building with shear wall

Table 4.7: Table of Comparison of stress results

4.9.4 General comparison for five-storey building

The maximum stresses applied to the building structure for the three areas (EL CENTRO, LOMA PRIETA and NORTHRIDGE) and for four types of structures are given in the following figure. In all areas, the use of a shear wall reduces the amount of stress applied to the structure significantly. This is while X-shaped reinforcements reduce the stress to a greater extent than V-shaped reinforcements.
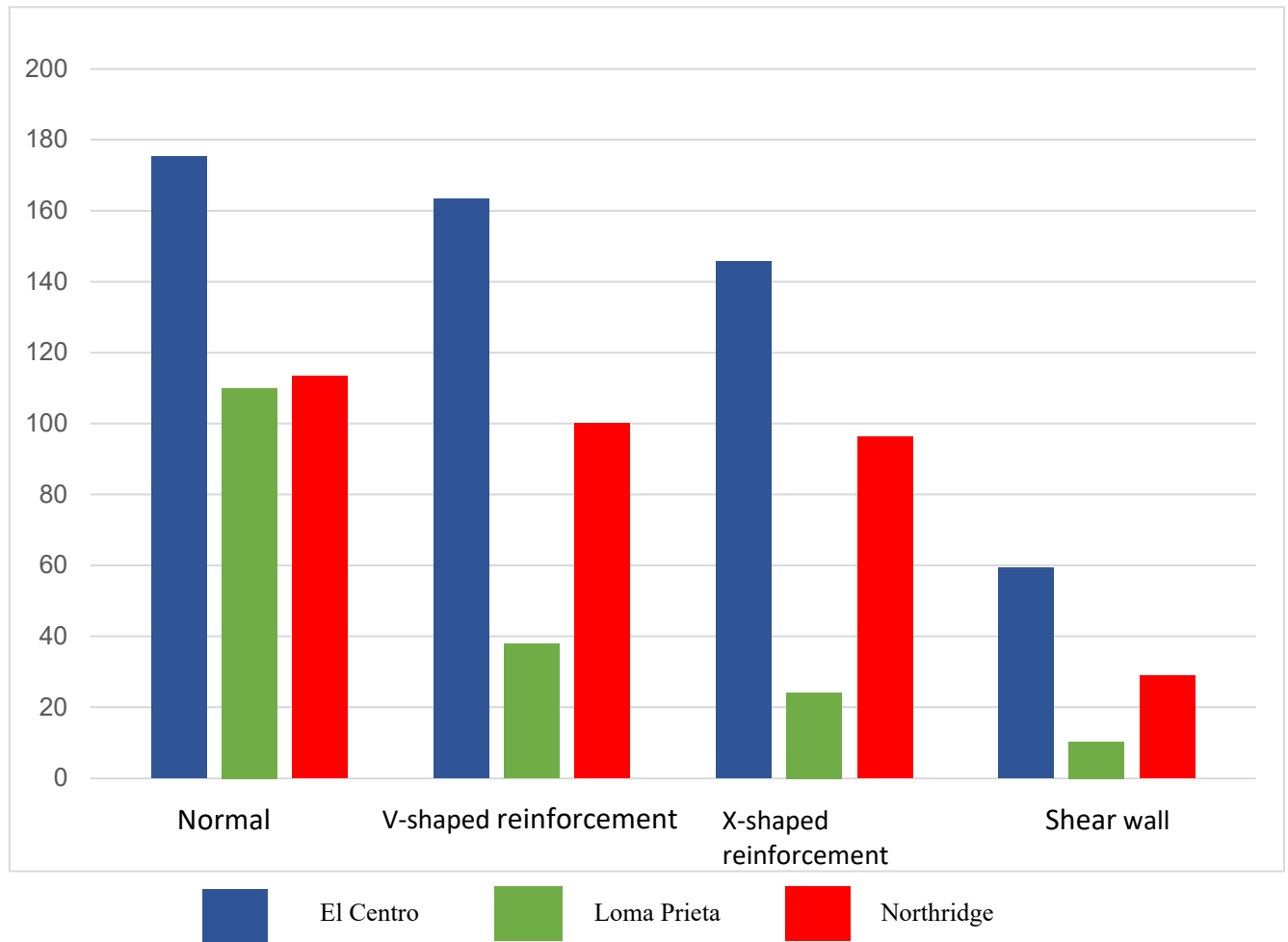
Figure 100: Comparison of stress results for five-storey building

5. CONCLUSION AND RECOMMENDATIONS

5.1 Conclusion

In this thesis, the structure of 3 and 5-storey buildings under the influence of various earthquakes, are examined using sequential accelerograms installed in the areas ELCENTRO, LOMA PRIETA and NORTHRIDGE. Then two types of V and X-shaped braces and also shear walls are used to retrofit the building and prevent the development of plastic hinges in columns at the base. To this end, the dynamic analysis in Abaqus Software was used. The results of this study indicate that the use of braces and shear walls in the building reduces the amount of stress and increases its strength to earthquakes. In fact, the shear walls reduce the tension more than X-shaped braces and the X-shaped braces also reduce the tension more than V-shaped braces in the building structure.

3 and 5-storey buildings and three types of earthquakes were used to validate the issue that use of braces and shear walls reduces the amount of stress in the building structure. In all modes, the use of braces, and in particular the shear walls, results in a significant reduction in stress levels and more structural strength to earthquake-induced forces. Also, the X-shaped brace reduces the amount of stress more than the V-shaped brace.

Due to the fact that use of experimental techniques on 3 and 5-storey buildings is very costly and time consuming, this factor prevents researchers from carrying out a comprehensive study. In this case, it is essential to use virtual simulations and computational methods such as finite element analysis to examine the changes in the performance of these structures. With the advancement of analytic modeling and finite element method, and the feasibility of a very varied modeling of mechanical properties, analytic and numerical models become more voluminous and advanced day-to-day, are confronted with experimental techniques, and may open the way for new research.

5.2 Hypotheses

Although the present study can model how to grow and expand the tension and displacement in different parts of the structure of 3 and 5-storey buildings under various earthquakes, it has several hypotheses of simplification and limitations, which are referred to below.

1. In this study, in order to model the structure of the building, the steel used in the building structure is assumed to be completely homogeneous and without any impurities. However, this mode does not exist in reality. The materials in the industry are not completely homogeneous and the presence of cavities and impurities increases the stress levels in the building structure.

2. When the earthquake occurs, other factors, such as wind-induced forces, soil moisture, the type of soil and materials used for the building structure, affect the changes in tension and displacements on its different parts, in addition to earth movements. These factors are disregarded here.

5.3 RECOMMENDATIONS

This study aims are to examine the performance of 3 and 5-storey buildings against accelerations caused by three different types of earthquakes. The results of the study are well consistent with those of previous studies. However, none of these studies have investigated the effect of using V and X-shaped braces and shear walls simultaneously and also the issue that use of which braces reinforces structures against the earthquake oscillations more. This has led the study to examine the effect of these reinforcements under various earthquakes. In future studies, reinforced concrete structures can also be used in addition to steel structures, and the results can be compared. Additionally, these braces can also be used in other parts of the building. To meet this objective, one can use the very important data provided in this thesis, and ultimately better and more accurate results can be extracted using this approach.

The main purpose of this thesis is to study the effect of increasing the number of floors on how to extend the stress on the building structure. To this end, the number of floors increased from three to five. Therefore, it can be concluded that an increase in the number of floors also more than 5 storey causes stress values, but these modes are quite consistent with the three- and five-storey buildings.

6. FIGURES

7. FORMULAS

8. TABLE

9. REFERENCES

[1] **Dan D, Fabian A, Stoian V**. Nonlinear behavior of composite shear walls with vertical steel encased profiles. Eng Struct 2011;33(10):2794–804.

[2] **Dan D, Fabian A, Stoian V**. Theoretical and experimental study on composite steel-concrete shear walls with vertical steel encased profiles. J Constr Steel Res 2011;67(5):800-13.

[3] **Qian J, Jiang Z, Ji X.** Behavior of steel tube-reinforced concrete composite walls subjected to high axial force and cyclic loading. Eng Struct 2012;36(3):173–84.

[4] **Liao F, Han L, Tao Z.** Performance of reinforced concrete shear walls with steel reinforced concrete boundary columns. Eng Struct 2012;44(11):186–209.

[5] **Dan D.** Experimental tests on seismically damaged composite steel concrete walls retrofitted with CFRP composites. Eng Struct 2012;45(12):338–48.

[6] **Ji X, Sun Y, Qian J, Lu X.** Seismic behavior and modeling of steel reinforced concrete (SRC) walls. Earthquake Eng Struct Dynam 2015;44(6):955–72.

[7] **Astaneh AA**. Seismic behaviour and design of composite steel plate shear walls. Steel tips. University of California: Berkeley, 2002.

[8] **EN 1992-1-1. Eurocode 2**: Design of concrete structures, part 1-1, general rules and rules for buildings.

[9] **Cao W, Zhang J, Zhang J, Wang M**. Experimental study on seismic behavior of mid-rise RC shear wall with concealed truss. Front Arch Civil Eng China 2009;3 (4):370–7.

[10] **Dan D, Fabian A, Stoian** V. Nonlinear behavior of composite shear walls with vertical steel encased profiles. Eng Struct 2011;33(10):2794–804.

[11] **EN 1998-1. Eurocode 8**: design of structures for earthquake resistance.

[12] **EN 1994-1-1. Eurocode 4**: design of composite steel and concrete structures, part 1–1, general rules and rules for buildings.

[13] **Liao F, Han L, Tao Z.** Performance of reinforced concrete shear walls with steel reinforced concrete boundary columns. Eng Struct 2012;44(11):186–209.

[14] **Tomii M.** Shear walls. In: Proceedings of international conference on planning and design of tall buildings, vol. 3, Lehigh University, American Society of Civil Engineering, New York; 1972. p. 203–22.

[15] **Gao XD.** Framed shear walls under cyclic loading. PhD thesis. Department of Civil and Environmental Engineering, University of Houston, Houston, USA; 1999

[16] **Xiaodong Ji, Tongseng Leong, Jiaru Qian, Wuhui Qi, Weibiao Yang**. Cyclic shear behavior of composite walls with encased steel braces. Engineering Structures 127 (2016) 117–128.

[17] **Weiyi Zhao, Quanquan Guo, Zeyu Huang, Li Tan, Jun Chen, Yinghua Ye**. Hysteretic model for steel–concrete composite shear walls subjected to in-plane cyclic loading. Engineering Structures 106 (2016) 461–470.

[18] **Akiyama H, Sekimoto H, Fukihara M, Nakanishi K, Hara K**. A compression and shear loading tests of concrete filled steel bearing wall. In: Proceedings of the 11th international conference on structural mechanics in reactor technology (SMiRT 11). Tokyo, Japan; 1991. p. 323–8.

[19] **Takeuchi M, Narikawa M, Matsuo I, Hara K, Usami S**. Study on a concrete filled structure for nuclear power plants. Nucl Eng Des 1998;179:209–23.

[20] **Ozaki M, Akita S, Niwa N, Matsuo I, Usami S**. Study on steel plate reinforced concrete bearing wall for nuclear power plants Part 1: shear and bending loading tests of SC walls. In: Proceedings of the 16th international conference on structural mechanics in reactor technology (SMiRT 16). Washington, DC, USA; 2001.

[21] **Ozaki M, Akita S, Osuga H, Nakayama T, Adachi N**. Study on steel plate reinforced concrete panels subjected to cyclic in-plane shear. Nucl Eng Des 2004;228:225–44.

[22] **Cheng W, Tian C, Wang C, Yang X, Sun Y.** Experimental study of steel– concrete– steel sandwich composite shear walls. Earthq Resistant Eng Retrofitting 2014:40–7.

[23] **Behnoosh Rassouli, Soheil Shafaei, Amir Ayazi, Farhang Farahbod**. Experimental and numerical study on steel-concrete composite shear wall using light-weight concrete. Journal of Constructional Steel Research 126 (2016) 117–128.

[24] **AISC, ANSI/AISC 341-10,** Seismic provisions for structural steel buildings, American Institute of Steel Construction, Chicago (IL), 2010.

[25] **Applied Technology Council (ATC)**, Guidelines for cyclic seismic testing of component of steel structures, ATC-24, Redwood City, CA, 1992.

[26] **Jungil Seo, Amit H. Varma, Kadir Sener, Deniz Ayhan**. Steel-plate composite (SC) walls: In-plane shear behavior, database, and design. Journal of Constructional Steel Research 119 (2016) 202–215

[27] **Yun-tian Wu, Dao-yang Kang, Yeong-Bin Yang**. Seismic performance of steel and concrete composite shear walls with embedded steel truss for use in high-rise buildings. Engineering Structures 125 (2016) 39–53.

[28] (GB50011-2010) Code for seismic design of buildings [in Chinese].

[29] **Jian-Guo Nie, Xiao-Wei Ma, Mu-Xuan Tao, Jian-Sheng Fan, Fan-Min Bu**. Effective stiffness of composite shear wall with double plates and filled concrete. Journal of Constructional Steel Research 99 (2014) 140–148

[30] **Nam H. Nguyen, Andrew S. Whittaker.** Numerical modelling of steel-plate concrete composite shear walls. Engineering Structures 150 (2017) 1–11.

[31] **Furlong, R.W. (1996)**, "Effective Stiffness of Composite Shear Walls," Proceedings of an Engineering Foundation Conference on Composite Construction in Steel and Concrete III, Irsee, Germany.

[32] **Eom, T-S; Park, H-G; Lee, C-H; Kim, J-H and Chang, I-H (2009)**, "Behaviour of Double Skin Composite Wall Subjected to In-Plane Cyclic Loading," Journal of Structural Engineering, ASCE, Vol. 135, No. 10, pp. 1239–1249.

[33] **Liang, Q.Q.; Uy, B.; Wright, H.D. and Bradford, M.A. (2004)**, "Buckling of Steel Plates in Double Skin Composite Panels under Biaxial Compression and Shear," Journal of Structural Engineering, ASCE, Vol. 130, No. 3, pp. 443–451.

[34] **Rahai, A.; Hatami, F. (2009)**, "Evaluation of composite shear wall behavior under cyclic loadings," Journal of Constructional Steel Research, Elsevier Ltd, Vol. 65, pp. 1528–1537.

[35] **Alinia, M.M. and Dastfan, M. (2007),** "Cyclic behaviour, deformability and rigidity of stiffened steel shear panels," Journal of Constructional Steel Research, Vol. 63, No. 4, pp. 554–563.

[36] **Zhao, Q. and Astaneh-Asl, A. (2004),** "Cyclic Behaviour of Traditional and Innovative Composite Shear Walls," Journal of Structural Engineering, ASCE, Vol. 130, No. 2, pp. 271–284.

[37] **Nie JG, Hu HS, Fan JS, Tao M, Li SY, Liu FJ.** Experimental study on seismic behavior of high-strength concrete filled double-steel-plate composite walls. J Constr Steel Res 2013;88:206–19.

[38] **Rafiei S, Hossain KMA, Lachemi M, Behdinan K.** Composite wall with high performance concrete subjected to monotonic shear. J Constr Steel Res 2015;107:124–36.

[39] **Hossain KMA, Rafiei S, Lachemi M, Behdinan K.** Structural performance of profiled composite wall under in-plane cyclic loading. Eng Struct 2016;110:88–104.

[40] **Chen L, Mahmoud H, Tong SM, Zhou Y.** Seismic behavior of double steel plate-HSC composite walls. Eng Struct 2015;102:1–12.

[41] **Design of Steel Structures for Buildings is Seismic Areas2007;** ECCS Eurocode design manuals

[42] **Dassault Systèmes Simulia Corp. (2008),** "ABAQUS/CAE Documentation, Version 6.8– 3," Providence, RI, USA (www.simulia.com).

[43] **Lubliner, J.; Oliver, J.; Oller, S. and Onate, E. (1989),** "A Plastic-Damage Model for Concrete," International Journal of Solids and Structures, Vol. 25, No. 3, pp. 299–326.

[44] **Lee, J. and Fenves, G.L. (1998),** "Plastic-Damage Model for Cyclic Loading of Concrete Structures," Journal of Engineering Mechanics, ASCE, Vol. 124, No. 8, pp. 892–900.

[45] **Popovics, S. (1973),** "A numerical approach to the complete stress strain curve for concrete," Cement and concrete research, Vol. 3, No. 5, pp. 583–599.

[46] **Wang, T. and Hus, T.T.C. (2001),** "Nonlinear finite element analysis of concrete structures using new constitutive models," Computers and Structures, Vol. 79, No. 32, pp. 2781–2791.

[47] **Shima, H.; Chou, L. and Okamura, H. (1987),** "Micro And Macro Models for Bond Behaviour in Reinforced Concrete," Journal of the Faculty of Engineering, University of Tokyo, Vol. 39, No. 564, pp. 297–316.

[48] **Eurocode-8**: Design provisions for earthquake resistance of structures, Part1.1: General rules, seismic actions and rules for buildings, European Committee for Standardization, 2003.

[49] **Iervolino I, Maddaloni G, Cosenza E. Eurocode 8** compliant real record sets for seismic analysis of structures, J Earthquake Eng 2008; 12(1): 54-90.

[50] **Eurocode-8:** Design provisions for earthquake resistance of structures, Part2: bridges, European Committee for Standardization, 1998.

[51] **Arabzadeh A, Soltani M, Ayazi A.** Experimental investigation of composite shear walls under shear loadings. Journal of Thin -Walled Structures, 49(2011) 842−54.

[52] Wikipedia.1940_El_Centro_earthquake

[53] Wikipedia. 1994_Northridge_earthquake

[54] Wikipedia.1989_Loma-Prieta_earthquake

[55] Wikipedia.1989_Loma-Prieta_earthquake

[56] **Rainer Flesch (Autor), Horst Pacht (Mitwirkende)** Baudynamik praxisgerecht, Bd.1, Berechnungsgrundlagen

10. ATTACHMENT

10.1 General information about ABAQUS/CAE

A wide range of applications in science and engineering, is the most important factors in choosing finite element modelling software by researchers. The ABAQUS as a professional and very powerful software, able to meet the range of needs of researchers in the fields of mechanical engineering, civil engineering, engineering, metallurgical, engineering and mining industries, and constantly improve their performance in these areas to the choice of reliable and efficient in the realm of engineering and science to be converted. Civil engineering fields is due to the scope of research topics and various educational topics, widely uses finite element modelling. Since ABAQUS able to provide various models and very good coverage of development issues, traditionally distinguish itself from other competitors selected to the researchers of civil engineers in the field of finite element simulation has become. ABAQUS, introduce itself as a serious competitor in the field of civil engineering finite element simulations and encourage researchers to make use of ABAQUS.

Civil engineering fields knew an enormous diversity of issues of a research in there. Analysis beams, columns, frames (Frame) and structures such as buildings, bridges, tubes buried in the soil, structural analysis under earthquake, identifying and analyzing the phenomenon of buckling and post buckling, analysis of reinforced structures such as reinforced concrete, the damage in concrete structures, analysis of stress concentration in the structure, analysis of hysterical beams and structural analysis under explosive loading, all of the issues common and widely used by civil engineers to research the deal and increasing software features. ABAQUS is a commercial software package for finite element analysis. The ABAQUS finite element system includes [42]:

- ABAQUS/Standard, a general-purpose finite element program;
- ABAQUS/Explicit, an explicit dynamics finite element program;
- ABAQUS/CFD, a general-purpose computational fluid dynamics program;
- ABAQUS/CAE, an interactive environment used to create finite element models, submit ABAQUS analyses, monitor and diagnose jobs, and evaluate results; and
- ABAQUS/Viewer, a subset of ABAQUS/CAE that contains only the postprocessing capabilities of the Visualization module.

ABAQUS was initially designed to address non-linear physical behavior; as a result, the package has an extensive range of material models. Its elastomeric (rubberlike) material capabilities are particularly noteworthy [42].

ABAQUS Documentation collection that includes full banking solution methods, the introduction of analytical steps, such as varied and practical as well as theoretical and mathematical relationships, one of the most complete and best references in the software step by step guide. Very detailed classification of information and Help, this opportunity is that beginners on how to modeling, usage instructions etc. along with experts and universities (about equations, solution formulation and behind the software) and solve their own needs.

ABAQUS / Standard and ABAQUS / Explicit are two main analysis products from ABAQUS / CAE. ABAQUS/Standard as general-purpose analysis software can solves a system of equations implicitly at each solution increment. It can solve a wide range of linear and nonlinear problems involving static, dynamic, thermal, and electrical response of components. The equilibrium for the implicit method is achieved by an iterative procedure.

ABAQUS/Explicit is a special-purpose analysis module which uses an explicit dynamic finite element formulation. It uses central difference method to integrate the equations of motion explicitly through time. In order to calculate the kinematic conditions in the next step, the explicit time-integration method uses the kinematic conditions in an increment.

This is capable for modelling, transient dynamic events such as shock problems and is also very useful for highly linear problems with contact conditions. The explicit method requires the use of small-time increments. Since there are no simultaneous equations to solve, each increment is inexpensive.

Tabell 10.1 shows the difference between ABAQUS/Standard and ABAQUS/Explicit which was excerpted from the ABAQUS documentations [42].

Parameter	ABAQUS/Standard	ABAQUS/Explicit
Element library	Offers an extensive element library	Offers an extensive library of elements well suited for explicit analyses. The elements available are a subset of those available in ABAQUS/Standard
Analysis procedures	General and linear perturbation procedures are available	General procedures are available
Material Models	Offers a wide range of material models	Similar to those available in ABAQUS/Standard; a notable difference is that failure material models are allowed
Contact formulation	Has a robust capability for solving contact problems	Has a robust contact functionality that readily solves even the most complex contact simulations
Solution technique	Uses a stiffness-based solution technique that is unconditionally stable	Uses an explicit integration solution technique that is conditionally stable
Disk space and Memory	Due to the large numbers of iterations possible in an increment, disk space and memory usage can be large	Disk space and memory usage is typically much smaller than that for ABAQUS/Standard

Table 10.1: Comparison between ABAQUS/Standard and ABAQUS [42]

For analyzing a nonlinear problem with a large number of degrees of freedoms (DOFs) such as composite walls, using ABAQUS/Standard will be impractical and time consuming. Since, for each iteration, ABAQUS/Standard requires solution of a large set of linear equations through iteration process. On the other hand, ABAQUS/Explicit determines the solution without iterating by explicitly advancing the kinematic state from the previous increment. Although for a large number of the DOFs the analysis may require a large number of time increments using the explicit method, the analysis can be more efficient in ABAQUS/Explicit compared to ABAQUS/Standard. The explicit method has great cost savings over the implicit method as the model size increases.

Figure 101 shows the variation of the computational cost versus number of DOF for ABAQUS/Explicit and ABAQUS/Standard. The relation between the computational costs and the number of DOF in ABAQUS/Explicit is almost linear.
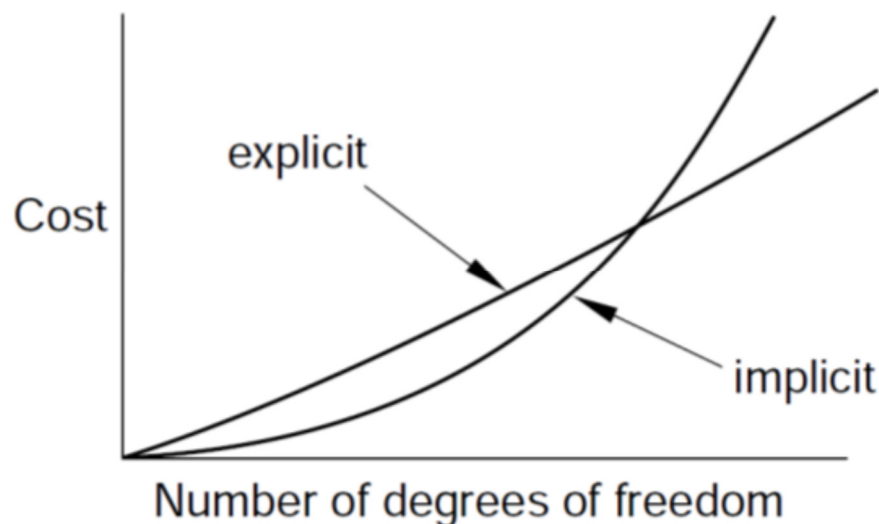
Figure 101: Cost versus model size in using the explicit and implicit methods [42]

The four main reasons that ABAQUS/Explicit is used in this study are as follows:

1. Concrete degradation can cause severe convergence difficulties in ABAQUS/Standard (implicit) analysis program but in the ABAQUS/Explicit can perform well,
2. Reduce the computational cost (time) for the composite wall model,
3. Formulation easier to contact conditions,
4. High-speed Analysis of dynamic phenomena

10.1.1 CONDITIONAL STABILITY AND TIME INCREMENT IN THE EXPLICIT METHOD

ABAQUS/Explicit automatically controls the time increment size throughout the analysis to maintain stability. ABAQUS/Explicit calculates the stable time increment based on the highest frequency in the model which can be estimated by individual elements. Based on the element-by element estimate, the stability time limit (Δt_{stable}) can be defined using the shortest element length (L_e) and the wave speed of the material (C_d) [42]:

(10.1)
$$\Delta t_{stable} = \frac{L_e}{C_d}$$

The wave speed is a property of the material. For a linear elastic material with a Poisson's ratio of zero the wave speed can be derived from the following equation:

(10.2)
$$C_d = \sqrt{\frac{E}{\rho}}$$

where E is Young's modulus and ρ is the mass density.

In a nonlinear material, such as a metal with plasticity or concrete, the wave speed changes as the material yields and the stiffness of the material changes. In the nonlinear portion of the analysis, the modulus of elasticity decreases which reduces the wave speed and increases the critical time increment. ABAQUS/Explicit monitors the effective wave speeds in the model throughout the analysis, and the current material state in each element is used for stability estimates.

The shortest element dimension has direct effect on the stability time limit (Eq. 3.2) and it is recommended to keep the element size as large as possible. On the other hand, for accurate analyses a fine mesh is needed. The best approach for meshing a FE model is to have a mesh which is as uniform as possible and also to make a balance in size of mesh that will not compromise the analysis accuracy or may result in very small stable time limit.

10.1.2 TIME HISTORY ANALYSIS WITH ABAQUS/EXPLICIT

As a general target objective finite element program, ABAQUS a brisk advancement in numerous regions. ABAQUS practically explosive improvement in the field of seismic investigation has encountered. It is not as recognized by the industry when it has barely been approved, anyway, mutually the consistently self-development and redevelopment from the users, it is seldom accepted by the industry, and soon ABAQUS has accumulated much helpful experiences in the field of seismic analysis which prompting itself as prime position in the area. Nevertheless, the assignment of ABAQUS to handle dynamic analysis is not the most complacent way, the idea is that the structural engineers prefer to pay a lot of brain effort during using ABAQUS to complete their work. The reason for that cause structural engineers require ABAQUS as their instrument is ABAQUS has several absolutely important advantages:

1. Powerful non-linear solution

ABAQUS is a powerful finite element software of engineering simulation, and its solution to the problem is in the range from relatively easily done linear analysis to many complicated non-linear problems, related to geometry, material nonlinearity and material damage accumulation of other complicated questions.

2. Explicit integration to solve two major problems

The core problem of time-history analysis is the numerical integration of dynamic equations. In the state of non-linear problems, the modal superposition method cannot relate to appropriate result, the direct integration approach should be used. Implicit and explicit are the main direct integration method. Implicit algorithm is, derive the next moment displacement according the balance equations, while the explicit algorithm is by the current balance to gain the next moment displacement. In general, unconditionally stable implicit algorithm is regularly used to solve dynamic problems, and NEWMARK method is the practically widely used implicit algorithm.

3. Wide library of materials

ABAQUS contains an extensive library of elements that can simulate virtually any geometry. The program also includes an extensive list of models of material behavior that can simulate the behavior of engineering materials such as metals, rubber, polymers, composites, reinforced concrete, brittle foams and geotechnical materials such as soil and rock. Issues with multiple components and different materials can be define with geometry of each component and assign its constituent materials and then define the interaction between the components to be simulated.

4. Successive modeling

In order to structural analyze and design, design engineer have to spend a lot of time and effort to time history analysis. In most modeling, even with the non-linear models, the engineer needs only determine and import engineering data, such as the geometry, material behavior of the boundary conditions and. ABAQUS in a non-linear analysis, automatically select the amount of development time and tolerances convergence as well as the analysis of their values is adjusted to achieve a correct answer. As a result, users rarely need to determine the numerical values of the control parameters.